University of Trento

Department of Mathematics

PhD Thesis

XXVIII Cicle

The influence of the population contact network on the dynamics of epidemics transmission

Author:

Stefania Ottaviano

Supervisors:

Prof. Stefano Bonaccorsi,

Dr. Francesco De Pellegrini

February 2016

To Marco

Introduction

The spread and persistence of infectious diseases are a result of the complex interaction between individual units (e.g. people, city, county, etc), disease characteristics and various control policies which aim at arresting disease transmission or bringing infection prevalence to as low a level as possible. Thus the main aim of many models is to gain insight into how diseases transmit and to identify the most effective strategies for their prevention and control.

The early modelling contributions for infectious disease spread date backs to the eighteenth century with the work of Bernoulli (1760) on the smallpox, another crucial work is that of Ross (1911) that modelled the transmission of malaria. One of the first more general and rigorous study was made by Kermack and McKendrick (1927), that has evolved along the years in an impressive quantity of improved works [21, 69].
Epidemiology modelling has been used in planning, implementing and evaluating various prevention, therapy and control programs [14]. The epidemic model has been used also to describe a wide range of others phenomena, like social behaviors, diffusion of information, computer viruses etc., indeed even if the basic mechanisms of these phenomena can be different, often their dynamical behavior can be described by the same type of equations [69].

Generally, the theoretical approach to epidemic spreading is based on compartmental models, i.e., we assume that the population can be divided into different classes (or compartments) depending on the stage of the disease. The main classes are those formed by the susceptibles (denoted by S)

that are healthy and hence can contract the infection, the infectives (denoted by I) that have contracted the disease and can infect the susceptible individuals and the removed (denoted by R) who recovered from the disease and received immunity. Additional compartments can be used to cover other possible states of individuals.

In the simplest models the population is considered closed, i.e. the population does not change over time. The implicit assumption, in this case, is that the time scale of the disease is much smaller than the lifetime of individuals. Consequently terms accounting for the births or natural deaths (but even demographic processes such as immigration or emigration) are not included in the equations that account for the evolution in time of contagion process, i.e. the transition of individuals from one compartment to the other [14].

The epidemic spreading is governed by an inherently probabilistic process. Thus a correct analysis of epidemic models should consider explicitly its stochastic nature, especially when dealing with small populations [42, 69].

In the simplest stochastic model the infectious period has the lack-of memory property, i.e., we assume that the duration of infectivity is exponential, this means that the process $(S, I) = \{(S(t), I(t)); t \geq 0\}$ is Markovian [42]. The first formulation of the epidemic Markov model is due to Barlett (1949). The assumption of an exponentially distributed infectious period is not epidemiologically motivated, rather often in conflict with the empirical evidence, however with this assumption the mathematical analysis becomes much simpler. Moreover using Markov process, we can obtain deterministic and diffusion approximations for the whole trajectory, in the case of large population sizes (see [53],[42, Chapter 5]). This is difficult to obtain when the stochastic process is not Markovian [42].

Models that choose other than the exponential interaction time for infection and/or recovery (see, for instance [96, 23, 48]), have appeared recently in literature.

Besides discrete time Markov chain (DTMC) and continuous time Markov chain (CTMC) (see [20]), another typical method for formulating stochastic epidemic models is through stochastic differential equations (SDE) [3, 2].
However most of the early epidemic models are deterministic, and over the years, works on deterministic models have dominated strongly over works on stochastic models, because of their greater simplicity and tractability [66].

The deterministic models assumes that the population is sufficiently large, in order to ignore the random fluctuations; by the application of the law of the large number the probability of an event (e.g. the infection) is equalized with the fraction of infected individuals. Thus, the number of individuals in each class, a discrete quantity, becomes a real number. The use of these deterministic model with real variables can be rigorously justified, as said before, as limit of stochastic model with integer variable, when the population tends to infinity (see [53]).
In these models, in absence of detailed data on human interactions, the most basic approach is to consider an *homogenous mixing approximation*, meaning that individuals in the population are well mixed and interact with each other completely at random, that is each member in a compartment is treated similarly and indistinguishably from the others [69, 5]. Thus, through the law of mass action (see [69]), which states that an individual becomes infected at a rate proportional to both the densities (i.e. the fraction) of infectious and susceptibles, one can write down a system of ordinary differential equations for the average densities of individuals in the various compartments.

There are many differences between the deterministic and stochastic epidemic models, one of the most important is their asymptotic dynamics. Eventually stochastic solutions (sample paths) may converge to the disease-free state even though the corresponding deterministic solution, under some pa-

rameter regimes, converges to an endemic equilibrium, meaning that the disease will persist indefinitely in the population, never dying out [3, 66, 65, 21]. Indeed, the deterministic version of models with compartments, has a threshold that is described in terms of the so-called basic reproduction ratio R_0, that depends on the basic parameters of the model. The basic reproduction ratio is the expected number of secondary cases produced by a typical infected individual, during its entire period of infectiousness, in a completely susceptible population [32]. The threshold value $R_0 = 1$ for the deterministic model identifies two parameter regions, i.e. one where $R_0 > 1$, and the other where $R_0 < 1$, with qualitatively different behaviors of the solutions of the ordinary differential equations. Instead, in the stochastic model, we can identify three parameter regions with qualitatively different behaviors. The boundaries between these regions depend on the value of the number of individuals N; the amplitude of the transition region near $R_0 = 1$ approaches zero when $N \to \infty$. This explains why this region is absent from the deterministic version of the model [66].

However, as it is showed in [66], some deterministic models are unacceptable approximations of the stochastic models for a large range of realistic parameter values.

Other properties that are unique to the stochastic epidemic models include the probability of an outbreak, the quasi-stationary probability distribution , the final size distribution of an epidemic and the expected duration of an epidemic, see [3] for a detailed explanation.

The assumption of homogeneous mixed population, both in deterministic and stochastic models (see e.g [21, Section 2.3]) is very strong and disputable, since details such as geographical location, presence of community structures, or the specific role of each individuals in the epidemic spreading are ignored [14, 69]. Moreover, an implicit assumption is that each infected individual has a small chance to infect every susceptible individual in popu-

lation. Conversely diseases spread through a network of social contacts, thus the epidemic has a much higher probability of spreading to a limited set of susceptible contacts [50]. Indeed the dynamics of disease transmission strongly depends on the properties of the population contact network.
The relationship between epidemiology and network theory dates back to the mid-1980s (Klovdahl, 1985; May and Anderson, 1987). However in the recent years great progress have been made in the understanding the role of network in the epidemic spread, regarding random graphs (Diekmann et al., 1990, Barbour and Mollison 1990, Andersson, 1998, Neal, 2003.), small word networks (Watts and Strogatz, 1998, More and Newmann, 2000), and scale-free networks (May and Llyod, 2001, Pastor-Satorras and Vespignani, 2001). In most of this works the individual-level network structure and behaviour are used to generate an approximation for the spread of infection [50]. For a short review on these kind of models see [69, 29]. A different approach is taken, e.g in [50], that aims to modify the standard ODE models of Kermack and McKendrick in order to capture the temporal dynamics of network. Generalization of the epidemic modeling to any network structure was recently proposed by Newman, 2002; Wang et al., 2003, Ganesh et al., 2005, VanMieghem et. al. 2009.

The increased interest in this field derives from the accumulated evidence for the emergence of complex and heterogeneous connectivity patterns in a wide range of biological and socio-technical systems [69]. We are, as individuals, units of a network of social relationships of different types, biological system are the result of biochemical reactions; network structure can be recognizable even in the Internet, or in an electric power grid, in the physical layer of the telecommunication systems, in highways and subways systems or neural networks [14].
The recent possibility of large-scale datasets have led to improve considerably the real-world accuracy of the models, thus simulations of entire populations down to the scale of single individuals [69, 8, 60]. The analysis of the re-

cent abundance of data has offered the possibility to observe interesting and unexpected behaviors whose theoretical understanding have stimulated an intense research activity. The new models try to take into account individual heterogeneity, multiple scales at play during the spread of epidemics, spactial structure, and the emergence of clustering and communities that characterize the connectivity patterns [69].

Another noteworthy aspect is that, in most of the models, the parameters are considered given and constant over time. However in population models, as well as in many other application fields, the parameters may have a great variability depending on errors in the observed and measured data, on uncertainties, e.g. when some variables cannot be measured, on lack of knowledge or, simply, on the presence of a random environment. Hence a more correct approach may be to consider the parameters as random variables with a specified given distribution, and study differential equations with random coefficients or incorporating stochastic effects. This kind of models are better in describing real behavior than model involving equations with deterministic coefficients [3, 86, 87].
The modeling of random perturbation is classically obtained in two different ways. On the one side, stochastic differential equations have been used to approximate the Markov chain model (see for instance [59] and [30]). On the other side, a simpler approach consists of introducing parameter perturbations in the ordinary differential equations to examine the effects of environmental stochasticity: see for instance [57, 41] and the review in [21, 86].

After this general overview on epidemics models, that clearly makes no claim to completeness, because of the huge amount of contributions and open problems in this field, we report in the next section a sketch of the thesis.

0.1 Scope and organization of the thesis

The major scope of this thesis is to understand how the viral propagation, between interacting agents, is determined by intrinsic characteristics of the contact networks; thus we aim to investigate how a particular network structure can impact on the long-term behavior of epidemics.
For this purpose we consider a given and static graph, i.e. one whose nodes set and edges sets do not change in time, that we can see, ideally as the result of some random experiment, or as a man made architectures. The use of theoretically constructed networks aims to capture some of the known (or postulated) features of real transmission networks.

We consider a closed population and an SIS (susceptible-infected-susceptible)-type model. In the SIS an individual can be repeatedly infected, recover and yet be infected again. This model covers those types of disease that does not confer immunity, e.g. common cold, sexually transmitted diseases, and other bacterial infections [38, 54]. Computer viruses also belong in this category, indeed once cured, without a constant upgrade of the antivirus softwares, the computer has no way to fend off subsequent attacks by the same virus [67]. The SIS model can be used also for describing some social behaviors and emotions [46].
Our continuous-time spreading process is described through an individual-based mean-field approximation [95, 81]. The basic idea [99, 26, 95, 40, 85] of this approach is to write down equations representing the evolution in time of the probability of each node to be infected, assuming that the dynamic state of every node is independent of the state of its nearest neighbors. Under this assumption the mean-field equations can be obtained [69].

The thesis is organized as follows.
In Chapter 1 we report some basic notions on graph theory, and in Chapter 2 some basic results on the stability of dynamical systems, that will be useful in the rest of the thesis.

In Chapter 3 we introduce the individual-based mean-field approximation, that we shall use for describing the exact spreading process through a reduced system of N non-linear differential equations. Then we report on the analysis of the stability properties of the dynamical systems obtained and the concept of *epidemic threshold*, the critical value of the rate parameters separating an absorbing state, where all nodes are healthy, from an endemic phase.

In Chapter 4 we consider a network divided in communities and report results in [17] and [16], where we have discussed the particular case of the *equitable partition* of the node set. The gross structure of hierarchical networks of this kind can be described by a quotient graph. The rational of our approach is that the epidemic process within the communities is faster compared to the rate at which it spreads across communities. We show that the spectral radius of this smaller quotient graph (which only captures the macroscopic structure of the community network) is all we need to know in order to decide whether the overall-healthy state defines a globally asymptotically stable or an unstable equilibrium. Indeed, the spectral radius is related to the epidemic threshold of the system.
We derive a tight lower bound for the threshold, as a function of network metrics; in practice this value can be adopted to determine a safety region for the extinction of epidemics.
Moreover we prove that, above the threshold, another steady-state exists that can be computed using a lower-dimensional dynamical system associated with the evolution of the process on the quotient graph. Finally, we have also considered the case when the partition is *almost equitable*.

In Chapter 5 we extend the results in Chapter 4 to the case of heterogeneous setting, reporting the result in [68]. Precisely we include the possibility for the infection rate to be different for each link, and that each node can have different recovery rate. Basically the epidemics spread over a directed weighted graph.
Here we also consider the important issue related to the control of the infectious disease. Taking into account the connectivity of the network, we

provide a cost-optimal distribution of resources to prevent the disease from persisting indefinitely in the population; for a particular case of two-level immunization problem we report on the construction of a polynomial time complexity algorithm (in Appendix A).

In Section 5.3 we include stochasticity in the parameters of the model. In the first part we discuss the case where the infection rates are i.i.d. random variables with a given distribution and investigate how the variance of such variables can influence the steady-state fraction of infected nodes.
Next, we consider that the parameters are not fixed in time; accordingly, we model the infection rates in the form of independent stochastic processes. This allows to get a stochastic differential equation for the probability of infection in each node. We prove that the unique global solution remains within $(0,1)^N$ whenever it starts from this region. Then we report on the asymptotic behaviour of the solution. We show that in a certain set parameters, the solution tends to extinction almost surely. We obtain this result by proving the global attractivity of the null solution of our system. After we discuss on stochastic permanence of the solution; this concept can be paraphrased by saying that the epidemic process will survive forever. We find a condition under which the epidemic process is stochastically permanent.

We find a gap between the two regions of extinction and persistence, given in terms of the parameters of the model. Thus, finally, we provide numerical results that investigate the behaviour of the solution into this middle region, comparing the solution of our stochastic system with that of the system with deterministic rate coefficients, introduced in Chapter 3.

Contents

Chapter 1

Notions on Graph Theory

1.1 Basic definitions

We report in this section some basic notions on graphs that will be useful in the rest of the thesis. As reference we use here [47, 89, 61].

Definition 1.1. A *simple graph* is a couple $G = (V, E)$, where V is the set of *nodes* (or vertices), and E is the set of *edges* (or links), i.e. it consists of some couples $e = \{i, j\}$, with $i, j \in V$, and $i \neq j$.

If $e = \{i, j\} \in E$ we say that i and j are *adjacent* (or that i is connected to j, or i is a neighbors of j). One can refer to i and j as the *endpoints* of e. The number of neighbors of a node i is called the *degree* of j.

Definition 1.2. A *simple digraph* is a coupled $G = (V, E)$, where V is the set of nodes and E is the set of *arcs* (or directed edges) of G, that are couples of the form $e = (i, j)$, with $i, j \in V$, and $i \neq j$.

For a digraph the arc e is called an *out-going arc* of i and an *in-coming arc* of j. The *out-degree* of a node i is the number of out-coming arcs and the *in-degree* of a node j is the number of in-coming arcs.

Simple (di)graphs have no loops and no multiple edges (arcs), i.e., edges with the same end nodes. Graphs which are permitted to have loops and

multiple edges is called *multigraphs*.

In this thesis only simple (di)graphs are considered. Therefore, we use (di)graphs to refer to simple (di)graphs for succinctness. Moreover along the thesis we refer to graphs also as *undirected graphs*, and to digraphs as *directed graphs*.

Definition 1.3. A *weighted digraph* is a triple $G = (V, E, \gamma)$, where (V, E) is a digraph and $\gamma : E \to [0, \infty)$ is a given function. $\gamma(e)$ is called the *weight* of e.

The *order* of G is the cardinality of V, the *size* of G is the cardinality of E.

1.2 Adjacency matrix, Laplace matrix and some spectral properties

The connectivity of a (di)graph G is encoded in the following matrix.

Definition 1.4. Let $G = (V, E)$ be a (di)graph. Letting N be the order of G, then the $N \times N$ adjacency matrix is defined by

$$a_{ij} = \begin{cases} 1 & \text{if } i \to j \\ 0 & \text{otherwise} \end{cases} \tag{1.1}$$

Where $i \to j$ means that i is connected with j.
The previous definition can be extended to the case of weighted graphs. In this case the entry $a_{ij} = \gamma(e)$, where e is the edges from i to j.

Let us denote by $\sigma(A)$ the *spectrum* of A, i.e. the set of all eigenvalues of A, and with $\rho = \max_{\lambda \in \sigma(A)} |\lambda|$ the *spectral radius* of A.
Now we report some remarkable results on the eigenvalue spectrum of the

adjacency matrix.

An outstanding result on nonnegative matrices is that given by the Perron-Frobenius Theorem. First we report the definition of irreducible matrix and its relation with graphs.

Definition 1.5. An $N \times N$ matrix A is said to be a *reducible matrix* when there exists a permutation matrix P such that

$$P^T AP = \begin{bmatrix} W & Y \\ 0 & Z \end{bmatrix}$$

where W and Z are both square. Otherwise A is said to be an *irreducible matrix.*

$P^T AP$ is called a symmetric permutation of A. The effect is to interchange rows in the same way as columns are interchanged.

A useful result is that the adjacency matrix A of a digraph G is irreducible if and only if G is strongly connected. We remember that in a strongly connected graph (or, simply, a connected graphs in the case of undirected graph) each node is reachable from any other node via a path (a sequence of adjacent links) by traversing edges in the direction in which they point.

Theorem 1.1 (Perron-Frobenius)**.** *Let A an $N \times N$ irreducible and nonnegative matrix, and suppose that $N \geq 2$. Then*
a) $\rho(A) > 0$
b) $\rho(A)$ is an algebraically simple eigenvalue of A
c) there is a unique real vector

$$x > 0 \quad \textit{such that} \quad Ax = \rho(A)x \quad \textit{and} \quad \|x\|_1 = 1.$$

This vector is called the Perron vector*. There are no nonnegative eigenvectors for A except for positive multiples of x, regardless of the eigenvalue.*

It is possible to give bounds on the position of eigenvalues.

Theorem 1.2 (Gershgorin)**.** *Every eigenvalue of an $N \times N$ matrix A lies in at least one of the closed discs centered in a_{ii} with radius $R_i \sum_{j \neq i} a_{ij}$.*

We underline that if the graph is undirected, then the adjacency matrix is real and symmetric. In this case A has N real eigenvalues that we may order as

$$\lambda_N \leq \ldots \leq \lambda_2 \leq \lambda_1.$$

By the Perron-Frobenius Theorem 1.1 we can assert that $\rho(A) = \lambda_1(A)$. Moreover let us denote with d_i the degree of the node i, then Gershgorin's Theorem 1.2, applied to the adjacency matrix, states that any eigenvalue of A lies in the interval $[-d_{\max}, d_{\max}]$, where $d_{\max} = \max_{1 \leq i \leq N} d_i$. Hence $\lambda_1(A) \leq N - 1$ and this maximum is attained in the complete graph (where all nodes are connected among themselves).

Let us consider an undirected graph $G = (V, E)$. In some applications, especially to physics, it would be desirable to associate with any graph a semidefinite matrix. The adjacency matrix A is not a good choice, its trace is always zero, hence one of its eigenvalues is necessarily strictly negative (unless the graph is trivial). Thus, in order to obtain a positive semidefinte matrix, we can shift the spectrum of $-A$ or A by adding the degree matrix $D = \mathrm{diag}(d_i)$ [64].

Definition 1.6. Let $G = (V, E)$ be a graph. Letting N be the order of G, then the $N \times N$ *Laplace matrix* L is defined by

$$l_{ij} = \begin{cases} d_i & \text{if } i = j \\ -1 & \text{if } i \to j \\ 0 & \text{otherwise} \end{cases} \tag{1.2}$$

i.e.

$$L = D - A.$$

Since we are considering undirected graphs, the Laplacian matrix is symmetric because A and D are both symmetric, and Gershgorins Theorem 1.2 states that each eigenvalue λ_i of the Laplacian lies in an interval $|\lambda_i - d_i| \leq 2d_i$, i.e. $0 \leq \lambda_i \leq 2d_i$.

Chapter 2

Stability of Dynamic Systems

For this section we refer to [6, Chapter 11] and [37, Chapter 5].
We underline that hereafter, unless otherwise specified, we indicate with $|X|$ the euclidean norm of X in $\mathbb{R}^d$.

2.1 Stability of deterministic systems

We report few basic facts on the stability of deterministic systems described by ordinary differential equations. Let us consider the following ordinary differential equation

$$\dot{X}_t = f(t, X_t), \qquad X_{t_0} = c, \quad t \geq t_0, \tag{2.1}$$

where X_t is a d-dimensional state vector. Let us assume that, for every initial condition $c \in \mathbb{R}^d$, there exists a global solution $X_t(c)$, that is one defined on $[t, \infty)$, and that $f(\cdot, x)$ is continuous. Moreover suppose that

$$f(t, 0) = 0, \qquad \text{for all} \quad t \geq t_0,$$

so that (2.1) has the solution $X_t \equiv 0$ corresponding to the initial condition $c = 0$. We shall refer to this solution as the zero (or null) solution (or state).

The zero solution is said to be *stable*, if for every $\varepsilon > 0$, there exists a $\delta = \delta(\varepsilon, t_0) > 0$ such that

$$\sup_{t_0 \le t < \infty} |X_t(c)| \le \varepsilon$$

whenever $|c| \le \delta$. Otherwise, it is said *unstable*.

The zero solution is said to be *asymptotically stable* if it is stable and if

$$\lim_{t \to \infty} X_t(c) = 0 \tag{2.2}$$

for all c in some neighborhood of $x = 0$.

If δ is not dependent on t_0, stability (resp. asymptotic stability) is said to be uniform.

If (2.2) holds for all $c \in \mathbb{R}^d$, then the zero solution is said *globally asymptotically stable* (or *asymptotically stable in the large*).

Definition 2.1. A continuous scalar function $v(x)$ defined on

$$U_h = \{x : |x| \le h\} \subset \mathbb{R}^d, \quad h > 0,$$

is said to be *positive-definite* (in the sense of Lyapunov) if

$$v(0) = 0, \quad v(x) > 0 \quad (\text{for all} \quad x \neq 0).$$

A continuous function $v(t, x)$ defined on $[t_0, \infty) \times U_h$ is said to be positive definite if $v(t, 0) = 0$ and there exists a positive-definite function $w(x)$ such that

$$v(t, x) \ge w(x) \quad \text{for all} \quad t \ge t_0.$$

A function v is said to be *negative-definite* if $-v$ is positive-definite.

A continuous nonnegative function $v(t, x)$ is said to be *decrescent* if there exists a positive-definite function $u(x)$ such that

$$v(t, x) \le u(x) \quad \text{for all} \quad t \ge t_0.$$

It is said to be *radially unbounded* if

$$\inf_{t \geq t_0} v(t,x) \to \infty \quad (|x| \to \infty).$$

Every positive-definite function that is independent of t is also decrescent.

The so called direct or second method, developed by Lyapunov, gives sufficient conditions to determine stability without solving explicitly the equation (2.1).

Theorem 2.1. *a) If there exists a positive-definite function $v(t,x)$ with continuous first partial derivatives such that the derivative formed along the trajectories of*

$$\dot{X}_t = f(t, X_t), \quad t \geq t_0, \quad f(t,0) \equiv 0,$$

satisfies the inequality

$$\dot{v}(t,x) = \frac{\partial v}{\partial t} + \sum_{i=1}^{d} \frac{\partial v}{\partial x_i} f_i(t,x) \leq 0$$

in a half-cylinder

$$\{(t,x) : t \geq t_0, |x| \leq h\}$$

then the zero solution of the differential equation is stable.
b) If there exists a positive-definite decrescent function $v(t,x)$ such that $\dot{v}(t,x)$ is negative-definite then the zero solution is asymptotically stable.
c) If the assumptions of a) and b) hold for all x and $v(t,x)$ is radially unbounded, then the zero solution is globally asymptotically stable.

A function $v(t,x)$ that satisfies the stability conditions of Theorem 2.1 is said to be a *Lyapunov function* corresponding to the differential equation in question.

2.2 Stability of stochastic systems

Now we report some definitions and notions on the stability properties of a stochastic system that we will use in Section 5.3.

Assumptions 2.1. Let us consider the stochastic differential equation

$$dX_t = f(t, X_t)dt + G(t, X_t)dW_t, \qquad X_{t_0} = c, \quad t_0 \leq t \leq T < \infty, \tag{2.3}$$

where W_t is an $\mathbb{R}^m$-valued Wiener process [6, Chapter 4] defined on a stochastic basis $(\Omega, \mathcal{F}, \{\mathcal{F}_t\}, \mathbb{P})$, and c is a random variable independent of $W_t - W_{t_0}$, for $t \geq t_0$; moreover the $\mathbb{R}^d$ valued function $f(t, x)$ and the ($d \times m$ matrix)-valued function $G(t, x)$ are defined and measurable on $[t_0, T] \times \mathbb{R}^d$.

Now let us assume that (2.3) satisfies the assumptions of the existence-and-uniqueness Theorem [6, Theorem 6.2.1] and has continuous coefficients with respect to t.

Then, in accordance with [6, Theorem 9.3.1], corresponding to every c that is independent of W, there exists a *unique global solution* $X_t = X_t(c)$ on $[t_0, \infty)$ which represents a d-dimensional diffusion process with drift vector $f(t, x)$ and diffusion matrix $B(t, x) = G(t, x)G(t, x)^T$. Moreover let us assume that c is a constant with probability 1, then Theorem [6, Thm. 7.1.2] implies the existence of all moments $\mathbb{E}|X_t|^k$ for $k > 0$ and also

$$\mathbb{P}(X_t \in B | X_{t_0} = c) = \mathbb{P}[X_t(c) \in B].$$

The solution beginning at the instant $s \geq t_0$ at the point x will be denoted by $X_t(s, x)$. In addition let us assume that

$$f(t, 0) = 0, \quad G(t, 0) = 0, \quad \text{for all} \quad t \geq t_0,$$

the latter ensures that the solution $X_t(0) = 0$ is the unique solution of (2.3), with initial value $c = 0$.

Now let X_t be the solution of (2.3) and let $v(t, x)$ denote a positive-definite function defined everywhere on $[t_0, \infty) \times \mathbb{R}^d$ that has continuous partial derivatives v_t, v_{x_i} and $v_{x_i x_j}$.

Then the process

$$V_t = v(t, X_t)$$

has, by Ito's theorem [6, Theorem 5.3.8], a stochastic differential. Let us consider the extension of the *infinitesimal operator* A (see [6, Section 2.4]) of X_t to all functions having continuous partial derivatives with respect to t and continuous second partial derivatives with respect to the x_i (see [6, Section 9.4]), and let us denote it with L, accordingly

$$L = \frac{\partial}{\partial t} + \mathcal{L}, \quad L \supset \mathcal{A}, \tag{2.4}$$

$$\mathcal{L} = \sum_{i=1}^{d} f_i(t,x)\frac{\partial}{\partial x_i} + \frac{1}{2}\sum_{i,j=1}^{d} \left(G(t,x)G(t,x)^T\right)_{ij} \frac{\partial^2}{\partial x_i \partial x_j} \tag{2.5}$$

then we have (see [6, Section 5.3])

$$dV_t = (Lv(t,X_t))dt + \sum_{i=1}^{d}\sum_{j=1}^{m} v_{x_i}(t,X_t)G_{ij}(t,X_t)dW_t^j.$$

Definition 2.2. Suppose that the assumptions 2.1 are satisfied. Then the zero solution is said to be *stochastically stable* (or stable with probability 1) if, for every $\varepsilon > 0$,

$$\lim_{c\to 0} \mathbb{P}\left[\sup_{t_0 \le t < \infty} |X_t(c)| \ge \varepsilon\right] = 0.$$

Otherwise, it is said to be *stochastically unstable*. The zero solution is said to be *stochastically asymptotically stable* if it is stochastically stable and

$$\lim_{c\to 0} \mathbb{P}\left[\lim_{t\to\infty} X_t(c) = 0\right] = 1.$$

The zero solution is said to be *stochastically asymptotically stable in the large* if it is stochastically stable and

$$\mathbb{P}\left[\lim_{t\to\infty} X_t(c) = 0\right] = 1$$

for all $c \in \mathbb{R}^d$.

Now let us assume that

$$Lv(t, X_t) \leq 0 \quad \text{for all} \quad t \geq t_0, \quad x \in \mathbb{R}^d, \tag{2.6}$$

this condition represents the stochastic analogue of the requirement that $\dot{v} \leq 0$ in the deterministic case and it reduces to that case if G vanishes. We shall refer to $v(t, X_t)$ as a *Lyapunov function* corresponding to the stochastic differential equation (2.3).

Through (2.6) it is easy to see that V_t is a (positive) supermartingale, i.e.

$$\mathbb{E}(V_t|\mathcal{F}_s) \leq V_s,$$

and by the supermartingale inequality to prove the following theorem (see [6] and [37] for a detailed proof).

Theorem 2.2. *Suppose that the assumptions 2.1 are satisfied.*
a) Suppose that there exists a positive-definite function $v(t, x)$ defined on a half-cylinder $[t_0, \infty) \times U_h$, $U_h = \{x : |x| < h\}$ where $h > 0$, that is everywhere, with the possible exception of the point $x = 0$, continuously differentiable with respect to t and twice continuously differentiable with respect to the components x_i of x.

Furthermore

$$Lv(t, x) \leq 0, \quad t \geq t_0, \quad 0 < |x| \leq h,$$

whith L as in (2.4). Then the zero solution of (2.3) is stochastically stable.

b) If, an addition, $v(t, x)$ is decrescent and $Lv(t, x)$ is negative-definite, then the zero solution is stochastically asymptotically stable. In both cases,

$$\mathbb{P}\left[\sup_{t \geq s} v(t, X_t(s, x)) \geq \varepsilon\right] \leq \frac{v(s, x)}{\varepsilon}, \quad \varepsilon > 0, \quad s \geq t_0.$$

c) If the assumptions of part b) hold for a radially unbounded function $v(t, x)$ defined everywhere on $[t_0, \infty) \times \mathbb{R}^d$, then the zero solution is stochastically asymptotically stable in the large.

Remark 2.1. A sufficient condition for negative-definiteness of Lv is the existence of a constant $k > 0$ such that

$$Lv(t, x) \leq -k\, v(t, x).$$

Remark 2.2. For an autonomous equation

$$dX_t = f(X_t)dt + G(X_t)dW_t, f(0) = 0, \quad G(0) = 0,$$

it is sufficient to consider a function $v(t, x) \equiv v(x)$ that is independent of t.

Khas'minskiy [52] has shown that the existence of a Lyapunov function $v(x)$ is a necessary condition for stochastic stability as long as the equation is "nondegenerate" on U_h, that is, as long as the smallest eigenvalue of $G(x)G(x)^T$ is greater than $k(x)$, with $k(x) > 0$ for $x \in U_h$. Under the condition of non-degenerate equation stochastic stability implies stochastic asymptotic stability.

Chapter 3

Individual-based SIS epidemic models on graphs

3.1 Introduction

Individual-based network models fall in two broad categories. First, theoretical network models that focus on understanding the impact of particular network metrics on outbreak threshold, final epidemic size and the efficacy of control measures (Keeling 1999, 2005; Kiss et al. 2005, 2008; May and Lloyd 2001, Wang et al., 2003, Ganesh et al., 2005, Van Mieghem2009), and that are used to establish some general principles. Second, those where network data is available and can be used to specify the contact network (Dent et al. 2008; Green et al. 2006; Kao et al. 2006; Kiss et al. 2006a). The latter are driven, at least partially, by the real-time predictive modelling of human (SARS, Hufnagel et al. 2004; Lipsitch et al. 2003; Meyers et al. 2005; and the current swine-flu outbreak, Smith et al. 2009) and animal disease outbreaks (foot-and-mouth disease, Ferguson et al. 2001; Kao et al. 2006; Avian Influenza, Dent et al. 2008) [85].

3.2 Individual-based SIS mean-field model

We introduce the susceptible–infected–susceptible (SIS) process spreading on an undirected graph $G = (V, E)$, where the cardinality of the node set V is N. In the SIS model an individual-node can be repeatedly infected, recover and yet be infected again. i.e a recovered node does not receive immunity and it is immediately susceptible to a new infection.

In our model the viral state of a node i, at time t, is described by a Bernoulli random variable $X_i(t)$, where we set $X_i(t) = 0$, if i is healthy, and $X_i(t) = 1$, if i is infected. Every node at time t is either infected with probability $p_i(t) = \mathbb{P}(X_i(t) = 1)$ or healthy (but susceptible) with probability $1 - p_i(t) = \mathbb{P}(X_i(t) = 0)$.
In the homogeneous setting we consider the curing (or recovery) process as a Poisson process with rate δ, that does not depend on the viral state of the neighbours of an infected node. Also, the infection process is a Poisson process with a rate β *per link* between an healthy and an infected node.

Clearly, the stochastic transition towards the infective state of a susceptible node, depends on the state of all its neighbours. All the infection and curing processes are independent, thus they compete for the production of an event (infection or recovery) [20, Chapter 8].

The state of the collective system of all nodes, i.e. the state of the network, is actually the joint state of all the nodes' state [81].

Since we assume that the infection and curing processes are of Poisson type, the SIS process, developing on a graph with N nodes, can be modeled as a continuous-time Markov process with 2^N states, covering all possible combinations in which N nodes can be infected [95, 97].

The transmission dynamics on the network can be formulated in terms of a transition matrix between all possible states. In the case of continuous time, this matrix, known as the infinitesimal generator [85, 51, 20], is explicitly computed for the SIS-case in e.g. [85, 95, 81]. Based on the infinitesimal

generator, we can write down the Kolmogorov's differential equations (i.e. a system of linear differential equations) that uniquely determine the probability of the process of being in a certain state [20]. However the number of equations increases exponentially with the number of nodes; this poses several limitations in order to determines the set of solutions even for small network order. Hence, often, it is necessary to derive models that are an approximation of the original one [85]. For a special class of graphs it is possible to reduce the number of states (i.e. number of equations) in the Markov chain and derive models that are either equivalent to the original system, but this is not generally the case (see [85]).

A direct approach for deriving an approximate model is to use a node level description of the underlying stochastic process, as proposed recently in [81], and then, through a mean-field approximation, passing from the linear differential equations of the exact Markov process, to a reduced set of non-linear differential equations.

The epidemic mean-field model in [81], where nodes can be in one of several states (or compartments), is a generalization of the *N-intertwined mean-field approximation* (NIMFA) proposed for the SIS model in [95].

The idea is to describe the node state $X_i(t + \Delta t)$ given the network state $X(t)$ at time t. Indeed, the spreading process is fully described if the probability for a node i to move from a state to the other, conditioned on the network state $X(t)$, is known for all i's [81].

Thus, since in Poisson processes the probability that q events occur in a time interval dt is in the order of $o(dt^q)$, we can write the probability of having an infection during the time interval $(t, t + dt]$ as

$$\mathbb{P}\left(X_i(t + dt) = 1 | X_i(t) = 0, X_{-i}(t)\right) = \beta \sum_{k=1}^{N} a_{ik} X_k(t) dt + o(dt),$$

considering that the sum of independent Poisson process is also a Poisson process with rate equal to the sum of the individual rates [20, Theorem 1.2].

Moreover, the probability to have no a transition from the infected state,

in the time interval $(t, t+dt]$, is

$$\mathbb{P}\left(X_i(t+dt)=1|X^i(t)t=1, X_{-i}(t)\right)=1-\delta dt+o(dt).$$

Thus we have

$$\mathbb{P}\left(X_i(t+\Delta t)=1|X_i(t), X_{-i}(t)\right)=(1-X_i(t))\left(\beta\sum_{k=1}^{N}a_{ik}X_k(t)dt\right)$$

$$+X_i(t)\left(1-\delta dt\right)+o(dt) \tag{3.1}$$

Now, by (3.1), and taking into account that $X_i(t)$ is a Bernoulli variable, we can compute the conditional expectation of $X_i(t+dt)$ w.r.t $X_i(t)$ and $X_{-i}(t)$

$$\mathbb{E}\left[X_i(t+dt)|X_i(t), X_{-i}(t)\right]=(1-X_i(t))\beta\sum_{k=1}^{N}a_{ik}X_k(t)dt-X_i(t)\delta dt+o(dt). \tag{3.2}$$

Computing the expected value of each side of (3.2), by the law of iterated expectations, we get

$$\mathbb{E}\left[X_i(t+dt)\right]=\beta\sum_{k=1}^{N}a_{i,k}\mathbb{E}\left[X_k(t)\right]+\beta\sum_{k=1}^{N}a_{i,k}\mathbb{E}\left[X_i(t)X_k(t)\right]dt-\mathbb{E}\left[X_i(t)\right]\delta dt+o(dt)$$

After dividing both members by dt and letting $dt\to 0$, we obtain

$$\frac{d\mathbb{E}(X_i(t))}{dt}=\mathbb{E}\left((1-X_i(t))\beta\sum_{k=1}^{N}a_{ik}X_k(t)-\delta X_i(t)\right),$$

whence

$$\frac{d\mathbb{E}(X_i(t))}{dt}=\beta\sum_{k=1}^{N}a_{ik}\mathbb{E}(X_k(t))-\beta\sum_{k=1}^{N}a_{ik}\mathbb{E}\left(X_i(t)X_k(t)\right)-\delta\mathbb{E}(X_i(t)) \tag{3.3}$$

The system given by (3.3) is not closed since it contains a new variable, that is the joint expectation $\mathbb{E}\left(X_i(t)X_k(t)\right)$. There are two ways to proceed.

First, we can derive the differential equations for each two-pair probabilities, followed by higher order joint probabilities until all 2^N SIS linear Markov equations, but again for large values of N, the system is neither analytically nor computationally tractable. Second, one can provide an approximation for the joint expectation in terms of $X_i(t)$ and $X_j(t)$ (i.e a pair approximation, or first-order approximation) [79, 49, 85, 81]. The simplest closing relation is based on the assumption of the absence of correlation between the infectious states of two nodes in the network, whence

$$\mathbb{E}\left(X_i(t)X_k(t)\right) = \mathbb{E}(X_i(t))\mathbb{E}(X_i(t)).$$

Applying this relation in (3.3), and taking into account that $X_i(t)$ is a Bernoulli random variable, thus $\mathbb{P}(X_i(t) = 1) = \mathbb{E}(X_i(t))$, we obtain the following first-order mean-field equation, for each node i in the network

$$\frac{dp_i(t)}{dt} = (1 - p_i(t))\beta \left(\sum_{j=1}^{N} a_{ij} p_j(t) \right) - \delta p_i(t),\ i = 1, \ldots, N. \tag{3.4}$$

The equation (3.4) is the same derived by means of the N-intertwined mean-field approximation (NIMFA) in [95].

Through the thesis, we shall refer to the system of differential equations (3.4) as the NIMFA system. The following matrix representation of (3.4) holds

$$\frac{dP(t)}{dt} = \beta A P(t) - \operatorname{diag}(p_i(t))(\beta A P(t) + \delta u), \tag{3.5}$$

where $P(t) = (\, p_1(t)\, p_2(t) \ldots p_N(t)\,)^T$, $\operatorname{diag}(p_i(t))$ is the diagonal matrix with elements $p_1(t), p_2(t), \ldots, p_N(t)$ on the diagonal, and u is the all-one vector. From (3.5), considering $P(t) = \operatorname{diag}(p_i(t))u$, we can write

$$\begin{aligned} \frac{dP(t)}{dt} &= \beta A P(t) - \delta \operatorname{diag}(p_i(t))u - \operatorname{diag}(p_i(t))\beta A P(t) \\ &= (\beta A - \delta I)P(t) - \beta \operatorname{diag}(p_i(t))AP(t). \end{aligned} \tag{3.6}$$

3.3 Epidemic threshold and long term prediction

For a network with finite order N, the exact SIS Markov process will always converge towards its unique absorbing state, that is the zero-state where all nodes are healthy. The other states form a transient class, from which one can reach the zero-state with positive probability. Transitions from the zero-state have zero probability and the probability that the process is in a transient state exponentially tends to zero with time [93], hence the stochastic model predicts that the virus will disappear from the network [75].

However the waiting time to absorption is a random variable whose distribution depends on the initial state of the system, on the parameters of the model and on the size of the population[65, 66]. In fact there is a critical value τ_c of the effective spreading rate $\tau = \beta/\delta$, whereby if τ is distinctly larger than τ_c the time to absorption grows exponentially in N, while for τ distinctly less than τ_c the lifetime of epidemic is rather small [65, 36].

The critical value τ_c is often called the *epidemic threshold* [95, 7, 28, 70].

Thus, above the threshold, a typical realization of the epidemic process may experience a very long waiting time before absorption to the zero-state. During such waiting time, the distribution of the number of infected individuals is close to the distribution of the same random variable under the condition that extinction has not occurred, the so-called *quasi-stationary distribution* [31, 65, 66].

The quasi-stationary distribution can be regarded as a limiting conditional distribution (quasi-limiting distribution), useful in representing the long-term behavior of the process before it evanesces [74, 75]. For a rich bibliography on quasi-stationary distribution see [74].

The exact computation of the exact quasi-stationary distribution is not analytical tractable, as it is showed in [65], hence it is important to consider an approximation of it. It is usual to consider two type of approximating

processes, both lack absorbing states. Therefore they have non-degenerate stationary distributions and these can be solved for explicitly. One possible approximation is to consider an SIS model with one permanently infected individual, another one is to consider a model with the origin removed, by not allowing the last infected individual to cure [65]. Recently, also models that include the possibility of a nodal self-infection are introduced in literature [46, 93]. Basically, besides receiving the infection from an infected neighbor, an individual can also itself produce a virus with rate a. For $a = 0$, the model corresponds to the classical SIS. The addition of a nodal infection component derive from the analogy of epidemics with information spread in social networks, where individuals can generate themselves information. This model has no absorbing state because if all individuals are healthy, the network does not permanently remain healthy but gets infected with rate Na [93]. In literature this type of model is called the SISa model in [46] or even the ε-SIS model in [93]. Along the thesis we shall refer to it as the a-SIS model.

Even so numerical simulations of SIS processes reveal that, already for reasonably small networks ($N \geq 100$) and when $\tau > \tau_c$, the overall-healthy state is only reached after an unrealistically long time. Hence, the indication of the model is that, in the case of real networks, one should expect that the extinction of epidemics is hardly ever attained [90, 33]. For this reason the literature is mainly concerned with establishing the value of the epidemic threshold, being a key parameter behind immunization strategies related to the network protection against viral infection.

For an SIS process on graphs, τ_c depends on the spectral radius $\lambda_1(A)$ of the adjacency matrix A [99, 95]. NIMFA determines the epidemic threshold for the effective spreading rate as

$$\tau_c^{(1)} = \frac{1}{\lambda_1(A)}, \tag{3.7}$$

where the superscript (1) refers to the first-order mean-field approxima-

tion [95, 91]. In Theorem 3.1, we report the analysis of the global dynamics of the model, carried out in [17], that give us an alternative way for identifying the epidemic threshold, studying also the stability properties of the NIMFA system.

However, with respect to the exact Markovian SIS model, due to the assumption of independence, NIMFA yields an upper bound for the probability of infection of each node, as well as a lower bound for the epidemic threshold, i.e., $\tau_c = \alpha\tau_c^{(1)}$ with $\alpha \geq 1$. This fact has been rigorously shown in [25], providing that the state of nodes are non-negatively correlated.

Thus, from the application standpoint, a key issue is to determine for which networks of given order NIMFA performs worst, meaning that $\alpha = \frac{\tau_c}{\tau_c^{(1)}}$ is largest.

First one can observe that, basically, NIMFA replaces the actual random infection rate for the node i, $\beta \sum_{i=1}^{N} a_{ij} X_j(t)$ (where the sum is done on all the neighbor nodes), by its average rate $\beta \sum_{i=1}^{N} a_{ij} \mathbb{E}[X_j(t)]$. If the states of the nearest nodes are sufficiently weakly dependent, and the the degree of node i (i.e. the number of neighbours of node i) is large enough so that the Lindberg's Central Limit Theorem [34] is applicable, then such replacement results in a good approximation. Informally, we can say that the mean-field approximation holds if in the underlying network, the degree of the nodes increase as the number of nodes N tends to infinity [97].

Moreover, evaluations on the variance of $\beta \sum_{i=1}^{N} a_{ij} X_j(t)$ in [95], shows that the deviations between the NIMFA model and the exact SIS are largest for intermediate values of τ, i.e. we expect large deviations in some τ-region around the exact τ_c.

A more accurate lower bound (the second order mean-field threshold) $\tau_c \geq \tau_c^{(2)} \geq \tau_c^{(1)}$ has been derived in [24], even if they found that this second-order approximation is not always possible: the network size N should be large enough. Further efforts have been made to satisfactorily quantify the

accuracy of the first-order meanfield approximation (see [97]).

Stability properties of the mean-field equation

In the NIMFA model, when $\tau > \tau_c^{(1)}$, a limiting occupancy probability appears as the second constant solution* of the non-linear system (3.5) which exists, apart from the zero-vector solution. Such non-zero steady-state reflects well the observed viral behavior [92]: it can be seen as the analogous of the quasi-stationary distribution of the exact stochastic SIS model.

Now we report the analysis of the global dynamics of the the NIMFA equation (3.6) that we have studied in [17].

We clearly study the system for $(p_1, \ldots, p_N) \in I_N = [0,1]^N$. It can be shown that the system (3.6) is positively invariant in I_N, i.e. if $P(0) \in I_N$ then $P(t) \in I_N$ for all $t > 0$ [54, Lemma 3.1].

The analysis of the global dynamics of (3.6) leads to identify the epidemic threshold $\tau_c^{(1)}$. We shall prove this, in Thm 3.1, by studying the stability of the equilibrium points of (3.6), that are solutions of the equation

$$P = \frac{\beta}{\delta}(I - \mathrm{diag}(p_i))AP. \tag{3.8}$$

To this aim we shall adapt the results in [54] to our individual-based SIS model. Let us denote by f the right hand side of (3.6), i.e., (3.6) can be re-written as a vector-valued differential equation

$$\frac{dP}{dt} = f(P), \tag{3.9}$$

where $f : [0,1]^N \to \mathbb{R}^N$ is a C^∞ function. Let $P_0 = 0$ be the vector of all zero components, one can easily check that P_0 is an equilibrium point of the system (3.9), i.e. $f(P_0) = 0$.

*We remember that all bounded trajectories of an autonomous first-order differential equation tend to an equilibrium, i.e., to a constant solution of the equation.

Theorem 3.1. *If $\tau \leq 1/\lambda_1(A)$ then P_0 is a globally asymptotically stable equilibrium of (3.6).*
If $\tau > 1/\lambda_1(A)$, P_0 is unstable and there exists another equilibrium point P_∞ that is globally asymptotically stable in $I_N - \{0\}$.

Proof. We can rewrite the system (3.9) in the following form (see [72, p. 108])

$$\dot{P} = D_f P + F(P), \tag{3.10}$$

where D_f is the Jacobian matrix of f at P_0 and $F(P)$ is a column vector whose i-th component is $-\beta \sum_{j=1}^{N} a_{ij} p_i p_j$.

From (3.6) we have

$$(Df(P_0))_{ij} = \begin{cases} \beta a_{ij} & i \neq j \\ -\delta & i = j \end{cases}$$

that is $D_f = \beta A - \delta I$. Since adjacency matrix A is real and symmetric its eigenvalues are real. Hence, the eigenvalues of D_f are real as well and of the form

$$\lambda_i(D_f) = \beta \lambda_i(A) - \delta.$$

In particular, let $\lambda_1(D_f) = \max_i \lambda_i(D_f)$, since the spectral radius of A is positive we have

$$\lambda_1(D_f) = \beta \lambda_1(A) - \delta.$$

Now we can apply [54, Thm. 3.1] to the system (3.10) and assert that when $\lambda_1(D_f) \leq 0$, i.e., $\tau \leq 1/\lambda_1(A)$, P_0 is a globally asymptotically stable equilibrium of (3.6).

Conversely, if $\lambda_1(D_f) > 0$, i.e. $\tau > 1/\lambda_1(A)$, there exists another equilibrium point P_∞. P_0 and P_∞ are the only equilibrium points in I_N and P_∞ is globally asymptotically stable in $I_N - \{0\}$.

Finally, since $\tau > 1/\lambda_1(A)$, we have $\lambda_1(D_f) > 0$. From Lyapunov's Linearization (or First) Method, it follows that P_0 is an unstable equilibrium point in I^N. □

Chapter 4

Community networks

4.1 Introduction

In this chapter we consider that the entire population is partitioned into communities (also called households, clusters, subgraphs, or patches). There is an extensive literature on the effect of network community structure on epidemics arising due to, for example, geographic separation. Models utilizing this structure are commonly known as *metapopulation models* (see, e.g., [43, 58, 4]). Such models assume that each community shares a common environment or is defined by a specific relationship. This framework captures the most salient structural inhomogeneity in contact patterns in many applied contexts [9].

In literature some of the most common works on metapopulation regard population divided into households, that consider two level of mixing ([10, 80, 11]. This models typically assume that contacts, and consequently infections, between individual in the same group occur at a higher rate than those between individual in different groups [9]. Moreover they define groups in terms of spatial proximity, considering the between-group contact rates (and consequently the infection rates) depending in some way on spatial distance, so that, each individual can be theoretically infected by each of the other individual.

However an underlying network contact structure may provide a more realistic approach for the study of the evolution of the epidemics, where infection can only be transmitted by individual directly linked by an edge [9]. Thus, an important challenge is to consider a realistic underlying structure to appropriately incorporate the influences of the topology of the network on the dynamics of epidemics [71, 12, 35, 13].

To this aim, in [17, 16] we have analyzed the dynamics of epidemics on networks that are partitioned into local communities, through the first-order mean-field approximation discussed in Chapter 3.

Our investigation has been based on the graph-theoretical notion of *equitable partition* [83, 39, 64] and of its recent and rather flexible generalization, that of *almost equitable partition* [22, 64]. The gross structure of hierarchical networks of this kind can be described by a *quotient graph*. The rationale of our approach was that individuals infect those belonging to the same community with higher probability than individuals in other communities. Thus, the nodal infection probability is expected to depend mainly on the interaction of a few, large interconnected clusters. We refers to such model also as *two-scale community model*.

Several authors also account for the effect of migration between communities [44, 27, 73]. Conversely, the model we are interested in suits better for the manmade architecture or stable social communities, which do not change during the infection period; hence we do not consider migration.

We shall report our results in the next section.

4.2 Equitable partitions

Let us consider the diffusion of epidemics over a simple graph $G = (V, E)$. We are interested in the case of networks that can be naturally partitioned into n communities: they are represented by a node set partition

$\pi = \{V_1, ..., V_n\}$, i.e., a sequence of mutually disjoint nonempty subsets of V, called cells, whose union is V.

The epidemic process is described through the first-order mean-field approximation NIMFA, described in Section 3.2. Compared to the homogeneous case where the infection rate is the same for all pairs of nodes, here we consider two infection rates: the *intra-community* infection rate β for infecting individuals in the same community and the *inter-community* infection rate $\varepsilon\beta$ i.e., the rate at which individuals among different communities get infected. We assume $0 < \varepsilon < 1$, the customary physical interpretation being that infection across communities occurs at a much smaller rate. Clearly the model can be extended to the case $\varepsilon \geq 1$.

The partition of the node set that we consider is *equitable*. First of all this means that all nodes belonging to the same community have the same internal degree: formally the subgraph G_i of G induced by V_i is regular for all i's (recall that $\pi = \{V_1, ..., V_n\}$ is a partition of the node set V, which is assumed to be given a priori). Furthermore, for any two subgraphs G_i, G_j, whenever there exists at least one connection between two nodes, one belonging to the first subgraph and the other to the second, then each node in G_i is connected with the same number of nodes in G_j (see as example 4.1).

In Section 4.4 we extend the study to the case of *almost equitable partitions* that does not require any specific structural condition inside each G_i.

Such network structure can be used for those models consisting of multiple smaller subpopulations (households, workplaces, classes in a schools) representing the internal structure of each community by a complete graph. This assumption appears natural because members of a small community usually know each other. Moreover we can consider that, given two connected communities, all of their individual are mutually linked, indeed each member of those two communities may potentially come into contact.

Furthermore such network structure can be observed, e.g., in the archi-

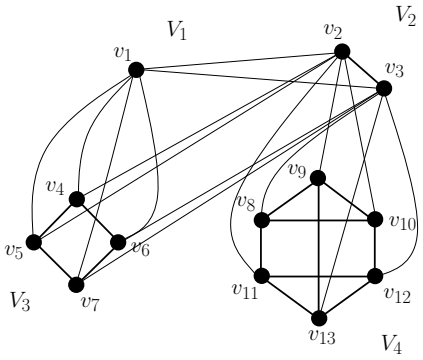

Figure 4.1: A sample graph with equitable partition $V = \{\{v_1\}, \{v_2, v_3\}, \{v_3, v_4, v_5, v_6\}, \{v_7, v_8, v_9, v_{10}, v_{11}, v_{12}, v_{13}\}\}$.

tecture of some computer networks where clusters of clients connect to single routers, whereas the routers' network has a connectivity structure with nodes' degree constrained by the number of ports. Also, graphs representing multi-layer networks may be characterized using equitable and almost equitable partitions [82].

The original definition of equitable partition is due to Schwenk [83].

Definition 4.1. Let $G = (V, E)$ be a graph. The partition $\pi = \{V_1, ..., V_n\}$ of the node set V is called *equitable* if for all $i, j \in \{1, \ldots, n\}$, there is an integer d_{ij} such that

$$d_{ij} = \deg(v, V_j) := \#\left\{e \in E : e = \{v, w\}, w \in V_j\right\}.$$

independently of $v \in V_i$.

We shall identify the set of all nodes in V_i with the i-th *community* of the whole population. In particular, each V_i induces a subgraph of G that is necessarily regular.

Remark 4.1. We use the notation lcm and gcd to denote the least common multiple and greatest common divisor, respectively. We can observe that the partition of a graph is equitable if and only if

$$d_{ij} = \alpha \frac{\operatorname{lcm}(k_i, k_j)}{k_i} \tag{4.1}$$

where α is an integer satisfying $1 \leq \alpha \leq \gcd(k_i, k_j)$

The macroscopic structure of such a network can be described by the *quotient graph* G/π which is a *multigraph* with cells as nodes and d_{ij} edges between V_i and V_j. For the sake of explanation, in the following we will identify G/π with the (simple) graph having the same node set, and where an edge exists between V_i and V_j if at least one exists in the original multigraph. We shall denote by B the adjacency matrix of the graph G/π.

Example 4.1. Let us assume that the adjacency matrix B of the quotient graph is given and that, for any $i, j \in \{1, \ldots, n\}$, $b_{ij} \neq 0$ implies $d_{ij} = k_j$, i.e., each node in V_i is connected with every node inside V_j. We can explicitly write a weighted adjacency matrix A in a block form. Let $C_{V_i} = (c_{ij})_{k_i \times k_i}$ be the adjacency matrix of the subgraph induced by V_i and $J_{k_i \times k_j}$ is an all ones $k_i \times k_j$ matrix; then

$$A = \begin{bmatrix} C_{V_1} & \varepsilon J_{k_1 \times k_2} b_{12} & . & . & \varepsilon J_{k_1 \times k_n} b_{1n} \\ \varepsilon J_{k_2 \times k_1} b_{21} & C_{V_2} & . & . & \varepsilon J_{k_2 \times k_n} b_{2n} \\ . & . & . & . & . \\ . & . & . & . & . \\ . & . & . & . & C_{V_n} \end{bmatrix} \tag{4.2}$$

We observe that (4.2) represents a block-weighted version of the usual adjacency matrix. The derivation of NIMFA for the case of two different infection rates, considered in this paper, results in the replacement of the unweighted adjacency matrix in the NIMFA system (3.5) with its weighted version.

4.2.1 The quotient matrix

We search for a smaller matrix Q that contains the relevant information for the evolution of the system. Such a matrix is the *quotient matrix* of the equitable partition. In Prop. 4.1 we will see that Q and A have the same spectral radii. As a consequence, we can compute the spectral radius of Q in order to estimate the epidemic threshold, instead of computing the spectral radius of matrix A.

The quotient matrix Q can be defined for any equitable partition: in view of the internal structure of a graph with an equitable partition, it is natural to consider the cell-wise average value of a function on the node set, that is to say the projection of the node space into the subspace of cell-wise constant functions.

Definition 4.2. Let $G = (V, E)$ be a graph. Let $\pi = \{V_i,\ i = 1, \dots, n\}$ be any partition of the node set V, let us consider the $n \times N$ matrix $S = (s_{iv})$, where

$$s_{iv} = \begin{cases} \frac{1}{\sqrt{|V_i|}} & v \in V_i \\ 0 & \text{otherwise.} \end{cases} \tag{4.3}$$

The *quotient matrix* of G (with respect to the given partition) is

$$Q := SAS^T.$$

Observe that by definition $SS^T = I$.

In the case of the example 4.1 the form of Q is rather simple:

$$q_{ii} = \sum_{h=1}^{k_i} \left(\frac{1}{\sqrt{k_i}}\right)^2 \sum_{k=1}^{k_i} (C_{V_i})_{kh} = \frac{1}{k_i} \sum_{h,k=1}^{k_i} (C_{V_i})_{kh}$$

and

$$q_{ij} = \frac{1}{\sqrt{k_i k_j}} \sum_{z \in V_i, l \in V_j} a_{zl} = \sqrt{k_i k_j}\varepsilon b_{ij}.$$

Hence we obtain that

$$Q = \mathrm{diag}(d_{ii}) + (\sqrt{k_i k_j}\varepsilon b_{ij})_{i,j=1,\dots n},$$

where $d_{ii} = \frac{1}{k_i} \sum_{h,k=1}^{k_i} (C_{V_i})_{kh}$ is the internal degree of the subgraph induced by V_i.

In the case of general equitable partitions, the expression for Q writes

$$Q = \mathrm{diag}(d_{ii}) + (\sqrt{d_{ij} d_{ji}}\varepsilon b_{ij})_{i,j=1,\dots n}.$$

There exists a close relationship between the spectral properties of Q and that of A. Being the order of Q smaller than that of A, a result in [39] basically shows that $\sigma(Q) \subseteq \sigma(A)$, Furthermore the following holds

Proposition 4.1. *Let $G = (V, E)$ be a graph. Let $\pi = \{V_i,\ i = 1, \ldots, n\}$ be an equitable partition of the node set V. The adjacency matrix A and the quotient matrix Q have the same spectral radius, i.e.*

$$\lambda_1(Q) = \lambda_1(A).$$

Proof. See [89, art. 62]. □

Complexity reduction.

Prop. 4.1 further details that, once the network structure is encoded in the connectivity of a quotient graph Q, then the epidemic threshold $\tau_c^{(1)}$ is expressed by the spectral radius of Q (see Section 3.3).

Now, since the order of Q is smaller than the order of A, this can provide a computational advantage. The complexity reduction can be evaluated easily, e.g, in the case of the power iteration method [62]. The power iteration method is a numerical technique for approximating a dominant eigenpair of a diagonalizable matrix L, using the following iteration

$$y^h = L\, y^{h-1}, \quad h = 1, 2, \ldots$$

for a given initial vector y^0. As the iteration step h increases, y^h approaches a vector which is proportional to a dominant eigenvector of L. If we order the eigenvalues of L such as as $|\lambda_1(L)| \geq |\lambda_2(L)| \geq \ldots \geq |\lambda_n(L)|$, the rate of convergence of the method is ruled by $|\lambda_2(L)|/|\lambda_1(L)|$.

In our case, for the Perron-Frobenius Theorem 1.1 the dominant eigenvalue $\lambda_1(A)$ is positive and by Proposition 4.1, $\lambda_1(A) = \lambda_1(Q)$. Furthermore $\sigma(Q) \subseteq \sigma(A)$, hence $\max_{i \geq 2} |\lambda_i(A)| \geq \max_{i \geq 2} |\lambda_i(Q)|$: this means that the convergence of power iteration for matrix Q is never slower than for matrix A. Finally, it is immediate that at each step the computational complexity is $O(n^2)$ for Q whereas for A it is $O(N^2)$.

4.2.2 A lower bound for the epidemic threshold

We can write $Q = D + \widehat{B}$, where $D = \mathrm{diag}(d_{ii})$ and $\widehat{B} = (\sqrt{d_{ij}d_{ji}}\varepsilon b_{ij})_{i,j=1,\dots n}$. By the Weyl's inequality [62] we have

$$\lambda_1(Q) \leq \lambda_1(D) + \lambda_1(\widehat{B}) = \max_{1\leq i\leq n} d_{ii} + \lambda_1(\widehat{B}). \tag{4.4}$$

From (3.7) and by Proposition 4.1

$$\tau_c^{(1)} = 1/\lambda_1(A) = 1/\lambda_1(Q),$$

thus a lower bound for the epidemic threshold can be derived from (4.4)

$$\tau_c^{(1)} \geq \tau^\star = \min_i \frac{1}{d_{ii} + \lambda_1(\widehat{B})}, \tag{4.5}$$

Moreover let us note that $\lambda_1(\widehat{B}) \leq \max_i \sum_j \hat{b}_{ij}$ [63, pp 24-26], hence

$$\tau_c^{(1)} \geq \frac{1}{\max_i(d_{ii} + \sum_j \hat{b}_{ij})}. \tag{4.6}$$

In applications, when designing or controlling a network, τ^* (or the more conservative bound in (4.6)) can be adopted to determine a safety region $\{\tau \leq \tau^\star\}$ for the effective spreading rate that guarantees the extinction of epidemics.

Figure 4.2 reports on the comparison of the lower bound and the actual threshold value: it refers to the case of a sample equitable partition composed of interconnected rings for increasing values of the community order.

We observe that obtaining a lower bound for $\tau_c^{(1)}$ is meaningful because $\tau_c^{(1)}$ is itself a lower bound for the epidemic threshold τ_c of the exact stochastic model, i.e., $\tau_c = \alpha\tau_c^{(1)}$ with $\alpha \geq 1$, as anticipated in Sec. 3.3. In fact, smaller values of the effective spreading rate τ, namely $\delta > \beta/\tau_c^{(1)}$, correspond, in the exact stochastic model, to a region where the infectious dies out exponentially fast [55]. By forcing the effective spreading rate below τ^*, one ensures that the epidemic will go extinct in a reasonable time frame (we recall that, above the threshold, the overall-healthy state is only reached after an unrealistically long time).

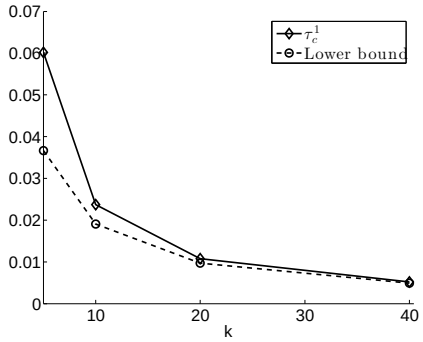

Figure 4.2: Lower bound (4.5) versus epidemic threshold: comparison for different values of k in a 40-communities network. The internal structure of each community is a ring and $d_{ij} = 2$ for all $i, j = 1, \ldots, n$.

Equality can be attained in (4.5): consider for instance the graph described by the adjacency matrix A in (4.2). Furthermore, we may require that all V_i's have the same number of nodes $k_i = k$ and same internal degree $d_{ii} = d$, $i = 1, \ldots, n$. In this case $Q = d\,\mathrm{Id}_n + \widehat{B}$, where $\widehat{B} := (k\varepsilon b_{ij})_{i,j=1,\ldots n}$, and

$$\lambda_1(Q) = d + k\varepsilon\lambda_1(B),$$

which is the exact value of $\lambda_1(A)$ and consequently of $\tau_c^{(1)}$.

Remark 4.2. Let us underline that if we remove edges between the communities, or inside the communities, in a network whose set nodes has an equitable partition, the lower bound (4.5) still holds. This because the spectral radius of an adjacency matrix is monotonically non increasing under the deletion of edges.

4.3 Infection Dynamics for Equitable Partitions

Now we show under which conditions matrix Q can be used in order to express the epidemic dynamics introduced in (3.6). This allows us to describe

the time-change of the infection probabilities by a system of n differential equations instead of N.

Theorem 4.1. *Let $G = (V, E)$ be a graph and $\pi = \{V_j,\ j = 1, \dots, n\}$ an equitable partition of the node set V. Let G_j be the subgraph of $G = (V, E)$ induced by cell V_j. If $p_h(0) = p_w(0)$ for all $h, w \in G_j$ and for all $j = 1, \dots, n$, then $p_h(t) = p_w(t)$ for all $t > 0$. In this case we can reduce the number of equations representing the time-change of infection probabilities using the quotient matrix Q.*

Proof. Let $\overline{p}_j(t) = \frac{1}{k_j} \sum_{h \in G_j} p_h(t)$ be the average value of the infection probabilities at time t of nodes in G_j. Then starting from (3.6), we can write a new system of differential equations

$$\frac{d\left(p_h(t) - \overline{p}_j(t)\right)}{dt} = -\delta(p_h(t) - \overline{p}_j(t)) + \beta(1 - p_h(t)) \sum_{z=1}^{N} a_{hz} p_z(t) - \frac{1}{k_j} \beta \sum_{l \in G_j} (1 - p_l(t)) \sum_{z=1}^{N} a_{lz} p_z(t), \qquad \forall h \in G_j, \quad j = 1, \dots, n \tag{4.7}$$

From (4.7) we have

$$\frac{d\left(p_h(t) - \overline{p}_j(t)\right)}{dt} = -\delta(p_h(t) - \overline{p}_j(t)) + \beta \left(\sum_{m=1}^{n} \sum_{z \in G_m} a_{hz} p_z(t) - \frac{1}{k_j} \sum_{l \in G_j} \sum_{m=1}^{n} \sum_{z \in G_m} a_{lz} p_z(t) \right) - \beta \left(p_h(t) \sum_{m=1}^{n} \sum_{z \in G_m} a_{hz} p_z(t) - \frac{1}{k_j} \sum_{l \in G_j} p_l(t) \sum_{m=1}^{n} \sum_{z \in G_m} a_{lz} p_z(t) \right),$$

that can be written as

$$\frac{d\left(p_h(t) - \overline{p}_j(t)\right)}{dt} = -\delta(p_h(t) - \overline{p}_j(t)) + \beta \left(\frac{1}{k_j} \sum_{l \in G_j} \sum_{m=1}^{n} \sum_{z \in G_m} (a_{hz} - a_{lz})\, p_z(t) \right) - \beta \frac{1}{k_j} \sum_{l \in G_j} \sum_{m=1}^{n} \sum_{z \in G_m} (a_{hz} p_h(t) - a_{lz} p_l(t))\, (p_z(t) - \overline{p}_m(t)) - \beta \frac{1}{k_j} \left(\sum_{l \in G_j} \sum_{m=1}^{n} \sum_{z \in G_m} (a_{hz} p_h(t) - a_{lz} p_l(t)) \right) \overline{p}_m(t).$$

Whence, since $\sum_{z\in G_m} a_{hz} = d_{jm}$, for $h \in G_j$ and for all $m = 1, \ldots, n$, we have

$$\begin{aligned}\frac{d\left(p_h(t) - \overline{p}_j(t)\right)}{dt} = &- \left[\sum_{m=1}^{n} \beta d_{jm}\overline{p}_m(t) + \delta\right](p_h(t) - \overline{p}_j(t)) \\ &+ \beta\frac{1}{k_j}\sum_{l\in G_j}\sum_{m=1}^{n}\sum_{z\in G_m}(a_{hz} - a_{lz})\,p_z(t) \\ &- \beta\frac{1}{k_j}\sum_{l\in G_j}\sum_{m=1}^{n}\sum_{z\in G_m}(a_{hz}p_h(t) - a_{lz}p_l(t))\,(p_z(t) - \overline{p}_m(t)).\end{aligned} \tag{4.8}$$

Now, we note that

$$-\frac{1}{k_j}\sum_{l\in G_j}\sum_{m=1}^{n}\sum_{z\in G_m}(a_{hz}p_h(t) - a_{lz}p_l(t))\,(p_z(t) - \overline{p}_m(t))$$

can be written as

$$-\frac{1}{k_j}\sum_{l\in G_j}\sum_{m=1}^{n}\sum_{z\in G_m}\left((p_h(t) - \overline{p}_j(t))a_{hz} - (p_l(t) - \overline{p}_j(t))a_{lz}\right)(p_z(t) - \overline{p}_m(t))$$

$$-\frac{1}{k_j}\sum_{l\in G_j}\sum_{m=1}^{n}\sum_{z\in G_m}\overline{p}_j(t)(a_{hz} - a_{lz})\,(p_z(t) - \overline{p}_m(t))\,,$$

whence we can rewrite (4.8) as

$$\begin{aligned}\frac{d\left(p_h(t) - \overline{p}_j(t)\right)}{dt} = &- \left[\sum_{m=1}^{n} \beta d_{jm}\overline{p}_m(t) + \delta\right](p_h(t) - \overline{p}_j(t)) \\ &+ \beta\frac{1}{k_j}\sum_{l\in G_j}\sum_{m=1}^{n}\sum_{z\in G_m}(a_{hz} - a_{lz})\,(p_z(t) - \overline{p}_m(t) + \overline{p}_m(t)) \\ &- \beta\frac{1}{k_j}\sum_{l\in G_j}\sum_{m=1}^{n}\sum_{z\in G_m}\left((p_h(t) - \overline{p}_j(t))a_{hz} - (p_l(t) - \overline{p}_j(t))a_{lz}\right)(p_z(t) - \overline{p}_m(t)) \\ &- \beta\frac{1}{k_j}\sum_{l\in G_j}\sum_{m=1}^{n}\sum_{z\in G_m}\overline{p}_j(t)(a_{hz} - a_{lz})\,(p_z(t) - \overline{p}_m(t))\,.\end{aligned}$$

Finally, since $\frac{1}{k_j}\sum_{l\in G_j}\sum_{m=1}^{n}\sum_{z\in G_m}(a_{hz} - a_{lz})\,\overline{p}_m(t) = 0$, we can consider

the following system

$$\frac{d\left(p_h(t)-\overline{p}_j(t)\right)}{dt} = -\left[\sum_{m=1}^{n}\beta d_{jm}\overline{p}_m(t)-\delta\right](p_h(t)-\overline{p}_j(t))$$
$$+\beta\frac{1}{k_j}\sum_{l\in G_j}\sum_{m=1}^{n}\sum_{z\in G_m}(a_{hz}-a_{lz})(p_z(t)-\overline{p}_m(t))(1-\overline{p}_j(t))$$
$$-\beta\frac{1}{k_j}\sum_{l\in G_j}\sum_{m=1}^{n}\sum_{z\in G_m}((p_h(t)-\overline{p}_j(t))a_{hz}-(p_l(t)-\overline{p}_j(t))a_{lz})(p_z(t)-\overline{p}_m(t)),$$
$$\forall h\in G_j,\quad j=1,\ldots,n$$

Now let us denote by $g(t)$ the solution of (4.7), where $g:\mathbb{R}\to\mathbb{R}^N$ and consider the case where

$$p_h(0)-\overline{p}_j(0)=0,\quad \forall h\in G_j,\quad j=1,\ldots,n, \tag{4.9}$$

i.e., $p_h(0)=p_w(0)$ for all $h,w\in G_j$. Then, from (4.9), we can easily see that the identically zero function $g\equiv 0$ is the unique solution of (4.7) with initial conditions (4.9). Indeed $g\equiv 0$ means that for all $t\geq 0$, $p_h(t)=p_w(t)$ for all $h,w\in G_j$, $j=1,\ldots,n$. Moreover the vector $P(t)$ such that $p_h(t)=p_w(t)$ for all $h,w\in G_j$, $j=1,\ldots,n$, is a solution of (3.6) and it is unique in $[0,1]^N$ with respect to the initial conditions (4.9), [72, Cap. 2, Sec. 2.2]. Thus we can conclude that also $g=0$ is a unique solution of (4.7) in $[-1,1]^N$.

Basically we have shown that the following subset of I_N

$$M=\left\{P\in[0,1]^N | p_1=\ldots=p_{k_1}=\overline{p}_1, p_{k_1+1}=\ldots=p_{k_1+k_2}=\overline{p_2},\right.$$
$$\left.\ldots, p_{(k_1+..k_{n-1}+1)}=\ldots=p_N=\overline{p}_n\right\}$$

is positively invariant for the system (3.6). This allows us to reduce the system (3.6) of N differential equations and describe the time-change of the infection probabilities by a system of n equations involving the matrix Q.

Indeed, let us consider $P(0)\in M$ and $\overline{P}=(\overline{p}_1,\ldots,\overline{p}_n)$, we can write

$$\begin{aligned}\frac{d\overline{p}_j(t)}{dt} &= \beta(1-\overline{p}_j(t))\sum_{m=1}^{n}\varepsilon b_{jm}d_{jm}\overline{p}_m(t) \\ &+ \beta d_j(1-\overline{p}_j(t))\overline{p}_j(t)-\delta\overline{p}_j(t), \qquad j=1,\ldots,n\end{aligned} \tag{4.10}$$

Hence, based on Thm. 2.1 in [39], we observe that

$$q_{ij} = (k_j/k_i)^{1/2} d_{ji},$$

This relation in our case brings

$$d_{jm} = \left(\frac{k_j}{k_m}\right)^{-1/2} \frac{q_{mj}}{\varepsilon} = \left(\frac{k_j}{k_m}\right)^{-1/2} \frac{q_{jm}}{\varepsilon},$$

where the last equality holds because Q is symmetric. We can rewrite (4.10) as

$$\begin{aligned} \frac{d\overline{p}_j(t)}{dt} \quad &= \beta(1-\overline{p}_j(t)) \sum_{m=1, m\neq j}^{n} \left(\frac{k_j}{k_m}\right)^{-1/2} q_{jm} p_m(t) \\ &+\beta q_{jj}(1-\overline{p}_j(t)) p_j(t) - \delta \overline{p}_j(t); \qquad j = 1, \ldots, n \end{aligned} \tag{4.11}$$

where $q_{jj} = d_{jj} = \lambda_1(C_{V_j})$. The matrix representation of (4.11) is the following

$$\frac{d\overline{P}(t)}{dt} = \beta \left(\mathrm{I}_n - \mathrm{diag}(\overline{p}_j(t))\right) \widetilde{Q}\overline{P}(t) - \delta \overline{P}(t), \tag{4.12}$$

where $\widetilde{Q} = \mathrm{diag}\left(\frac{1}{\sqrt{k_j}}\right) Q \,\mathrm{diag}(\sqrt{k_j})$. It is immediate to observe that $\sigma(Q) = \sigma(\tilde{Q})$. □

Corollary 4.1. *When $\tau > \tau_c^{(1)}$ the non-zero steady-state P_∞ of the system (3.6) belongs to $M - \{0\}$.*

Proof. In Theorem 3.1 we have shown that when $\tau > \tau_c^{(1)}$, the system (3.6) has a globally asymptotically stable equilibrium P_∞ in $I_N - \{0\}$; hence for any initial state $P(0) \in I_N - \{0\}$

$$\lim_{t\to\infty} |P(t) - P_\infty| = 0.$$

We have proved in Thm. 4.1 that if $P(0) \in M$ then $P(t) \in M$ for all $t > 0$, thus we can conclude that P_∞ must be in $M - \{0\}$ when $\tau > \tau_c^{(1)}$. □

Basically, Corollary 4.1 says that one can compute the $n \times 1$ vector, $\overline{P}_\infty$, of the reduced system (4.12) in order to obtain the $N \times 1$ vector, P_∞, of (3.6):

indeed $p_{z\infty}, \ldots, p_{x\infty} = \overline{p}_{j\infty}$, for all $z, x \in G_j$ and $j = 1, \ldots, n$. This provides a computational advantage by solving a system of n equations instead of N. Moreover, since P_∞ is a globally asymptotically stable equilibrium in $I^N - \{0\}$, the trajectories starting outside M will approach those starting in $M - \{0\}$. The same holds clearly for trajectories starting in I^N and in M when $\tau \leq \tau_c^{(1)}$. Numerical experiments in Fig. 4.6 depict this fact.

The statements proved above can be easily verified, with a direct computation, in the simple case where the subgraphs of G, induced by each V_i, is complete, i.e., $d_{ii} = k_i - 1$ for all $i = 1, ..., n$, and all nodes belonging to two linked communities i and j are connected, i.e., $d_{ij} = k_j$ (see Section 4.3.1). Indeed for all $h, w \in G_j$, $j = 1, \ldots, n$, we have

$$\begin{aligned}\frac{d(p_h(t) - p_w(t))}{dt} = \quad & -\delta\,(p_h(t) - p_w(t)) + \beta \sum_{z \notin G_j} \left[(1 - p_h(t))a_{hz} - (1 - p_w(t))a_{wz}\right] p_z(t) \\ & + \beta \sum_{z \in G_j, z \neq h,w} \left[(1 - p_h(t))a_{hz} - (1 - p_w(t))a_{wz}\right] p_z(t) \\ & + \beta \sum_{z = h,w} \left[(1 - p_h(t))a_{hz} - (1 - p_w(t))a_{wz}\right] p_z(t) \qquad (4.13)\end{aligned}$$

Since in this special case $a_{hz} = a_{wz}$, for all $z \in V$ s.t. $z \neq h, j$, we can rewrite (4.13) as

$$\frac{d(p_h(t) - p_w(t))}{dt} = -\left[\delta + \beta\left(\sum_{z=1, z \neq h,w}^{N} a_{hz} p_z(t) + 1\right)\right](p_h(t) - p_w(t))\,.$$

whence

$$p_h(t) - p_w(t) = (p_h(0) - p_w(0))\, e^{-\int_0^t \delta + \beta\left(\sum_{z=1, z\neq h,w}^{N} a_{hz} p_z(s) + 1\right) ds}.$$

Thus, if $p_h(0) = p_w(0)$ for the uniqueness of solution it will occur $p_h(t) = p_w(t)$ for all $t > 0$, as we have proved in Thm. 4.1, but if the initial conditions are different, the distance between $p_w(t)$ and $p_z(t)$ decreases exponentially.

Remark 4.3. The framework of quotient graphs extends the NIMFA model to graphs with prescribed community network structure. It reduces to the original NIMFA model when $k_j = 1$ for all $j = 1, .., n$.

Steady-state

We focus now on the computation of the steady-state $P_\infty = \left(p_{i\infty}\right)_{i=1,\dots,N}$ of system (3.6). To this aim, by Corollary 4.1, we can compute the steady-state $\overline{P}_\infty = \left(\overline{p}_{j\infty}\right)_{j=1,\dots,n}$ of the reduced system (4.12) and obtain

$$\beta(1-\overline{p}_{j\infty})\sum_{m=1}^{n}\left(\frac{k_j}{k_m}\right)^{-1/2} q_{jm}\overline{p}_{m\infty} - \delta\overline{p}_{j\infty} = 0, \qquad j = 1,\dots,n$$

whence

$$\begin{aligned}\overline{p}_{j\infty} &= \frac{\beta\sum_{m=1}^{n}\left(\frac{k_j}{k_m}\right)^{-1/2} q_{jm}\overline{p}_{m\infty}}{\beta\sum_{m=1}^{n}\left(\frac{k_j}{k_m}\right)^{-1/2} q_{jm}\overline{p}_{m\infty} + \delta} = 1 - \frac{1}{1+\tau\sum_{m=1}^{n}\left(\frac{k_j}{k_m}\right)^{-1/2} q_{jm}\overline{p}_{m\infty}} \\ &= 1 - \frac{1}{1+\tau g_j\left(\overline{P}\right)} \end{aligned} \tag{4.14}$$

where

$$g_j\left(\overline{P}\right) := \left(d_{jj} + \varepsilon\sum_{m=1}^{n}\left(\frac{k_j}{k_m}\right)^{-1/2}\sqrt{d_{jm}d_{mj}}\right) - \sum_{m=1}^{n}\left(\frac{k_j}{k_m}\right)^{-1/2} q_{jm}(1-\overline{p}_{m\infty}).$$

From (4.14) follows that the steady-state infection probability of any node j is bounded by

$$0 \le \overline{p}_{j\infty} \le 1 - \frac{1}{1+\tau(d_{jj} + \varepsilon\sum_{m=1}^{n}\left(\frac{k_j}{k_m}\right)^{-1/2}\sqrt{d_{jm}d_{mj}})}, \tag{4.15}$$

where the inequality holds true because $\overline{p}_{j\infty} \in [0,1]$ for all $j = 1,\dots,n$.

By introducing $1-\overline{p}_{m\infty} = \frac{1}{1+\tau\sum_{z=1}^{n}\left(\frac{k_m}{k_z}\right)^{-1/2} q_{mz}\overline{p}_{z\infty}}$ in (4.14), we can express $\overline{p}_{j\infty}$ as a continued fraction iterating the formula

$$x_{j,s+1} = f(x_{1;s},..,x_{n;s}) = 1 - \frac{1}{1+\tau g_j(x_{1;s},..,x_{n;s})},$$

As showed in [95], after a few iterations of the formula above, one can obtain a good approximation of $\overline{p}_{j\infty}$, with a loss in the accuracy of the calculation around $\tau = \tau_c$. Ultimately, such numerical estimation can be used to improve the bound in (4.15).

If we consider a regular graph where communities have the same number of nodes, then

$$\overline{p}_{j\infty} = 1 - \left(1/\tau \left(d_{jj} + \varepsilon \sum_{m=1}^{n} \left(\frac{k_j}{k_m}\right)^{-1/2} \sqrt{d_{jm} d_{mj}}\right)\right)$$

is the exact solution of (4.14).

Now let $r_j = d_{jj} + \varepsilon \sum_{m=1}^{n} \left(\frac{k_j}{k_m}\right)^{-1/2} \sqrt{d_{jm} d_{mj}}$ and $r(1) = \min_j r_j$; relying on the estimate $\overline{p}_{j\infty} \approx 1 - (1/\tau r_j)$ we can express the steady-state average fraction of infected nodes $y_\infty(\tau) = (1/N) \sum_{j=1}^{n} k_j \overline{p}_{j\infty}(\tau)$ by

$$y_\infty(\tau) \approx 1 - \frac{1}{\tau N} \sum_{j=1}^{n} k_j \frac{1}{d_{jj} + \varepsilon \sum_{m=1}^{n} \left(\frac{k_j}{k_m}\right)^{-1/2} \sqrt{d_{jm} d_{mj}}}. \tag{4.16}$$

According to the analysis reported in [95], approximation (4.16) becomes the more precise the more the difference $r(2) - r(1)$ is small, where $r(2)$ is the second smallest of the r_j's. Afterward we report on some related numerical experiments (see Figure 4.7).

Example 4.2. In Fig. 4.1 we provide an example of a graph which has an equitable partition with respect to $V_1 = \{v_1\}$, $V_2 = \{v_2, v_3\}$, $V_3 = \{v_3, v_4, v_5, v_6\}$, $V_4 = \{v_7, v_8, v_9, v_{10}, v_{11}, v_{12}, v_{13}\}\}$.

The corresponding quotient matrix reads

$$Q = \begin{bmatrix} 0 & \varepsilon\sqrt{2} & \varepsilon 2 & 0 \\ \varepsilon\sqrt{2} & 1 & \varepsilon\sqrt{2} & \varepsilon\sqrt{3} \\ \varepsilon 2 & \varepsilon\sqrt{2} & 2 & 0 \\ 0 & \varepsilon\sqrt{3} & 0 & 3 \end{bmatrix}$$

From (4.12) we have that the steady-state can be computed by

$$\overline{P}_\infty = \frac{\beta}{\delta} (\mathrm{I}_n - \mathrm{diag}(\overline{p}_\infty)) \, \mathrm{diag}(1/s_j) Q \, \mathrm{diag}(s_j) \overline{P}_\infty,$$

where s_j is the j-th entry of vector $s = (1, \sqrt{2}, 2, \sqrt{6})$.

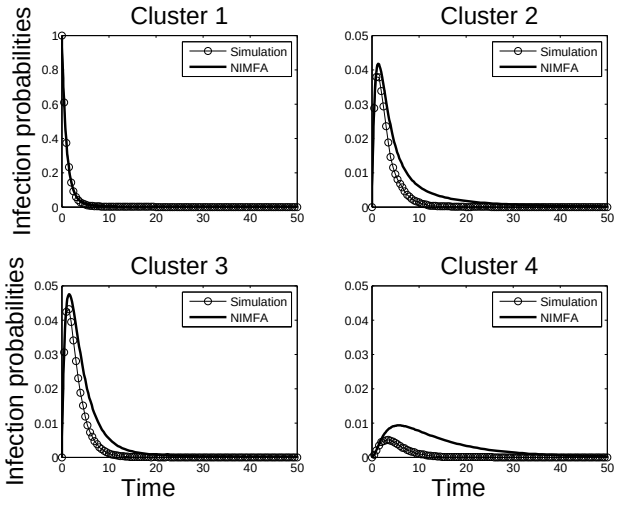

Figure 4.3: Dynamics of infection probabilities for each community of the network in Fig.4.1: simulation versus numerical solutions of (4.12); $\tau = \beta/\delta < \tau_c^{(1)} = 0.3178$, with $\beta = 0.29$ and $\delta = 1$, $\varepsilon = 0.3$. At time 0 the only infected node is node 1.

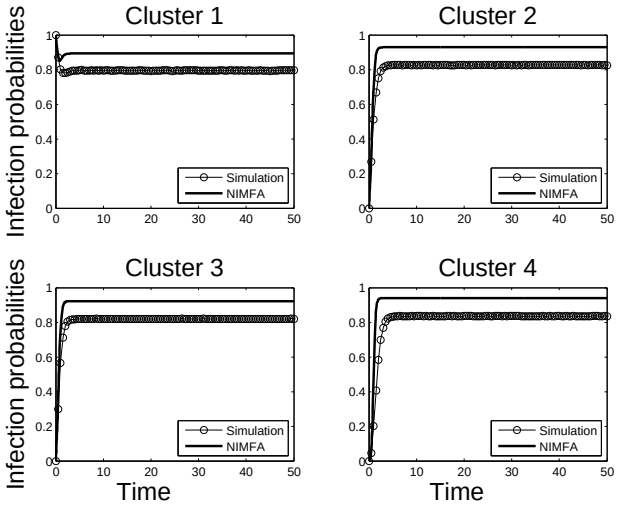

Figure 4.4: Dynamics of infection probabilities for each community of the network in Fig.4.1: simulation versus numerical solutions of (4.12); $\tau = \beta/\delta > \tau_c^{(1)} = 0.3178$, with $\beta = 1.5$ and $\delta = 0.3$, $\varepsilon = 0.3$; initial conditions as in Fig. 4.3.

Numerical experiments. In Figures 4.3 and 4.4 we provide a comparison between the solution of the reduced ODE system (4.12) for the graph in

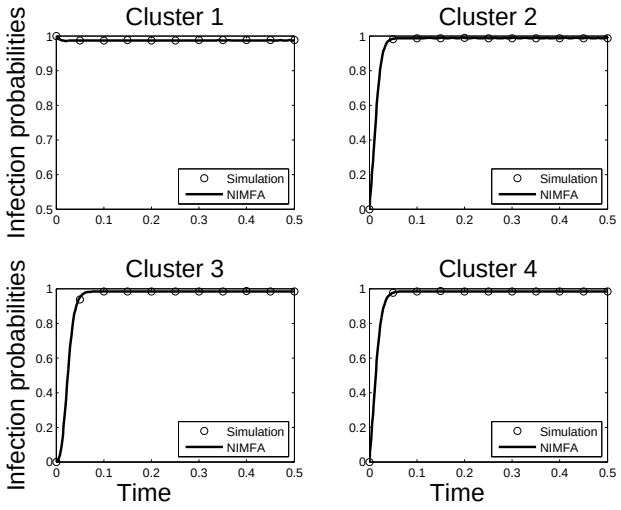

Figure 4.5: Infection probabilities for each community in a network with $N = 80$, $d_{ii} = k_i - 1 = 19$ and $d_{ij} = 20$, for all $i, j = 1, .., 4$: simulation versus numerical solutions of (4.12); $\tau = \beta/\delta > \tau_c^{(1)} = 0.0348$, with $\beta = 5$ and $\delta = 2$, $\varepsilon = 0.3$; at time 0 all nodes of the 1-st community are infected.

Figure 4.1 and the averaged $50 \cdot 10^4$ sample paths resulting from a discrete event simulation of the exact SIS process. The discrete event simulation is based on the generation of independent Poisson processes for both the infection of healthy nodes and the recovery of infected ones. We observe that, as expected, NIMFA provides an upper bound to the dynamics of the infection probabilities (see Section 3.3). Also, in Figure 4.3 we observe that the dynamics for the communities that are initially healthy is characterized by a unique maximum for the infection probability, which decreases afterward. The communities initially infected, conversely, show a monotonic decrease of the infection probability.

Figure 4.5 depicts the same comparison in the case of a network with eighty nodes partitioned into four communities; each community is a complete graph and all nodes belonging to two linked communities are connected. The agreement between NIMFA and simulations improves compared to Figure. 4.4. This is expected, because, as we said in Section 3.3, the accuracy of NIMFA is known to increase with network order N, under the assumption

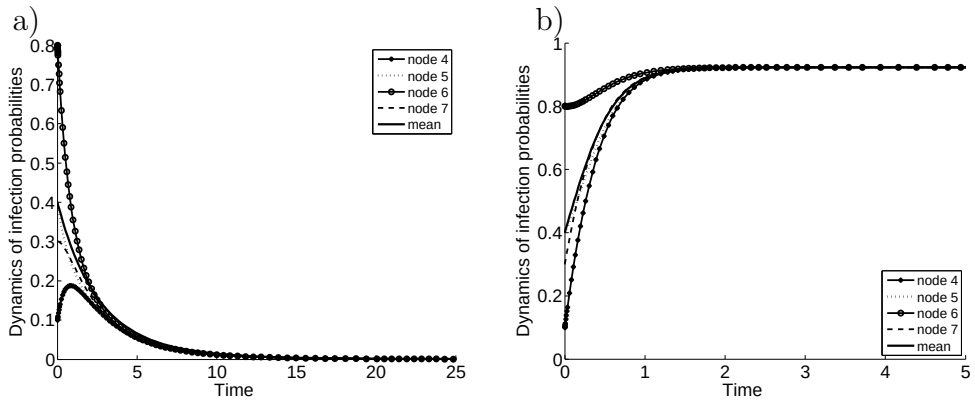

Figure 4.6: Comparison between the dynamics of the original system (3.6) for each of the nodes belonging to V_3 in Fig. 4.1, for different initial conditions and the dynamics of the reduced system (4.12). In the latter case the initial conditions for each node are the mean value of the $p_i(0)$s. a) case below the threshold: $\beta = 0.29$, $\delta = 1$, $\varepsilon = 0.3$ b) case above the threshold: $\beta = 1.5$, $\delta = 0.3$, $\varepsilon = 0.3$

.

that the nodes' degree also increases with the number of nodes. Conversely, it is less accurate, e.g., in lattice graphs or regular graphs with fixed degree not depending on N [95, 97].

Figure 4.6 depicts the solutions of system (3.6) for each node belonging to V_3 in the graph of Figure 4.1; here nodes in V_3 have different initial infection probabilities $p_i(0)$'s. These solutions are compared with the one computed using the reduced system (4.12), in the case when the initial conditions for those nodes are the same, precisely equal to the mean value of the $p_i(0)$'s. As expected, trajectories starting outside invariant set M described in Thm. 4.1 tend to approach the one starting in M as time elapses. Finally, we report on numerical experiments about the steady-state average fraction of infected nodes. More precisely, Figure 4.7 compares the value obtained by solving the original system (3.8) and the value obtained from approximation (4.16), as a function of τ.

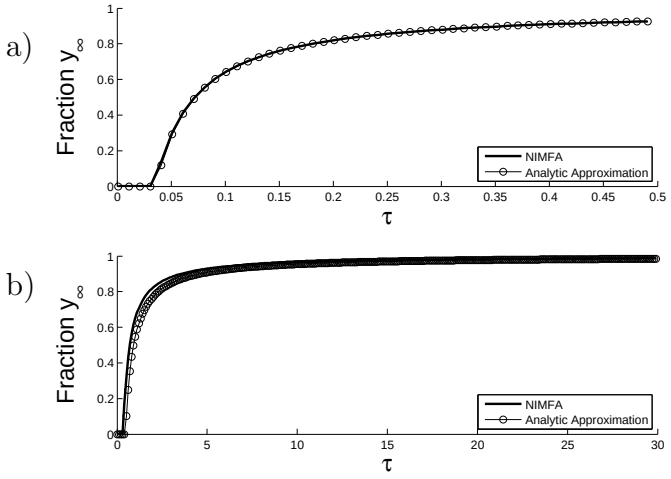

Figure 4.7: Steady-state average fraction of infected nodes, for different values of τ: comparison between the approximation (4.16) and the exact computation (3.8); a) the graph is the one considered in Fig. 4.1 and b) the one considered in Fig. 4.5.

4.3.1 Clique case

A *clique* of a graph is a set of vertices that induces a complete subgraph of that graph. Here we consider the specific case, analyzed in [16], where we have a *clique cover* of the graph, i.e., a set of cliques that partition its vertex set.

Thus, basically, all elements in a community are connected, i.e, $d_{ii} = k_i - 1$ for all $i = 1, ..., n$. Moreover we assume that all nodes belonging to two linked communities i and j are connected, i.e., $d_{ij} = k_j$ and $d_{ji} = k_i$. A sample graph is depicted in Figure 4.8.

In [16] sufficient conditions for the extinction of epidemics have been found explicitly in terms of the dimension of the communities, their connectivity, and the parameters of the model. In the following we report the main results.

Let us consider the computation of the equilibrium points of the system (4.12). In this case, it is easy to see that $\tilde{Q} = \mathrm{diag}(k_j - 1) + \varepsilon B\,\mathrm{diag}(k_j)$.

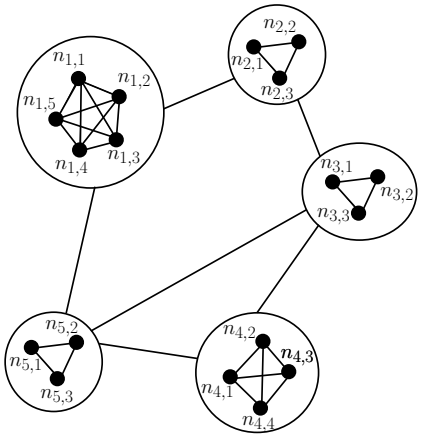

Figure 4.8: The two-scale community model: the contagion spreads within each cluster node with intra-cluster infection rate β and among clusters with inter-cluster infection rate $\varepsilon\beta$, with $0 < \varepsilon < 1$. A link between two clusters means that each node in one cluster is linked with all nodes in the other cluster.

The equilibrium points can be computed as the solution of

$$\delta\,\overline{P}_\infty = \beta\left(\tilde{Q}\overline{P}_\infty - \mathrm{diag}(\overline{P}_\infty)\tilde{Q}\overline{P}_\infty\right). \tag{4.17}$$

We underline that in a connected graph either $p_{i\infty} = 0$, for all $i = 1, \ldots, N$, or none of the components $p_{i\infty}$ is zero [95, Lemma 4].
Ignoring extreme virus spread conditions (the absence of curing, $\delta = 0$, and an infinitely strong infection rate, $\beta \to \infty$), then the infection probabilities $p_{j\infty}$ cannot be one such that the matrix $I - \mathrm{diag}(\overline{p}_{j\infty}) = \mathrm{diag}(1 - \overline{p}_{j\infty})$ is invertible [94].

Then from (4.17) we get

$$\beta\,\tilde{Q}\overline{P}_\infty = \mathrm{diag}\left(\frac{\delta}{1-\overline{p}_{j\infty}}\right)\overline{P}_\infty. \tag{4.18}$$

Let us write $\kappa = (k_1, \ldots, k_n)$. From the definition of $\tilde{Q}$ we can rewrite (4.18) as

$$B\,\mathrm{diag}(\kappa)\overline{P}_\infty = \mathrm{diag}\left(\frac{1}{\frac{\varepsilon\beta}{\delta}(1-\overline{p}_{j\infty})} - \frac{(k_j-1)}{\varepsilon}\right)\overline{P}_\infty. \tag{4.19}$$

Now let us denote by d_j the number of communities with which the j-th is connected. Then the Laplacian of the graph whose adjacency matrix is B (that encodes the connectivity of the communities) is the matrix $L = \mathrm{diag}(d_j) - B$; L is a $n \times n$ singular, positive semidefinite matrix, and the eigenvector corresponding to the zero eigenvalue is the all-one vector $u = (1, \ldots, 1)^T$.
Now let us define $B_\kappa := B\,\mathrm{diag}(\kappa)$, i.e., the matrix obtained from B by multiplying the j-th column by k_j, $j = 1, \ldots, n$, then we introduce the *modified Laplacian* matrix

$$\mathcal{L}_\kappa(\alpha) = \mathrm{diag}\,(\alpha) - B_\kappa, \qquad \alpha = (\alpha_1, \ldots, \alpha_n)^T,$$

where

$$\alpha_j = \frac{1}{\frac{\varepsilon\beta}{\delta}(1 - \overline{p}_{j\infty})} - \frac{(k_j - 1)}{\varepsilon}.$$

We can write the relation (4.19) by means of the modified Laplacian to get the (nonlinear) equation

$$\mathcal{L}_\kappa \left(\frac{1}{\frac{\varepsilon\beta}{\delta}(1 - \overline{p}_{j\infty})} - \frac{(k_j - 1)}{\varepsilon} \right) \overline{P}_\infty = 0. \tag{4.20}$$

Hence, if it exists, a nonzero steady-state vector $\overline{P}_\infty$ is an eigenvector of $\mathcal{L}_k(\alpha)$ corresponding to the zero eigenvalue.
It shall be noticed that B_κ is not a symmetric matrix, unless all $V_i's$ have the same number of nodes $k_j = k$. In order to find conditions that implies the existence of the zero eigenvalue for the modified Laplacian $\mathcal{L}_\kappa(\alpha)$, we apply Gerschgorin's Theorem 1.2 both to B_κ and B_κ^T.

Proposition 4.2. *Every eigenvalue of the modified Laplacian $\mathcal{L}_\kappa(\alpha)$ lies in (at least) one of the circular discs with center α_i and radius R_i, where*

$$R_i = \max\Big(\sum_{i \neq j} k_j b_{ij}, k_i \sum_{j \neq i} b_{ji} \Big) = \max\Big(\sum_{j \neq i} k_j b_{ji}, k_i d_i \Big).$$

Graphs with homogeneous partition into communities.

As mentioned above, in the case all $V_i's$ have the same order $k_j = k$, the matrix B_κ is symmetric, hence also the matrix $\mathcal{L}_\kappa(\alpha)$ is symmetric, which implies that all the eigenvalues are real. Moreover, in this case, all its eigenvalues are positive, except for the smallest one that is equal to 0 [94, Theorem 1].

Hence, precisely one, say the j-th, of the Gerschgorin line segments contains the zero eigenvalue, i.e. it must hold

$$\alpha_j - R_j < 0 < \alpha_j + R_j.$$

We can further express the above inequality as follows:

$$\frac{1}{\frac{\varepsilon\beta}{\delta}(1-\overline{p}_{j\infty})} - \frac{(k_j-1)}{\varepsilon} - R_j < 0,$$
$$\frac{1}{\frac{\varepsilon\beta}{\delta}(1-\overline{p}_{j\infty})} - \frac{(k_j-1)}{\varepsilon} + R_j > 0,$$

which, with a little algebra, leads to

$$\frac{1}{(1-\overline{p}_{j\infty})} < (k_j-1)\frac{\beta}{\delta} + R_j\,\frac{\varepsilon\beta}{\delta},$$
$$\frac{1}{(1-\overline{p}_{j\infty})} > (k_j-1)\frac{\beta}{\delta} - R_j\,\frac{\varepsilon\beta}{\delta}.$$

Considering that $k_j = k$, the first inequality implies that

$$\overline{p}_{j\infty} < 1 - \frac{\delta}{(k-1)\beta + R_j\,\varepsilon\beta}$$

and since we require $p_{j\infty} > 0$, we obtain that existence of an endemic state implies

$$\frac{(k-1)\beta + k\,d_j\,\varepsilon\beta}{\delta} > 1. \tag{4.21}$$

The second inequality leads to no further conditions. Actually, if the right-hand side is negative, i.e., in the regime $(k-1)\beta_L < k\,d_j\,\beta_G$, the inequality is trivially satisfied, since we require $v_{j;\infty} < 1$. Otherwise, in the regime $(k-1)\beta > k\,d_j\,\varepsilon\beta$, we get $1 > \frac{\delta}{(k-1)\beta - k\,d_j\,\varepsilon\beta}$ which leads to the lower bound for the probability $\overline{p}_{j\infty} > 1 - \frac{\delta}{(k-1)\beta - k\,d_j\,\varepsilon\beta}$.

Theorem 4.2. *Let $G = (V, E)$ be a graph with partition $\pi = \{V_j, j = 1, ..., n\}$, such that all V_i's induce a complete subgraph G_i of G, and all V_i's have the same order $k_j = k$. Moreover let us consider that whenever a node of G_i is connected with a node in G_j, then it is connected with all nodes in G_j. Therefore a sufficient condition for the uniqueness of the zero steady-state is the following:*

$$\frac{d_{\max}\varepsilon\beta + (1 - \frac{1}{k})\beta}{\delta} < \frac{1}{k},$$

where $d_{\max} = \max_j d_j$.

Inhomogeneous community dimension.

Now we extend previous results including the possibility for each community to have a different number of elements. The starting point is equation (4.19); however, instead of using directly Corollary 4.2, we first state the problem in terms of the vector $\overline{W}_\infty = \mathrm{diag}(\kappa)\overline{P}_\infty$. Then we consider the modified Laplacian matrix with respect to B:

$$\mathcal{L}(\alpha) = \mathrm{diag}(\alpha) - B,$$

where

$$\alpha_j = \frac{1}{\frac{\varepsilon\beta}{k_j\,\delta}(1 - \overline{p}_{j;\infty})} - \frac{(k_j - 1)}{\varepsilon k_j}.$$

The existence of a nonzero steady state $\overline{P}_\infty$ requires that $\overline{W}_\infty$ is a nonzero eigenvector of $\mathcal{L}(\alpha)$ related to the eigenvalue zero; now $\mathcal{L}(\alpha)$ is symmetric and, with the same reasoning as above, taking into account Proposition 4.2, we have that for at least one j

$$\alpha_j - R_j < 0 < \alpha_j + R_j.$$

Clearly, in this case the radius R_j is expressed in terms of the adjacency matrix B, hence $R_j = d_j$.

Therefore, a sufficient condition for the uniqueness of the trivial steady state is the following:

$$\frac{1}{\frac{\varepsilon\beta}{\delta}(1 - \overline{p}_{j\infty})} - \frac{(k_j - 1)}{\varepsilon} > d_j\,k_j$$

and, since it must be $0 < \overline{p}_{j\infty} < 1$, we have proved the following result.

Theorem 4.3. *Let $G = (V, E)$ be a graph with partition $\pi = \{V_j, j = 1, ..., n\}$, such that all V_i's induce a complete subgraph G_i of G, each of arbitrary order k_i. Moreover let us consider that whenever a node of G_i is connected with a node in G_j, then it is connected with all nodes in G_j. Therefore a sufficient condition for the uniqueness of the zero steady state is the following:*

$$\forall\, j = 1, \ldots, n: \qquad \frac{d_j\, \varepsilon\beta + (1 - \frac{1}{k_j})\beta}{\delta} < \frac{1}{k_j}.$$

The above result confirms the intuition that just the presence of communities, i.e. of a group of individuals that may get infected each other at much higher rate, implies an increase of the probability of persistence of the epidemics. Actually, it is sufficient to compare the condition in Theorem 4.3 for $k_j > 1$ with the condition $d_j\beta\delta < 1$ that results in case $k_j \equiv 1$ and $\varepsilon = 1$ (we implicit assume that if the network is not partitioned in communities, the infection rate is constant among the population). Furthermore, the same formula implies that the higher the value of β, the smaller is the region of extinction of epidemics. Finally, the result in Theorem 4.3 becomes apparent in the limit cases. Suppose, for instance, that β converges to zero. Then the inequality in Theorem 4.3 is trivially satisfied and the system is in the region of extinction for the epidemics. Conversely, if β converges to infinity, then the system enters in the region of persistence.

Numerical Experiments.

Our NIMFA-like approximation is validated here by comparison with the exact SIS model. From the operative standpoint, we compare NIMFA with the a-SIS model [46, 93] where a nodal self-infection is allowed. This model has no absorbing state and its stationary distribution, that can be computed for explicitly, can be made arbitrarily close to the quasi-stationary distribution of the original SIS model, by considering appropriate and small values of $a > 0$ (see Section 3.3) [93, 55]. For a detailed explanation on the simulation process see [55].

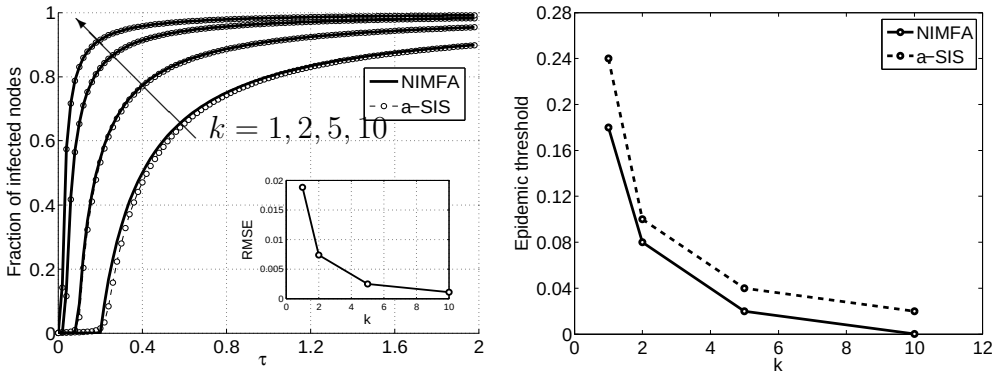

(a) (b)

Figure 4.9: (a) Fraction of infected nodes for different values of k as a function of $\tau = \beta/\delta$, with fixed the ratio $\varepsilon = 1/2$ and the value $\delta = 1$. The network of the communities is a regular graph with degree 10; the number of nodes is $N = 500$. The inserted plot represents the root mean square error between the simulated and the approximated fraction of infected nodes (b) The corresponding value of the epidemic threshold for the NIMFA and the exact a-SIS model.

Effect of community dimension. We depict first, in Figure 4.9(a), the impact of the community dimension k on the fraction of infected nodes in the steady-state, and compare the results of our model to the a-SIS model. The epidemic threshold of the a-SIS model is measured as the value of τ where the second derivative of the steady-state fraction of infected nodes equals zero. We consider a range for $\tau = \beta/\delta$, for constant ratio $\varepsilon = 1/2$ and fixed $\delta = 1$.

The sample network, representing the connections between the communities, has constant degree $d = 10$. The total number of nodes is $N = 500$. The number of elements k is the same for all communities: curves are drawn for increasing values of k ($k = 1, 2, 5, 10$), where $k = 1$ denotes the absence of local clusters. The threshold effect is well visible in the graphs depicted in Figure 4.9(a). As can be further observed, our model and the exact SIS model are in good agreement and the root mean square error between them decreases as k increases.

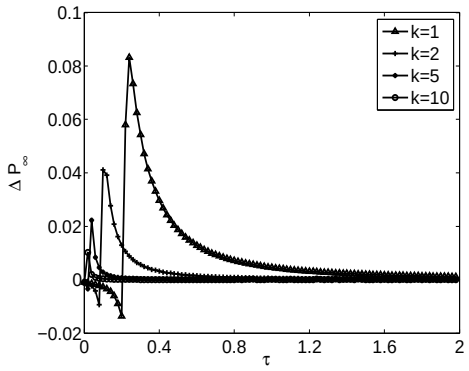

Figure 4.10: Difference between the exact a-SIS model and the NIMFA fractions of infected nodes as a function of τ and for different values of k, for the sample network in Fig. 4.9.

In Figure 4.9(b) the corresponding value of the epidemic threshold for the NIMFA and the a-SIS model is reported. As expected from Theorem 4.2, the critical threshold above which a persistent infection exists decreases with the dimension of the communities. Thus, for large values of the community dimension, a very small value of τ is sufficient to cause epidemic outbreaks, irrespective of the actual network structure.

Figure. 4.10 illustrates the difference between the NIMFA and the a-SIS fraction of infected nodes as a function of τ and for various k, for the sample network in Figure 4.9: we observe that, as we expect (see Section 3.3) the maximum difference between the two models occurs when τ equals the a-SIS epidemic threshold. This means that for τ greater than the a-SIS epidemic threshold, the difference between the two models decreases and the two models get increasingly closer.

In Figures 4.11(a) and (b), the network of communities is an Erdős-Rényi random graphs * with $n = 10$, generated according to edge connection probability $p = 0.3$. The plots have been derived averaging over 300 instances of random graphs, and setting $\varepsilon = 1/2$ and $\delta = 1$. The confidence intervals for

*An Erdős-Rényi random graph can be generated from a set of N nodes by randomly assigning a link with probability p to each pair of nodes.

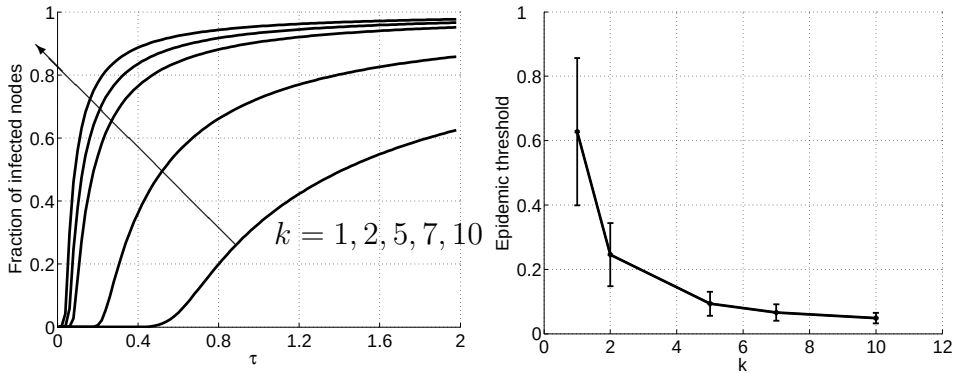

(a) Fraction of infected nodes. (b) Epidemic Threshold.

Figure 4.11: (a) Fraction of infected nodes for different values of k and τ, being fixed the ratio $\varepsilon = 1/2$, $n = 10$, and the value $\delta = 1$. (b) The corresponding value of the epidemic threshold. All plots have been obtained averaging over 300 instances of Erdős-Rényi random graphs, each representing the network of the communities, for $p = 0.3$, the level of confidence is set to 98%.

the epidemic threshold is set to 98%.

Larger community dimensions, $k > 1$, cause the epidemic threshold to drop of one order of magnitude, i.e. it starts above 0.3 for $k = 1$ and it decreases to around 0.1 already for $k = 2$, while it finally drops below 0.03 for $k \geq 7$.

By taking into account one instance of this set of Erdős-Rényi graphs for $k = 5$, we report, in Figure 4.12, the behavior of the fraction of infected nodes as a function of $\tau_G = \varepsilon\beta/\delta$ and $\tau_L = \beta/\delta$, where the subscripts G and L stay for "global"(i.e between communities) and "local" (i.e within the communities) respectively. We can observe that the epidemic threshold behaves linearly for a given cluster dimension, in agreement with the expression derived in Theorem 4.2.

Finally, we consider a sample Erdős-Rényi network, for the communities' connection, with order $n = 20$ and $p = 0.3$. Figures 4.13(a) and (b) show a good agreement between the two models for cluster size $k = 5, 7, 10$. On the contrary, for networks with few individuals, $N = 20$ corresponding to

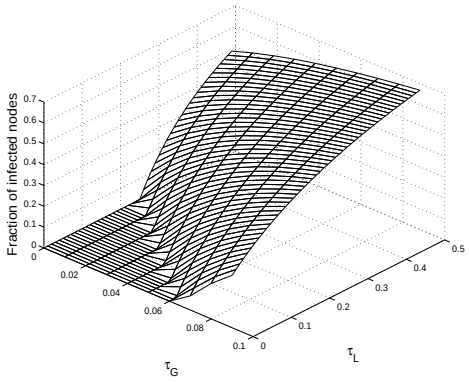

Figure 4.12: (a) Fraction of infected nodes as a function of $\tau_G = \varepsilon\beta/\delta$ and $\tau_L\beta/\delta$ for a network with 10 communities and $k = 5$.

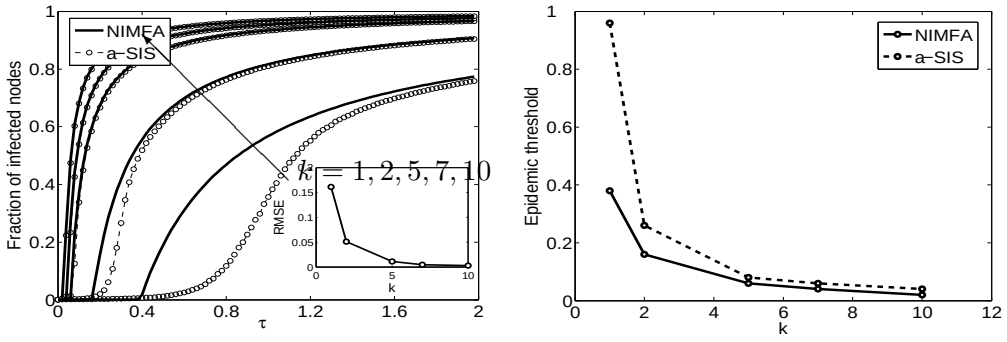

(a) (b)

Figure 4.13: (a) Fraction of infected nodes for different values of k and $\tau_G = \beta_G/\delta$, being fixed the ratio $\varepsilon = 1/2$ and the value $\delta = 1$, for the case where the network of the communities is an Erdős-Rényi graph of order $n = 20$ and $p = 0.3$. Both the NIMFA and the exact $a = 10^{-3}$ SIS model are shown. The inserted plot represents the root mean square error between the simulated and the approximated fraction of infected nodes. (b) The corresponding value of the epidemic threshold for the NIMFA and the exact a-SIS model.

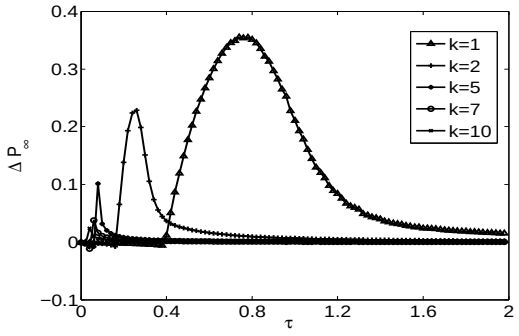

Figure 4.14: Difference between the exact a-SIS model and the NIMFA fractions of infected nodes as a function of τ and for different values of k, for the case where the network of the communities is an Erdős-Rényi graph of order $n = 20$, $p = 0.3$.

$k = 1$, and $N = 40$ for $k = 2$, the epidemic threshold of the NIMFA model is less close to that of the a-SIS model. As further observed from Figure 4.14, the maximum difference between the NIMFA and the a-SIS fractions of infected nodes corresponds to the a-SIS epidemic threshold for networks with communities' dimension equal to $k = 5, 7, 10$.

Effect of the heterogeneity of the community dimension.

One interesting question that concerns the two-scale epidemic model is the influence of the community dimension distribution onto the epidemic threshold. In general, it is not obvious whether, fixing all remaining system's parameters, a constant community dimension will lead to a lower or larger epidemic threshold for the same network.

In Figure 4.15 we performed a test using a set of 300 sample tree graphs for depicting the connectivity of the communities. Each graph is the spanning tree of an Erdős-Rényi graph of order $n = 10$ and $p = 0.3$. The ratio ε is set to $1/8$. The plot draws the difference Δ_τ, obtained averaging over the 300 sample graphs, between the epidemic threshold measured for homogeneous cluster distribution, and the epidemic threshold measured in the case of inhomogeneous cluster distribution.
In particular, for each sample tree, we considered different values of the average cluster dimension $k = 5, 10, 15$. In the case of heterogeneous cluster

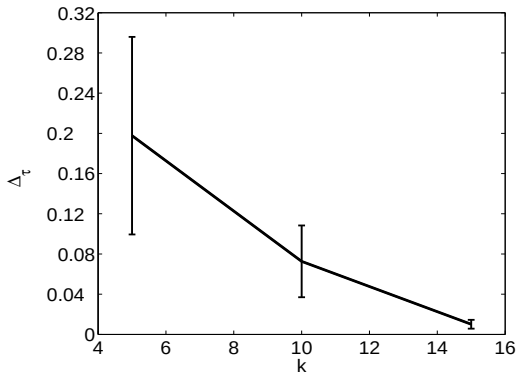

Figure 4.15: Difference Δ_τ between the epidemic threshold in the case of homogeneous cluster distribution and inhomogeneous cluster distribution for different values of k (5,10,15), being fixed the ratio $\varepsilon = 1/8$. The difference was obtained averaging over 300 instances of tree graphs of 10 clusters, the level of confidence is set to 98%

distribution half of the communities have dimension 2 and half of them have dimension $2k - 2$.

Figure. 4.15 exemplifies that heterogeneity of communities' dimension lowers the epidemic threshold compared to the case of constant dimension. This observation agrees with the theory, indeed from the inequality [89, (3.34) on p. 47]:

$$\lambda_1 \geq \frac{2L}{N}\sqrt{1 + \frac{\mathrm{Var}[d]}{(\mathbb{E}[d])^2}},$$

where λ_1 is the spectral radius of a given graph with N nodes and L links, and d is the degree of a randomly chosen node in the graph, we have

$$\tau_c^{(1)} = \frac{1}{\lambda_1} \leq \frac{N}{2L}\frac{1}{\sqrt{1 + \frac{\mathrm{Var}[d]}{(\mathbb{E}[d])^2}}}$$

implying that, the larger the variance in the degree d, the lower the NIMFA epidemic threshold $\tau_c^{(1)}$. Unfortunately, since $\tau_c^{(1)} \leq \tau_c$, we cannot conclude that an increase in $\mathrm{Var}[d]$ also always lowers the exact epidemic threshold τ_c.

Figure 4.16 shows the epidemic threshold measured for homogeneous community dimension and the epidemic threshold measured for inhomogeneous

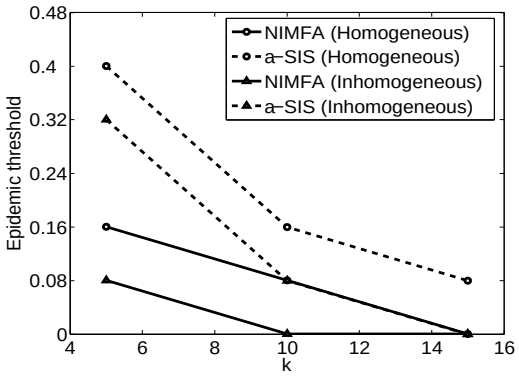

Figure 4.16: The epidemic threshold in the case of homogeneous cluster distribution and inhomogeneous cluster distribution for different values of k, where the network of the communities is a spanning tree of an Erdős-Rényi graph of order $n = 10$ and $p = 0.3$. Both the NIMFA and the a-SIS thresholds are shown.

community dimension, by considering one instance of the previous set of spanning trees of an Erdős-Rényi graph. We report both the results obtained for our model and the results obtained for the a-SIS model: the NIMFA epidemic threshold well estimates the a-SIS epidemic threshold in both community dimension distributions.

Effect of community internal structure.

Here we analyze the impact of the cluster internal structure on the epidemic process, thus we compare a network whose clusters are fully connected, i.e $d_{jj} = k - 1$, for all $j = 1, \ldots, n$, with another one with clusters having a ring topology, i.e. $d_{jj} = 2$, for all $j = 1, \ldots, n$.

Figure 4.17 illustrates the results for clusters with a ring topology, compared to fully connected clusters. The figure shows, for different values of k, the difference Δ_τ between the epidemic threshold in the case of ring clusters and fully connected clusters. The results have been obtained by averaging over 300 instances of Erdős-Rényi random graphs (as before, $n = 10$, $p = 0.3$ and the level of confidence is set to 98%). For $k > 2$, the difference in the value of the epidemic threshold confirms that the community structure has an impact on the epidemic threshold, and as we actually expect, having sparser

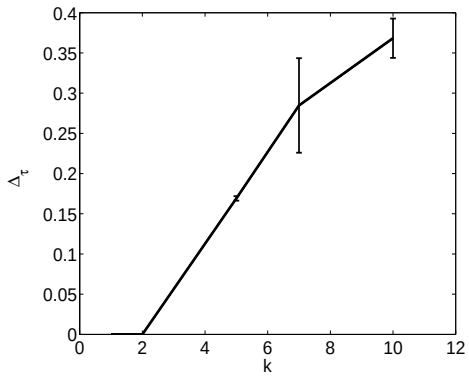

Figure 4.17: Ring clusters v.s. fully connected clusters: difference Δ_τ between the epidemic threshold in the case of ring clusters and fully connected clusters for different values of k. The difference was obtained averaging over 300 instance of Erdos-Renyi random graphs of 10 clusters, for $p = 0.3$, the level of confidence is set to 98%.

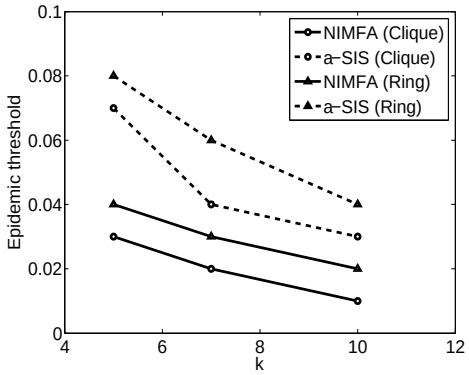

Figure 4.18: Epidemic threshold in the case of ring and fully connected clusters for different values of k, for an instance of Erdős-Rényi random graph of order $n = 10$ and $p = 0.3$. Both the NIMFA and the exact ε-SIS model thresholds are shown.

communities in a network increases the epidemic threshold. This behavior is further observed in Figure 4.18 where we compare the NIMFA and the a-SIS thresholds for the two cluster topologies. Moreover, as for the previous test cases, the NIMFA epidemic threshold is close to that of the a-SIS model.

4.3.2 Interconnected Stars

Here we consider a specific undirected graphs, which result by interconnecting star graphs, where stars' central nodes may be connected among themselves. We call such kind of topology *interconnected stars networks* (NSIs). A sample network of this type is depicted in Figure 4.19.
We can consider the following partition of the node set V: the set $\{V_1^0, ..., V_m^0\}$, namely the star central nodes, where $|V_i^0| = 1$, for all $i = 1, \ldots, m$, and the set $\{V_1, ..., V_m\}$, namely the stars' leaves, where $|V_i| = k_i$.
As before we shall identify the set of all nodes in each V_i with a community of the whole population.

We define the set of star central nodes as the set of *central communities* (or *central nodes*), and that of the stars' leaves as the set of the *terminal communities*.

Each central community is connected with all elements in one of the terminal communities (it acts as the hub in a star). The terminal communities are not connected among themselves but each of them is related only with its corresponding central community, i.e., all nodes in V_i are connected only with V_i^0, for $i = 1, .., m$. Actually, if we look at the connections between V_i^0 with nodes of V_i, the corresponding subgraph is a star. Thus, the whole network is a set of interconnected stars. It is straightforward to see that the partition $\pi = \{V_1^0, ..., V_m^0, V_1, ..., V_m\}$ of this kind of network is *equitable*.

The two-scale model for the diffusion sets β infection rate between the central nodes and $\varepsilon\beta$ the infection rate between a central node and a node in its adjacent terminal community, where $\varepsilon > 0$. Here, the same curing rate δ holds for all nodes.

Let B be the $m \times m$ adjacency matrix of the central nodes, the $N \times N$ adjacency matrix A of the whole network is

$$A = \begin{bmatrix} B_{m\times m} & \varepsilon Z_{m\times(N-m)} \\ \varepsilon Z^T_{(N-m)\times m} & 0_{(N-m)\times(N-m)} \end{bmatrix}$$

where $Z = \mathrm{diag}(\mathbf{1}_{k_1}, \ldots, \mathbf{1}_{k_m})$ with $\mathbf{1}_{k_i}$ the $1 \times k_i$ vector of all ones. Thus the

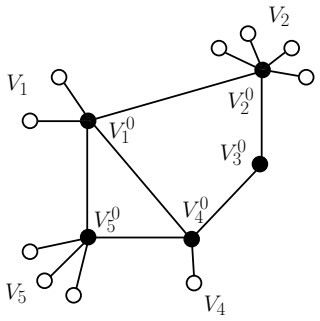

Figure 4.19: A sample network of interconnected stars; the resulting graph with $m = 5$ and $k_1 = 2$, $k_2 = 4$, $k_3 = 0$, $k_4 = 1$, $k_5 = 3$: central communities are filled black, terminal communities are filled white.

quotient matrix writes

$$Q = \begin{bmatrix} B_{m\times m} & \varepsilon\sqrt{\Lambda}_{m\times m} \\ \varepsilon\sqrt{\Lambda}_{m\times m} & 0_{m\times m} \end{bmatrix}$$

where $\Lambda := \operatorname{diag}(k_i)$.

We may assume that, at time $t = 0$, the infection probability is the same in all nodes of a terminal community, and may differ from one community to the other. Then by Theorem 4.1 we know that the epidemic diffusion (3.6) can be expressed by means of the modified quotient matrix which reduces the original system of N differential equations to a system of $2m$ differential equations. We have

$$\tilde{Q} = \begin{bmatrix} I & 0 \\ 0 & \Lambda^{-\frac{1}{2}} \end{bmatrix} Q \begin{bmatrix} I & 0 \\ 0 & \Lambda^{\frac{1}{2}} \end{bmatrix} = \begin{bmatrix} B & \varepsilon\Lambda \\ \varepsilon I & 0 \end{bmatrix}$$

then the reduced system (4.12) writes

$$\frac{d}{dt}\overline{P}(t) = \beta \operatorname{diag}(\mathbf{1}_N - \overline{P}(t)) \begin{bmatrix} B & \varepsilon\Lambda \\ \varepsilon I & 0 \end{bmatrix} \overline{P}(t) - \delta\overline{P}(t), \tag{4.22}$$

and by partitioning the $2m \times 1$ vector $\overline{P} = (P^0\overline{P}^1)^T$ finally we have

$$\begin{aligned} \tfrac{d}{dt}P^0(t) = \; & -\delta P^0(t) + \varepsilon\beta \operatorname{diag}(\mathbf{1}_m - P^0(t))\Lambda\overline{P}^1(t) \\ & +\beta \operatorname{diag}(\mathbf{1}_m - P^0(t))BP^0(t) \\ \tfrac{d}{dt}\overline{P}^1(t) = \; & -\delta\overline{P}^1(t) + \varepsilon\beta \operatorname{diag}(\mathbf{1}_m - \overline{P}^1(t))P^0(t) \end{aligned}$$

We note, however, that if nodes in the same terminal community have different initial conditions, the stability properties of the original system (3.6) cause the dynamics to converge exponentially fast to the reduced dynamics (4.22) (see Section 4.3).

In order to study the long term behavior of the system, we have to compute the vector of steady state infection probabilities.

Corollary 4.1 shows that, irrespective of the initial conditions of terminal nodes, it is sufficient to compute the positive steady-state vector of the reduced system (4.22) to obtain that of the original system (3.6). Indeed, the components of the steady-state vector P_∞, corresponding to nodes in the same terminal community, are equal. Thus, starting from (4.23) the positive steady-state vector can be obtained from the following conditions

$$\frac{p^0_{i\infty}}{1-p^0_{i\infty}} = \varepsilon\tau k_i \overline{p}^1_{i\infty} + \tau\left(\sum_{j=1}^{c} b_{ij} p^0_{j\infty}\right),\ \frac{\overline{p}^1_{i\infty}}{1-\overline{p}^1_{i\infty}} = \varepsilon\tau p^0_{i\infty}$$

which is equivalent to the following m equations

$$\frac{p^0_{i\infty}}{1-p^0_{i\infty}} = (\varepsilon\tau)^2 k_i \frac{p^0_{i\infty}}{1+\varepsilon\tau p^0_{i\infty}} + \tau\left(\sum_{j=1}^{c} b_{ij} p^0_{j\infty}\right)$$

The steady-state for the terminal communities writes simply

$$\overline{p}^1_{i\infty} = \frac{\varepsilon\tau p^0_{i\infty}}{1+\varepsilon\tau p^0_{i\infty}} \xrightarrow{p^0_{i\infty}\to 1} \frac{\varepsilon\tau}{1+\varepsilon\tau}$$

suggesting that, when $\tau\varepsilon$ is not too large, terminal communities are less likely to be infected than the adjacent central communities, hence they eventually require lesser curing resources.

Now we derive bounds for the NIMFA epidemic threshold $\tau_c^{(1)} = \frac{1}{\lambda_1(A)} = \frac{1}{\lambda_1(Q)}$. A general bound is obtained from Gershgorin's theorem 1.2,

$$\frac{1}{\lambda_1(Q)} \geq \frac{1}{\max_i \sum_j Q_{ij}} \geq \frac{1}{\max_i \left(d_i + \varepsilon\sqrt{k_i}\right)},$$

where $d_i = \sum_{j=1}^{m} b_{ij}$.

A tighter bound is found in the following proposition.

Proposition 4.3. *For the NSIs it holds*

$$\tau_c^{(1)} = \frac{1}{\lambda_1(Q)} \geq \frac{1}{\lambda_1(B) + \varepsilon \cdot \max_i \sqrt{k_i}}.$$

Proof. We can write

$$Q = \begin{bmatrix} B & 0 \\ 0 & 0 \end{bmatrix} + \begin{bmatrix} 0 & \varepsilon\Lambda^{\frac{1}{2}} \\ \varepsilon\Lambda^{\frac{1}{2}} & 0 \end{bmatrix} = \widehat{B} + \widehat{L}$$

From the property of the determinant of 2×2 block matrices [84] we write the characteristic polynomial of the second matrix as

$$p_{\widehat{L}}(\lambda) = (\lambda I - \varepsilon\Lambda^{\frac{1}{2}})(\lambda I + \varepsilon\Lambda^{\frac{1}{2}})$$

so that clearly $\lambda_1(\widehat{L}) = \varepsilon \max_i \sqrt{k_i}$. By Weyl's inequality we have

$$\lambda_1(Q) \leq \lambda_1(B) + \varepsilon \cdot \max_i \sqrt{k_i}$$

Since $\lambda_1(A) = \lambda_1(\tilde{Q}) = \lambda_1(Q)$ the proposition is proved.

□

Two-layers Networks. The NSIs can be seen as a two-layer, interdependent network. Such case is interesting for specific closed forms giving insight into the properties of virus diffusion and immunization strategies (see Section 5.2).

In a multilayer network $G = (V_M, E_M)$, it is given a partition of vertex set V_M into layers $\{V_\alpha\}_\alpha$, $\alpha = 1, \ldots, n$ [82]. A quotient graph is hence induced by such partition and each layer α, with $\alpha = 1, ..., n$ corresponds to the respective induced subgraph $G_\alpha = (V_\alpha, E_\alpha)$.

In our case, the natural node set partition is $\pi = V_0 \cup V_1$, where $V_0 = (\cup_i V_i^0)$ and $V_1 = (\cup_i V_i)$. This corresponds to a two-layers network.

Observe that π is an equitable partition only under the assumption that $G_0 = (V_0, E_0)$ is a regular graph with degree d_0 and that $G_1 = (V_1, E_1)$ has

an empty edges set. Moreover, each central node belonging to V_0 must have $d_{01} = d_1$ neighbors in V_1, and each terminal nodes must be connected with only one central node. The 2×2 quotient and modified quotient matrices write

$$Q = \begin{bmatrix} d_0 & \varepsilon\sqrt{d_1} \\ \varepsilon\sqrt{d_1} & 0 \end{bmatrix}, \quad \tilde{Q} = \begin{bmatrix} d_0 & \varepsilon\sqrt{\frac{d_1 k_1}{k_0}} \\ \varepsilon\sqrt{\frac{d_1 k_0}{k_1}} & 0 \end{bmatrix} \tag{4.23}$$

whose largest eigenvalue is

$$\lambda_1(Q) = \frac{d_0}{2}\left(1 + \sqrt{1 + 4\frac{d_1}{d_0^2}\varepsilon^2}\right),$$

and consequently the epidemic threshold is

$$\tau_c^{(1)} = \frac{1}{\lambda_1(Q)} = -\frac{d_0}{2d_1\varepsilon^2}\left(1 - \sqrt{1 + 4\frac{d_1}{d_0^2}\varepsilon^2}\right).$$

The infection probability in steady-state is obtained in closed form as

$$(1 - p_0)d_0 p_0 + \varepsilon\sqrt{\frac{d_1 k_1}{k_0}}\overline{p}_1(1 - p_0) - \frac{1}{\tau}p_0 = 0,$$

$$\varepsilon\sqrt{\frac{d_1 k_0}{k_1}}(1 - \overline{p}_1)p_0 - \frac{1}{\tau}\overline{p}_1 = 0.$$

Let $\varepsilon\sqrt{\frac{d_1 k_1}{k_0}} = a$ and $\varepsilon\sqrt{\frac{d_1 k_0}{k_1}} = b$ from the second equation:

$$\overline{p}_1 = \frac{bp_0}{\frac{1}{\tau} + bp_0},$$

substituting this value into the first equation yields

$$(1 - p_0)d_0 p_0 + \frac{bp_0}{\frac{1}{\tau} + bp_0}a(1 - p_0) - \frac{1}{\tau}p_0 = 0,$$

from which p_0 is obtain and consequently $\overline{p}_1$.

4.4 Almost equitable partitions

In this section we consider graphs where the partition of the vertex set is *almost equitable*.

Definition 4.3. The partition $\pi = \{V_1, ..., V_n\}$ is called *almost equitable* if for all $i, j \in \{1, \ldots, n\}$ with $i \neq j$, there is an integer d_{ij} such that for all $v \in V_i$, it holds

$$d_{ij} = deg(v, V_j) := \#\left\{e \in E : e = \{v, w\}, w \in V_j\right\}$$

independently of $v \in V_i$.

The difference between equitable and almost equitable partitions is that, in the former case, subgraph G_i of G induced by V_i has regular structure, whereas the latter definition does not impose any structural condition into G_i.

Ideally we can think of a network $\tilde{G}$ whose node set has an almost equitable partition as a network G with equitable partition where links between nodes in one or more communities have been added or removed.

The objective is to obtain lower bounds on threshold $\tau_c^{(1)}$, useful in determining a safety region for the extinction of epidemics. We start assuming that links are added only.

To this aim, let us consider two graphs $G = (V, E)$ and $\tilde{G} = (V, \tilde{E})$ with the same partition $\{V_1, \ldots, V_n\}$, but different edge sets $E \subsetneq \tilde{E}$, and assume G to have an equitable partition but $\tilde{G}$ to have merely an almost equitable partition. Then if $\tilde{A}$ and A are the adjacency matrices of $\tilde{G}$ and G respectively it holds

$$\tilde{A} = A + R,$$

where $R = \text{diag}(R_1, \ldots, R_n)$; the dimension of R_i is $k_i \times k_i$ for $i = 1, ..., n$, as before k_i is the order of G_i and n is the number of the communities.

The Weyl's inequality can be applied to $\tilde{A} = A + R$, and then it yields

$$\lambda_1(\tilde{A}) \leq \lambda_1(A) + \lambda_1(R). \tag{4.24}$$

In the following we shall provide a more explicit formulation of the right hand side of (4.24) involving the number of added edges.

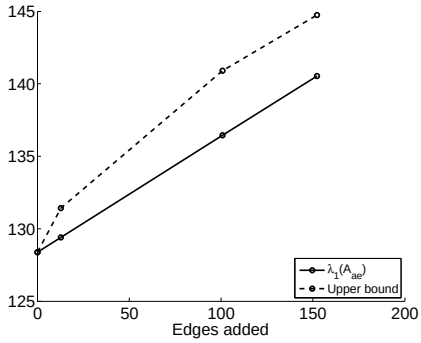

Figure 4.20: Comparison of the bound and the spectral radius for a 40-communities network. Each community has $k = 25$ nodes, whose internal structure is initially a ring; the perturbation graph is obtained by adding in each of them the same increasing number of links. The spectral radius of the adjacency matrix $\tilde{A}$ (A_{ae} in the legend, where the subscript "ae" stays for "almost equitable") is compared to the upper bound as a function of the links added in each community.

Proposition 4.4. *Let $G = (V, E)$ and $\tilde{G} = (V, \tilde{E})$ be two graphs and consider a partition $\{V_1, \ldots, V_n\}$ of the set of vertices V; we shall denote by $G_i = (V_i, E_i)$ and $\tilde{G}_i = (V_i, \tilde{E}_i)$ the subgraph of G and $\tilde{G}$ induced by the cell V_i, respectively, for $i = 1, ...n$. Assume this partition to be equitable for G and almost equitable for $\tilde{G}$. Let $E \subset \tilde{E}$ with*

$$\tilde{E} \setminus E = \bigcup_{i=1}^{n} (\tilde{E}_i \setminus E_i)$$

(i.e., the edge sets can only differ within cells) and denote by R the adjacency matrix corresponding to a graph with $\tilde{E} \setminus E$ as edge set. Finally, let us denote by G_i^C the graph with edge set $\tilde{E}_i \setminus E_i$ and whose node set is simply the set of endpoints of its edges (i.e., no further isolated nodes).

1. *If $\Delta(G_i^C)$ denotes the maximal degree in G_i^C, $i = 1, \ldots, n$, then*

$$\lambda_1(R) \leq \max_{1 \leq i \leq n} \min \left\{ \sqrt{\frac{2e_i(k_i - 1)}{k_i}}, \Delta(G_i^C) \right\} ,$$

where e_i is the number of edges added to G_i, i.e., $e_i = (|\tilde{E}_i| - |E_i|)$, and k_i is the number of nodes in V_i.

2. If additionally G_i^C is connected for each $i = 1, \ldots, n$, then

$$\lambda_1(R) \leq \max_{1\leq i\leq n} \min\left\{\sqrt{2e_i - k_i' + 1}, \Delta(G_i^C)\right\} ,$$

where k_i' is the number of nodes of G_i^C.

Proof. (1) By assumption, R is a diagonal block matrix whose blocks R_i are the adjacency matrices of the induced subgraphs G_i^C. Thus, $\lambda_1(R)$ is the maximum of all spectral radii $\lambda_1(R_i)$. On the other hand, one has by [89, (3.45)] that

$$\lambda_1(R_i) \leq \min\left\{\sqrt{\frac{2e_i(k_i-1)}{k_i}}, \Delta(G_i^C)\right\}.$$

and the claim follows.
(2) By Gershgorin's theorem 1.2, the spectral radius of an adjacency matrix of a graph without loops is never larger than the graph's maximal degree, i.e., $\lambda_1(R_i) \leq \Delta(G_i^C)$. By assumption, there exists a permutation of the nodes in V_i such that the matrix R_i has the form

$$R_i = \begin{bmatrix} R_i' & \mathbf{0} \\ \mathbf{0} & \mathbf{0} \end{bmatrix}$$

where R_i' is the adjacency matrix of a connected graph with k_i' nodes (i.e., the block R_i' has dimension $k_i' \times k_i'$). Now, we deduce from [89, art. 50] that

$$\lambda_1(R_i') \leq \sqrt{2e_i - k_i' - 1},$$

and since $\lambda(R_i) = \lambda(R_i')$, the statement follows. □

By using estimate (4.4) and Proposition 4.4 in the first and the second term on the right hand side of (4.24), respectively, we deduce

$$\lambda_1(\tilde{A}) \leq \max_{1\leq i\leq n} \lambda_1(C_{V_i}) + \lambda_1(\widehat{B}) + \max_{1\leq i\leq n} \min\left\{\sqrt{\frac{2e_i(k_i-1)}{k_i}}, \Delta(G_i^C)\right\}. \quad (4.25)$$

The inequality in (4.25) gives us a lower bound for the epidemic threshold in the case of a graph whose partition of nodes set is almost equitable. Actually

$$\tau_c^{(1)} = \frac{1}{\lambda_1(\tilde{A})} \geq \tau^\star = \frac{1}{\max\limits_{1\leq i\leq n} \lambda_1(C_{V_i}) + \lambda_1(\widehat{B}) + \max\limits_{1\leq i\leq n} \min\left\{\sqrt{\frac{2e_i(k_i-1)}{k_i}}, \Delta(G_i^C)\right\}}. \tag{4.26}$$

Now let us consider the case where we remove edges inside the communities, in a network whose set nodes has an equitable partition, then, as we said in Remark 4.2, it holds that

$$\lambda_1(\tilde{A}) \leq \lambda_1(A),$$

whence

$$\frac{1}{\lambda_1(\tilde{A})} \geq \frac{1}{\lambda_1(A)} \geq \min_i \frac{1}{d_{ii} + \lambda_1(\widehat{B})} \geq \frac{1}{\max_i(d_{ii} + \sum_j \hat{b}_{ij})}.$$

The bounds developed so far support the design of community networks with safety region for the effective spreading rate, that guarantees the extinction of epidemics. E.g. if we consider some G_i, $i = 1, \ldots, n$, it is possible to connect them such in a way to form a graph $\tilde{G} = (V, \tilde{E})$ with an almost equitable partition. Now, any subgraph obtained from $\tilde{G}$, by removing edges inside the communities, will have smaller spectral radius than $\tilde{G}$, and consequently a larger epidemic threshold. Thus the lower bound in (4.26) still holds.

Chapter 5

Heterogeneous SIS on graphs

Most studies refer to epidemic process with homogeneous infection (recovery) rate. However in many real situations, in social, biological and data communications networks, it is more appropriate to consider an heterogeneous setting than an homogeneiteous one [94].

A short overview on works in literature that consider heterogeneous populations can be found in [100, 78].

In this section we report the results in [68]. We include the possibility for the infection rate to be different for each link, thus we denote by β_{ij} the infection rate of the node j towards the node i, where $\beta_{ii} = 0$. Basically the epidemic spreads over a *directed weighted* graph. Moreover a node i can recover at rate δ_i.

As for the homogeneous SIS (introduced in Section 3.2), the SIS model with heterogeneous infection and recovery rates is as well a Markovian process, where the time for an infected node j to infect its susceptible neighbours i is an exponential random variable with average β_{ij}, and the time for a node j to recover is an exponential random variable with average δ_j.

We underline that in the first formulation of NIMFA for the heterogenous

setting in [94], a node i can infect all its neighbors with the same infection rate β_i. Here, instead, we include the possibility that the infection rates depend on the type of connection between two nodes, that may represent a wider range of more realistic scenarios.

The NIMFA governing equation in the heterogeneous setting writes

$$\frac{dp_i(t)}{dt} = \sum_{j=1}^{N} \beta_{ij} p_j(t) - \sum_{j=1}^{N} \beta_{ij} p_i(t) p_j(t) - \delta_i p_i(t),\ i = 1, \dots, N. \tag{5.1}$$

Letting $P = (p_1, \dots, p_N)^T$ and let $\overline{A} = (\overline{a}_{ij})$ be the matrix defined by $\overline{a}_{ij} = \beta_{ij}$ when $i \neq j$, and $\overline{a}_{ii} = -\delta_i$; more let $F(P)$ be a column vector whose i-th component is $-\sum_{j=1}^{N} \beta_{ij} p_i(t) p_j(t)$. Then we can rewrite (5.1) in the following form:

$$\frac{dP(t)}{dt} = \overline{A} P(t) + F(P). \tag{5.2}$$

Let $r(\overline{A}) = \max_{1 \leq j \leq N} Re(\lambda_j(\overline{A}))$ be the *stability modulus* [54] of $\overline{A}$, where $Re(\lambda_j(\overline{A}))$ denotes the real part of the eigenvalues of $\overline{A}$, $j = 1, \dots, N$. We report a result from [54] that lead us to extend the stability analysis of NIMFA in Section 3.3 to the heterogeneous case.

Theorem 5.1. *If $r(\overline{A}) \leq 0$ then $P = 0$ is a globally asymptotically stable equilibrium point in I_N for the system (5.1), instead if $r(\overline{A}) > 0$ then there exists a constant solution $P^{\infty} \in I_N - \{0\}$, such that P^{∞} is globally asymptotically stable in $I_N - \{0\}$ for (5.1) .*

Proof. See [54, Thm. 3.1]. □

5.1 Community Networks

5.1.1 Equitable partitions (an extension)

In this section we provide an extension of Section 4.2: more than two level of mixing have been considered, including, in this way, a wider range of realistic situations. More precisely, as in Section 4.2, all pairs of connected nodes in community j can infect each other with rate β_{jj}, but the rate β_{ij} at which individuals in community j infect those in community i can be different from β_{ji}, that is the rate at which individuals belonging to community i infect those in community j.
However we assume that if $\beta_{ij} \neq 0$ then $\beta_{ji} \neq 0$, for all $i, j = 1, \dots, n$. In practice this assumption means that we are considering directed weighted graphs, with the restriction that the arc $(z, w) \in E$ if and only if $(w, z) \in E$; it can only happen that their weights are different, i.e. $\gamma(w, z) \neq \gamma(z, w)$ (see Def. 1.3), when $w \in V_i$ and $z \in V_j$.
Moreover, since β_{ji} is the same for any arc from V_i to V_j, for all $i, j = 1, \dots, n$, we can use the definition of d_{ij} and, hence, of equitable partition given in Section 4.2, i.e. we do not need an alternative definition of equitable partition (see e.g. [64, Def. 8.24]). A more complex scenario may be treated in the future.

Thus, recalling that $B = (b_{ij})$ is the adjacency matrix encoding for the connectivity of the communities, we have that the transpose of the weighted adjacency matrix of our graph is $A = (a_{wz})$, where

$$a_{wz} = \begin{cases} \beta_{jj} & \text{if } w \leftarrow z, \quad w, z \in V_j \\ \beta_{ij} & \text{if } w \leftarrow z, \quad w \in V_i, \quad \text{and } z \in V_j \\ 0 & \text{if } b_{ij} = 0 \end{cases} \tag{5.3}$$

In this heterogeneous setting the transpose of the quotient matrix writes

$$Q = \mathrm{diag}(d_{ii}\beta_{ii}) + (\sqrt{d_{ij}d_{ji}}\beta_{ij}b_{ij})_{i,j=1,\dots n}. \tag{5.4}$$

We call this matrix still Q, as in Def. 4.2, for simplicity in the notation. Let us note that this matrix is not symmetric, despite the case of two infection rates discussed in Section 4.2.

When one consider a population divided in communities, it is appropriate to take into account the case where all nodes of the same community j can recover at the same rate δ_j, $j = 1, \dots, n$, and that it may differ from one community to the other. Thus let us define the $1 \times n$ vector of nonzero curing rates $\overline{\Delta} = (\overline{\delta}_1, ..., \overline{\delta}_n)$.
Under the conditions of Theorem 4.1, i.e. when at time $t = 0$, the infection probability is equal for all nodes in the same community (and may differ from one community to the other), we can reduce the number of equations in (5.2) using the matrix Q, in the following way

$$\frac{d\overline{P}(t)}{dt} = \left(\tilde{Q} - \overline{D}\right)\overline{P}(t) - \mathrm{diag}(\overline{P}(t))\tilde{Q}\overline{P}(t), \tag{5.5}$$

where $\overline{D} = \mathrm{diag}\left(\overline{\Delta}\right)$ is the curing rate matrix and

$$\widetilde{Q} = \mathrm{diag}\left(\frac{1}{\sqrt{k_j}}\right) Q\, \mathrm{diag}(\sqrt{k_j}).$$

It is immediate to observe that $\sigma(Q) = \sigma(\tilde{Q})$.

Now let us define the $1 \times N$ curing rates vector $\Delta = (\delta_1, \dots, \delta_N)$, where $\delta_z = \overline{\delta}_j$ for all $z \in V_j$ and $j = 1, \dots, n$, and $D = \mathrm{diag}(\Delta)$ is the $N \times N$ curing rate matrix. It holds the following.

Lemma 5.1. *Let $\pi = \{V_1, \dots, V_n\}$ be an equitable partition. Let A and Q weighted matrices as in* (5.3) *and* (5.4) *respectively, and S as in* (4.3)*. Then it holds that*
i) $(A - D)S^T = S^T(Q - \overline{D})$.
ii) For all $\lambda \in \mathbb{C}$ and all $x \in \mathbb{C}^n$

$$(Q - \overline{D})x = \lambda x \qquad \textit{if and only if} \qquad (A - D)S^T x = \lambda S^T x.$$

Proof. i) $AS^T = S^T Q$, indeed

$$(AS^T)_{i,j} = d_{hj}\frac{\beta_{hj}}{\sqrt{k_j}},$$

if $i \in V_h$ and

$$(S^T Q)_{i,j} = \frac{\beta_{hj}}{\sqrt{k_h}}\sqrt{d_{hj}d_{jh}},$$

if $b_{hj} \neq 0$. By (4.1) one can easily see that

$$\frac{\beta_{hj}}{\sqrt{k_h}}\sqrt{d_{hj}d_{jh}} = d_{hj}\frac{\beta_{hj}}{\sqrt{k_j}}.$$

Moreover $(DS^T)_{ih} = (S^T\overline{D})_{ih} = \frac{1}{\sqrt{k_h}}\delta_h$, if $i \in V_h$, otherwise $(DS^T)_{ih} = 0$. Thus the statement holds.
ii) Using the result in i), one can immediately apply the proof in [39, Thm. 2.2].

□

Next we report some technical facts that we will use later.

Proposition 5.1. *Let A be an $n \times n$ irreducible and non negative matrix and let $D = \mathrm{diag}(\delta_1, ..., \delta_n)$. Then it holds:*
i. $A - D$ is irreducible, for each $(\delta_1, ..., \delta_n)$.
ii. There exists an eigenvector w of $A - D$ such that $w > 0$ and the corresponding eigenvalue is $r(A - D)$, for each $(\delta_1, ..., \delta_n)$.

Proof. i. From [54]: a $n \times n$ matrix A is said to be irreducible if for any proper subset $S \subseteq \{1, \ldots, n\}$ there exists $i \in S$ and $j \in S' = \{1, \ldots, n\} - S$ such that $a_{ij} \neq 0$; since A is irreducible, the definition applies immediately to $A - D$;
ii. See [54, Lemma 4.2]. □

Now let us consider the system of N differential equations (5.2). We can prove that, in the case of a graph whose node set has an equitable partition, and regardless to the initial conditions, it is possible to determine the critical threshold for (5.2), applying Thm. 5.1, directly on the reduced system (5.5).

Proposition 5.2. *The elements of the curing rates vector $\Delta = (\delta_1, ..., \delta_N)$, that determines the critical threshold of (5.2), is identified by the elements of $\overline{\Delta} = (\overline{\delta}_1, ..., \overline{\delta}_n)$, in such a way that $\delta_z = \overline{\delta}_j$ for all $z \in V_j$, $j = 1, \ldots, n$, for which*

$$r(Q - \overline{D}) = 0, \tag{5.6}$$

where r is the stability modulus.

Proof. Basically, by Theorem 5.1, we have to show that

$$r(A - D) = r(\tilde{Q} - \overline{D}) = r(Q - \overline{D}). \tag{5.7}$$

We first prove that

$$r(Q - \overline{D}) = r(A - D). \tag{5.8}$$

By the definition of Q we have

$$S\,(A - D)\,S^T = SAS^T - SDS^T = Q - \overline{D}.$$

Now, let $c \in \mathbb{R}$ such that both $a_{zz} - \delta_z + c \geq 0$, for all $z = 1, \ldots, N$ and $q_{ii} - \overline{\delta}_i + c \geq 0$ for all $i = 1 \ldots, n$. Let us define $A - D + cI_{N\times N} = \hat{A}$ and $Q - \overline{D} + cI_{n\times n} = \hat{Q}$. $\tilde{A}$ and $\tilde{Q}$ are non negative and irreducible (see i)) in Proposition 5.1) matrices. We order the eigenvalues of $\hat{Q}$ so that $|\lambda_1(\hat{Q})| \geq |\lambda_2(\hat{Q})| \geq \ldots \geq |\lambda_n(\hat{Q})|$, making the same also for $\hat{A}$. By the Perron-Frobenius theorem, the eigenvalues of maximum modulus of an irreducible and non negative matrix is real and positive and its corresponding eigenvector, the Perron vector, is the unique (up to a factor) strictly positive eigenvector of the matrix. Hence there exists $\omega > 0$, eigenvector of $\hat{Q}$ corresponding to $\lambda_1(\hat{Q})$.

By ii) in Lemma 5.1 and since, obviously, $S^T I_{n\times n} = I_{N\times N} S^T$, we have that $S^T\omega > 0$ is the eigenvector of $\hat{A}$ corresponding to $\lambda_1(\hat{Q})$. However, since

$S^T\omega$ is strictly positive, it must be the Perron vector of $\hat{A}$, consequently $\lambda_1(\hat{A}) = \lambda_1(\hat{Q})$.

It can be immediately shown that

$$r(\hat{Q}) = \lambda_1(\hat{Q}) = \lambda_1(\hat{A}) = r(\hat{A}),$$

and that

$$r(Q - \overline{D}) + c = r(\hat{Q}) = r(\hat{A}) = r(A - D) + c, \tag{5.9}$$

thus (5.8) holds.

Now we prove that

$$r(\tilde{Q} - \overline{D}) = r(Q - \overline{D}). \tag{5.10}$$

For any n-vector v and scalar $\lambda \in \mathbb{C}$ we have

$$\left(\tilde{Q} - \overline{D}\right) v = \lambda v \Longleftrightarrow \left(\Lambda^{-\frac{1}{2}} Q \Lambda^{\frac{1}{2}} - \overline{D}\right) v = \lambda v \Longleftrightarrow$$

$$\left(Q\Lambda^{\frac{1}{2}} - \overline{D}\Lambda^{\frac{1}{2}}\right) v = \lambda\Lambda^{\frac{1}{2}} v \Longleftrightarrow \left(Q - \overline{D}\right)\left(\Lambda^{\frac{1}{2}} v\right) = \lambda\left(\Lambda^{\frac{1}{2}} v\right),$$

hence $\lambda \in \sigma(\tilde{Q} - \overline{D}) \Longleftrightarrow \lambda \in \sigma(Q - \overline{D})$, and (5.10) holds.

In conclusion from (5.10) and (5.8) we have (5.7).

□

Remark 5.1. Let us note that if A is an $n \times n$ irreducible and non negative matrix, and D a diagonal matrix with positive entries, then the eigenvalue $\lambda \in \sigma(A - D)$, such that $Re(\lambda) = r(A - D)$, is real.

Furthermore we underline that, by Corollary 4.1, irrespective of the initial conditions of nodes in the same community, it is sufficient to compute the positive steady-state vector $\overline{P}_\infty$ of the reduced system (5.5) to obtain that of the original system (5.2).

5.2 Optimal Immunization

An important challenge in epidemiology is to understand how to control the infectious disease, both in public health and in other domains, such as,

e.g., protection of computer architectures.

Here we propose an optimal antidote allocation strategy. Our problem is related to the different allocation of antidotes to each node in order to increase its recovery rate. We consider that the amount of resource allocated for a node is proportional to its recovery rate.
We know that the structure of the network plays a crucial role in the diffusion of epidemic, thus a uniform distribution of resources among nodes, that does not take into account the connectivity of the network, does not seems to work efficiently in order to eradicate the infection, or reduce the number of infected nodes [76]. Moreover the distribution of resources for the recovery have a cost, which can vary from individual to individual. Thus, a crucial aspect is to individuate a cost-optimal distribution of resources to prevent the disease from persisting indefinitely in the population.

Based on these considerations and taking into account the results of Theorem 5.1, we have designed our immunization strategy, as we shall explain into details below.

Proposed approach to the problem.

We adopt the following linear cost function , where the cost may well depend on the node itself

$$U(\Delta) = \sum_{i=1}^{N} c_i \delta_i, \tag{5.11}$$

where Δ is the immunization rate vector, and c is the cost vector, where the component $c_i > 0$, for $i = 1, \ldots, N$, is the cost for the immunization of node i at unitary rate.

Now let us consider the case where $\beta_{ij} = \beta_{ji}$, for all $i, j = 1, \ldots, N$, i.e. the weighted adjacency matrix A is symmetric. We seek for the solution of the following

Problem 5.1 (Immunization: Eigenvalue Constraint Formulation)**.** Find

$\Delta \geq 0$ which solves

$$\begin{aligned} &\text{minimize} && c \cdot \Delta^T \\ &\text{subject to:} && \lambda_1\big(A - \operatorname{diag}(\Delta)\big) \leq 0, \qquad \Delta \geq 0 \end{aligned}$$

The immunization problem can be reformulated as a semidefinite programming that is a convex optimization problem [19]. In fact we observe that $\operatorname{diag}(\Delta) = \sum_{i=1}^{N} \Delta_i \operatorname{diag}(\mathbf{e}_i)$, where Δ_i is the i-th component of Δ and $\mathbf{e}_i$ is the i-th element of the standard basis, so that $\operatorname{diag}(\mathbf{e}_i) \geq 0$; hereafter the inequality sign in $M \geq 0$ when M is a matrix, means that M is positive semidefinite. Thus we can express the optimization problem with eigenvalue constraint as a semidefinite programming problem in the following way

Problem 5.2 (Immunization: Semidefinite Programming Formulation)**.** Find Δ which solves

$$\begin{aligned} &\text{minimize} && c \cdot \Delta^T \\ &\text{subject to:} && \operatorname{diag}(\Delta) - A \geq 0 \\ & && \Delta \geq 0 \end{aligned}$$

The feasibility of the problem is always guaranteed, as showed in the following

Theorem 5.2 (Feasibility)**.** *The immunization problem is feasible.*

Proof. We define $l_{\max} := \max_i \sum_j a_{ij}$ and choose $\Delta = l_{\max} u$, where u is the all-one vector: $D = l_{\max} I_N$. Then for any vector $w = \sum_{i=1}^{N} z_i v_i$, where $\{v_1, \ldots, v_N\}$ is an eigenvector basis of A, it holds

$$w^T(A - D)w = w^T(\sum \lambda_i(A) z_i v_i - l_{\max} w) \leq (\lambda_1(A) - l_{\max})|w|^2 \leq 0,$$

where the last inequality follows since $\lambda_1(A) \leq \max_i \sum_j a_{ij}$. Hence the chosen vector satisfies the constraint and we can assert that the feasible region is not empty. □

Since the problem is feasible there is always an optimal point on the boundary [19] and, by a fundamental result of convex optimization, any locally optimal point of a convex problem is globally optimal [18, Sec. 4.4.2].

A semidefinite programming (SDP) approach for the study of optimal resource allocation in a network has been discussed also in [77]. However the problem statement is different. First, each node i can infect all its neighbors with the same infection rate β_i, while in our construction β_{ji} depends on the arrival node j; moreover they try to minimize an arbitrary convex function of the infection rates, considering, unlike us, a given curing rate profile.
In the next section we shall extend our approach to a network divided in communities. Indeed, in most of the real situations, it may be more appropriate consider policies for different entire groups (hospitals, schools, villages, cities, etc,...), rather than for each individual.

5.2.1 Optimization for Networks with Equitable Partitions.

In this section we consider a different allocation of antidotes to each community. Let us consider the case where $\beta_{ij} = \beta_{ji}$, $i, j = 1, \ldots, n$. In this case the matrix Q is symmetric and its eigenvalues are real. Considering the reduced curing rate vector $\overline{\Delta}$ and the $1 \times n$ cost vector c, where each component refers to the cost for the immunization of a community at unitary rate, then we seek for the solution of the following

Problem 5.3 (Immunization: Eigenvalue Constraint Formulation)**.** Find $\overline{\Delta} \geq 0$ which solves

$$\begin{aligned} &\text{minimize} && c \cdot \overline{\Delta}^T \\ &\text{subject to:} && \lambda_1\big(Q - \operatorname{diag}(\overline{\Delta})\big) \leq 0, \qquad \overline{\Delta} \geq 0 \end{aligned}$$

Problem 5.4 (Immunization: Semidefinite Programming Formulation)**.** Find

$\overline{\Delta} \geq 0$ which solves

$$\begin{aligned} &\text{minimize} && c \cdot \overline{\Delta}^T \\ &\text{subject to:} && \operatorname{diag}(\overline{\Delta}) - Q \geq 0 \\ & && \overline{\Delta} \geq 0 \end{aligned}$$

Semidefinite programs can be solved using standard tools [88]. For systems of moderate size (e.g., on the order of $n = 100$ communities), the number of involved variables does not represent a serious performance bottleneck and standard solvers perform well in practice. We further observe that from Thm. 5.2, the feasibility of the problem is always guaranteed. Scalability properties limit the usage of semidefinite programming for very large graphs, which in general need not to be sparse.

Now we tackle a simplified case where an accurate polynomial time complexity algorithm (that we shall discuss in Appendix A) can be employed instead. In order to do so, we need a few technical facts recalled next:

Proposition 5.3. *Let A be an $n \times n$ symmetric, irreducible and non negative matrix and let $D = \operatorname{diag}(\delta_1, ..., \delta_n)$. Then it holds:*
i. Let $\delta_i = 0$ for some $i = 1, \dots n$, then $\lambda_1(A - D) \geq 0$.
ii. The function $(\delta_1, ..., \delta_n) \longmapsto \lambda_1(D - A)$ is continuous.

Proof. i) Let consider $\delta_i = 0$ for some $i = 1, \dots n$ and assume by contradiction that $\lambda_1(A - D) < 0$, this means that the matrix $A - D$ must be definite negative; however if we take the vector $\mathbf{e}_i$ of the canonical basis of $\mathbb{R}^n$, then it holds that $\mathbf{e}_i^T(A - D)\mathbf{e}_i = \mathbf{e}_i^T A \mathbf{e}_i \geq 0$ and we have a contradiction.
ii) It follows since the eigenvalues of a matrix A vary with continuity with the entries of A, see [47, Appendix D]. □

Two-level immunization

Now we consider the case where the set of communities is divided in two categories: one where the communities have curing rate δ_0, and the other, with communities whose curing rate is δ_1; as above, $\beta_{ij} = \beta_{ji}$, for all $i, j = 1, \dots, n$.

This kind of situation can be well represented by a quotient graph that is, e.g., bipartite (where each node may represent a full-meshed community), or an interconnected stars network (see Section 4.3.2).

We can consider the following partition of the node set: the set $\{V_1^0, ..., V_m^0\}$, and the set $\{V_1, ..., V_{m'}\}$, clearly the set partition $\pi = V_0 \cup V_1$, where $V_0 = (\cup_i V_i^0)$ and $V_1 = (\cup_i V_i)$ must be equitable.
For convenience we define the central communities, those whose elements have curing rate δ_0, and terminal communities those whose elements have curing rate δ_1.

Thus, let us consider the curing matrix $D = \text{diag}\,(\delta_0 \mathbf{1}_m, \delta_1 \mathbf{1}_{m'})$. We also define

$$I_m^0 = \begin{bmatrix} I_m & 0 \\ 0 & 0 \end{bmatrix}, \qquad I_{m'}^1 = \begin{bmatrix} 0 & 0 \\ 0 & I_{m'} \end{bmatrix}$$

where I_m is the identity matrix of order m.

The semidefinite programming for the two-level curing rates, shortly the $2D$ immunization problem, is resumed below:

Problem 5.5 (Semidefinite Programming 2D Formulation)**.** Find $\Delta_2 = (\delta_0, \delta_1)$ which solves

$$\begin{aligned} &\text{minimize} && U(\Delta_2) \\ &\text{subject to:} && \delta_0 I_m^0 + \delta_1 I_{m'}^1 - Q \geq 0 \\ & && \Delta_2 \geq 0 \end{aligned}$$

where $c = (c_0, c_1)$ with $c_0 = \sum_i c_i^0$ and $c_1 = \sum_i c_i$ are the sum of the costs for the immunization of the central communities and the terminal communities, respectively.

In the design of our algorithmic solution we will need some properties of the $2D$ problem.

Lemma 5.2 (Monotonicity)**.** *Let $\phi : \delta_0 \longmapsto \phi(\delta_0)$ be the function that associates to each $\delta_0 \in \mathbb{R}^+$ the value $\delta_1 = \phi(\delta_0) \in \mathbb{R}^+$ such that $\lambda_1(Q - \text{diag}\,(\delta_0 \mathbf{1}_m, \delta_1 \mathbf{1}_{m'})) = 0$. Then ϕ is decreasing.*

Proof. Let $z > 0$ and assume that $\phi(\delta_0 + z) = \phi(\delta_0) + \zeta > \phi(\delta_0)$, for some $\zeta > 0$, i.e, that ϕ is not decreasing. From the definition of ϕ there exists $0 \neq w \in \ker\Big(\operatorname{diag}\left(((\delta_0 + z)\mathbf{1}_m, \phi(\delta_0 + z)\mathbf{1}_{m'}\right) - Q\Big)$. Hence, we can write

$$\begin{aligned} &w^T\Big(Q - \operatorname{diag}\left(\delta_0\mathbf{1}_m, \phi(\delta_0)\mathbf{1}_{m'}\right)\Big)w = w^T \operatorname{diag}\left(z\mathbf{1}_m, \zeta\mathbf{1}_{m'}\right)w + \\ &w^T\Big(Q - \operatorname{diag}\left((\delta_0 + z)\mathbf{1}_m, \phi(\delta_0 + z)\mathbf{1}_{m'}\right)\Big)w \\ &= w^T \operatorname{diag}\left((z\mathbf{1}_m, \zeta\mathbf{1}_{m'})\right)w > 0 \end{aligned} \tag{5.12}$$

where the strict inequality holds because $\operatorname{diag}\left(z\mathbf{1}_m, \zeta\mathbf{1}_{m'}\right) > 0$; hence because $\lambda_1\Big(Q - \operatorname{diag}(\delta_0\mathbf{1}_m, \phi(\delta_0)\mathbf{1}_{m'}\Big) = 0$, this means that $Q - \operatorname{diag}(\delta_0\mathbf{1}_m, \phi(\delta_0)\mathbf{1}_{m'})$ must be semidefinite negative and we have a contradiction. □

Let us denote by Γ the feasibility region of Prob. 5.5; it is convex [18]. We prove that the search for the optimal solution can be confined to a compact subset of the feasibility region.

Theorem 5.3 (Compact search set)**.** *There exist two pairs* $(\delta_0^{\min}, \delta_0^{\max})$ *and* $(\delta_1^{\min}, \delta_1^{\max})$ *such that a solution* $\Delta_2^* = (\delta_0^*, \delta_1^*)$ *of Prob. 5.5 belongs to a compact subset* $\Gamma' \subseteq [\delta_0^{\min}, \delta_0^{\max}] \times [\delta_1^{\min}, \delta_1^{\max}]$.

Proof. Let us define $\Delta_2^{l_{\max}} = (l_{\max}, l_{\max})$, $U_{l_{\max}} = c_0 l_{\max} + c_1 l_{\max}$ and $U^* = c_0\delta_0^* + c_1\delta_1^*$.

By Thm. 5.2, $\Delta_2^{l_{\max}} \in \Gamma$, hence $U_{l_{\max}} \geq U^*$ and, letting $\Omega = \{(\delta_0, \delta_1) : c_0\delta_0 + c_1\delta_1 \leq U_{l_{\max}})\}$, it follows that $(\delta_0^*, \delta_1^*) \in \Gamma' = \Gamma \cap \Omega$; Γ' is closed as intersection of closed set.

Now, feasibility conditions of Prob. 5.5 require matrix $Q - \delta_0 I_m^0 + \delta_1 I_{m'}^1$ to be semidefinite negative. We define $f(\delta_0) = \lambda_1\Big(Q - \delta_0 I_m^0 + (\frac{U_{l_{\max}} - c_0\delta_0}{c_1})I_{m'}^1\Big)$: we have $f(l_{\max}) \leq 0$ since $(l_{\max}, l_{\max}) \in \Gamma$ and $f(0) > 0$ by $i)$ of Prop. 5.3. By assertion $ii)$ in Prop. 5.3, $f(\delta_0)$ is a continuous function, hence, there exists $\delta_0^{\min}$ such that $f(\delta_0^{\min}) = 0$, and since ϕ is decreasing $\phi(\delta_0^{\min}) = \delta_1^{\max}$. We can repeat the same reasoning by inverting the role of δ_1 and δ_0 defining $g(\delta_1) = \lambda_1\Big(Q - (\frac{U_{l_{\max}} - c_1\delta_1}{c_0})I_m^0 + \delta_1 I_{m'}^1\Big)$; then assert that exists $\delta_1^{\min}$ such that $g(\delta_1^{\min}) = 0$ and $\phi(\delta_1^{\min}) = \delta_0^{\max}$.

Hence let $r : c_0\delta_0 + c_1\delta_1 = U_{l_{\max}}$, the points $(\delta_0^{\min}, \delta_1^{\max})$ and $(\delta_0^{\max}, \delta_1^{\min})$ belong to $\partial\Gamma \cap r$, i.e. they belong to $\partial\Gamma'$, so $\Gamma' \subseteq [\delta_0^{\min}, \delta_0^{\max}] \times [\delta_1^{\min}, \delta_1^{\max}]$, and consequently, being Γ' closed, it is also compact. □

Remark 5.2. Thm. 5.3 allows us to identify the interval of the values of δ_0 and δ_1 restrict the search of (δ_0^*, δ_1^*), indeed since $\Gamma' \subseteq [\delta_0^{\min}, \delta_0^{\min}] \times [\delta_1^{\min}, \delta_1^{\max}]$ and $(\delta_0^*, \delta_1^*) \in \Gamma'$, then $\delta_0^* \in [\delta_0^{\min},\ \delta_0^{\max}]$ and $\delta_1^* \in [\delta_1^{\min}, \delta_1^{\max}]$. This is one key property in the numerical search of the optimal solution proposed in Appendix A.

A direct proof that the optimal solution lies on $\partial\Gamma'$ follows:

Corollary 5.1. *A solution $\Delta_2^* = (\delta_0^*, \delta_1^*)$ of Prob. 5.5 belongs to $\partial\Gamma' \cap \Omega$.*

Proof. Let us assume $\Delta_2^* = (\delta_0^*, \delta_1^*) \in \Gamma' \setminus \partial\Gamma'$. Δ_2^* is feasible, hence $\lambda_1(\beta Q - D) < 0$, with $D = \mathrm{diag}\,(\delta_0\mathbf{1}_m, \delta_1\mathbf{1}_{m'})$. From Thm. 5.3 ii., again we can find $0 < \delta_1' < \delta_1^*$ such that $\lambda_1(\beta Q - \mathrm{diag}(\delta_0^*\mathbf{1}_m, \delta_1'\mathbf{1}_{m'})) = 0$, where, i.e., $\Delta_2' \in \partial\Gamma'$. But, $U(\Delta_2^*) - U(\Delta_2') = c_1(\delta_1^* - \delta_1') > 0$. Contradiction. □

Two-layers networks. In order to provide further insight, the closed form of the optimal solution is reported below for the two-layer networks that we have discussed, as a special case of interconnected stars networks, in Section 4.3.2. We consider here the case where the rate of infection β is constant among the population.
According to (5.6) we have to find the value of δ_0 and δ_1 for which $\beta Q - D$ has a maximal eigenvalue equal to zero, with Q as in (4.23). The characteristic polynomial of $\beta Q - D$ is

$$p_\lambda(\beta Q - D) = \lambda^2 + (\delta_0 + \delta_1 - \beta d_0)\lambda + \delta_0\delta_1 - \beta d_0\delta_1 - \beta^2\varepsilon^2 d_1.$$

First of all 0 belongs to the spectrum of $\beta Q - D$ when $\delta_1\delta_0 = \beta^2\varepsilon^2 d_1 + \beta d_0\delta_1$. This also ensures that the second eigenvalue is negative and, consequently, 0 must be the largest eigenvalue of $\beta Q - D$. The linear cost optimization is solved for

$$\delta_0 = \beta d_0 + \beta\varepsilon\sqrt{\frac{c_1 d_1}{c_0}}, \quad \delta_1 = \beta\varepsilon\sqrt{\frac{c_0 d_1}{c_1}}. \tag{5.13}$$

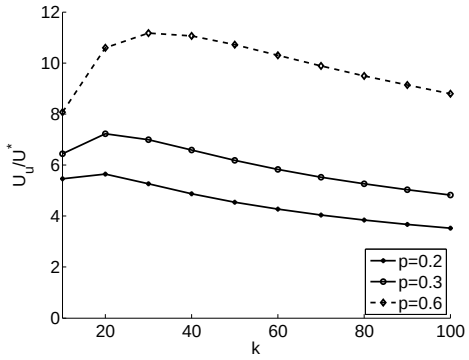

Figure 5.1: (a) Ratio U_u/U^* for increasing dimension k of the terminal communities: $c_i^0 = c_i^1 = 1$, $i = 1 \dots m$. The curves refer to three Erdős-Rényi networks with 50 central nodes, generated for $p = 0.2$, $p = 0.3$ and $p = 0.6$ respectively.

Remark 5.3. Closed form (5.13) provides a simple connection between the NSIs topology – under regularity assumptions – and optimal immunization strategies: 1) linear term βd_0 appearing in δ_0 is due to the cost sustained to protect from virus exchanged across central communities; 2) optimal immunization of central communities requires an additional term $\sqrt{c_1\, d_1/c_0}$ due to infections of terminal community nodes. Overall, from (5.13) we see that limiting the number of terminal connections per subnetwork may represent only partially a good practice, and it should be combined to frequent allocation of resource at central communities.

Numerical Results.

Here, for our numerical experiments, we consider the case of an interconnected stars network (see Section 4.3.2), moreover we consider that only the curing rates may be different, hence the infection rate is the same among all nodes. We plan to investigate numerically, in the future, also the implication of others network topology on our two-level immunization algorithm and the influence of considering different infection rates.

In Figure 5.1 we compare the ratio between the cost U_u of the uniform curing rate vector and the optimal cost $U^* = U(\Delta^*)$ solving the $2D$ immunization Prob. 5.5. The uniform curing rate vector is $\Delta = \delta \mathbf{1}_N$ where δ is the minimum value of the components of $\overline{\Delta}$, such that the threshold in (5.6) is attained.

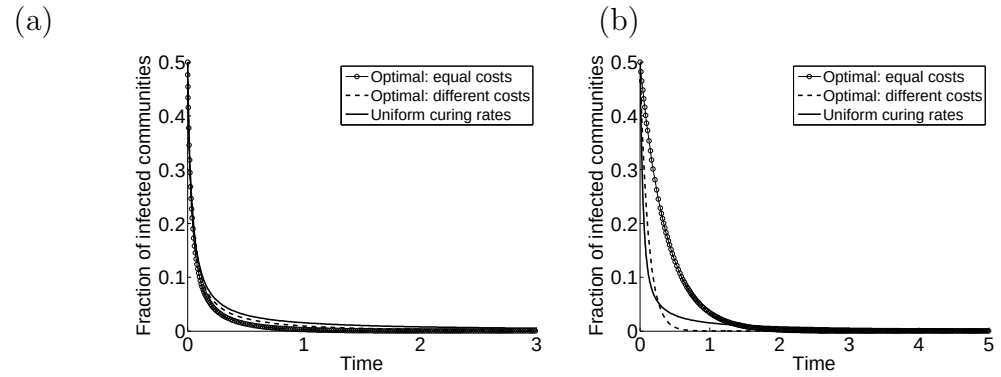

Figure 5.2: Fraction of infected communities as a function of the time. The three curves represent respectively: 1) optimal vector of curing rates (Prob. 5.5) for $c_i^0 = c_1^i = 1$, $i = 1 \dots m$, 2) for $c_i^0 = 10$ and $c_i^1 = 1$, $i = 1 \dots m$, 3) uniform vector of curing rates that satisfies (5.6). Initial conditions:(a) central nodes infected. (b) terminal communities infected.

The computation is made for different values of k, i.e., we consider uniform terminal community dimension, and for three different networks. The networks considered have $m = 50$ central nodes and $m = 50$ terminal communities that differ, each other, for the average degree of the central nodes: the connectivity of the central nodes correspond to three sample Erdős-Rényi graphs with $p = 0.2$, $p = 0.3$, $p = 0.6$, respectively. The ratio increases with k until a maximum value: after the maximum the ratio is decreasing. The plot confirms that the gain obtained by $2D$ immunization policies versus a uniform approach is large, in particular, the larger the denser the network (i.e. when p increases). Such advantage decreases, as expected, when the dimension of the terminal communities becomes dominant compared to the number of central communities. Also, the value of k where the maximum is attained increases with the network's density (i.e. with increasing p). Given a certain topology for the network of the communities, the best relative performance for the $2D$ optimization corresponds to an optimal number of terminal connections per subnetwork.

Figure 5.2(a) and Figure 5.2(b) describe the speed of recovery from a virus infection for various immunization strategies. In particular, we consider two

cases: Figure 5.2(a) represents the case when all central nodes are initially infected, while Figure. 5.2(b) when all terminal communities are infected. There we report on the dynamics of the fraction of infected communities for a network with $m = 50$ central nodes, and with $k = 20$ per terminal community. In these figures, we compare the dynamics under the uniform curing rate vector, and the optimal solutions for the $2D$ immunization, for the case $c_i^0 = c_i^1 = 1$ and $c_i^0 = 10$, $c_i^1 = 1$, $i = 1 \dots m$, respectively. We observe that different curing vectors have a little impact in the dynamics when the infection originates at central nodes (see Figure 5.2(a)), anyhow having different curing rate still provide an advantage in terms of costs, as depicted in Figure 5.1. In Figure 5.2(b) we observe that by putting more weight onto the central nodes, the optimal solution tend to immunize terminal communities at higher rate, providing faster response to the infections originating from terminal communities.

5.3 Heterogeneous SIS on graphs with stochastic rates

The model that we have studied until now assumes that the the infection rate (such as the recovery rate) is given a *priori*, and it does not change in time.

These assumptions can be a good start point in order to study the evolution of epidemics on graphs, however the parameters of the model may have a great variability, because, e.g, most of the approaches to empirically obtain them, from external data, are fraught with errors and uncertainty [30]. Moreover this variability can also derive, simply, on the presence of a random environment, indeed the system environment may be subject to randomly occurring fluctuations which appear as fluctuation of the parameters around some average values.

Thus, in order to include this random effects we modify the NIMFA model considering that the rate parameters can be affected by some stochastic fluc-

tuations.

Precisely, let Ω be a given reference sample space, and $\omega \in \Omega$ one possible outcome that represents a possible perturbation of the population's parameters. We consider that the disease spreads among the population according to the dynamics

$$\begin{aligned} \dot{x}_i(t,\omega) =& \beta(\omega)s_i(t,\omega)(1-x_i(t,\omega)) - \delta(\omega)x_i(t,\omega), \qquad i \in \{1,\dots,N\} \\ s_i(t,\omega) =& \sum_{j=1}^{N} a_{ij}x_j(t,\omega) \end{aligned} \tag{5.14}$$

Hence, the rate coefficients, $\beta(\omega)$ and $\delta(\omega)$, as well as the unknowns $x_i(t,\omega)$, are assumed to be random variables on the probability space $(\Omega, \mathcal{F}, \mathbb{P})$, for a given σ-algebra $\mathcal{F}$ and a probability measure $\mathbb{P}$ on it.

Log-normal distribution. In most cases, where the rate parameters cannot be fixed a priori, we only know their statistical properties.

The following questions arise:

- Assume that the rate parameters have distributions with known mean values and variances, then what is the probability of extinction for the epidemic?
- Can we compute the average value of epidemics in the population, in the long range?

Let us try to understand what might happen, considering the following "toy model", i.e. a simple one-dimensional logistic equation

$$\dot{x}(t) = -\delta x(t) + \beta x(t)(1-x(t)). \tag{5.15}$$

The equation has the global solution

$$x(t) = \frac{(\beta-\delta)e^{(\beta-\delta)t}x_0}{(\beta-\delta)+\beta(e^{(\beta-\delta)t}-1)x_0}.$$

For $\frac{\beta}{\delta} > 1$, the equation has a global solution which is positive and bounded and has the asymptotic limit $x(t) \to \frac{\beta-\delta}{\beta}$ as $t \to \infty$. On the other hand, for $\frac{\beta}{\delta} < 1$ then the solution remains positive and bounded, but asymptotically converges to 0 as $t \to \infty$.

Now we consider that the parameters characterizing the infection, β and δ, follow a log-normal distribution. This assumption is inspired by works that consider real-world datasets, e.g., in [98] the authors find that infection rates with the log-normal distribution fit best the data of SARS in 2003 [78].

In particular, we assume that β and δ have the same average $\mathbb{E}[\beta] = \mathbb{E}[\delta] = \mu$. In such a case, for deterministic β and δ, one should expect to stay in the critical region. Below we study the probability of being in the over-threshold region (the epidemics remains endemic) and, in this case, what is the average x_∞ for the asymptotic limit of the epidemic distribution.

Thus, let us assume $\beta \sim \ln \mathcal{N}(a, b^2)$, i.e., there exists a standard normal distribution Z such that

$$\beta = e^{a+bZ}.$$

It follows:

$$\mu_\beta = \mathbb{E}[\beta] = e^{a+b^2/2}, \qquad \sigma_\beta^2 = \mathrm{Var}(\beta) = (e^{b^2} - 1)\mu_\beta^2.$$

If $\delta \sim \ln \mathcal{N}(c, d^2)$ is independent from β, then the ratio $\zeta = \beta/\delta$ has again a log-normal distribution $\ln \mathcal{N}(a - c, b^2 + d^2)$, hence

$$\mathbb{E}[\zeta] = e^{d^2} \frac{\mathbb{E}[\beta]}{\mathbb{E}[\delta]}, \qquad \mathrm{Var}(\zeta) = (e^{b^2+d^2} - 1)e^{d^2} \left(\frac{\mathbb{E}[\beta]}{\mathbb{E}[\delta]}\right)^2$$
$$= (e^{b^2+d^2} - 1)e^{d^2} \left(\frac{\mathrm{Var}(\beta)}{(e^{b^2} - 1)} \frac{(e^{d^2} - 1)}{\mathrm{Var}(\delta)}\right)$$

Let us denote $m = (a - c)$ and $s^2 = (b^2 + d^2)$ the parameters of ζ. The probability density function has the form

$$f_\zeta(x) = \frac{1}{\sqrt{2\pi s^2 x^2}} \exp\left(-\frac{1}{2s^2}(\ln(x) - m)^2\right).$$

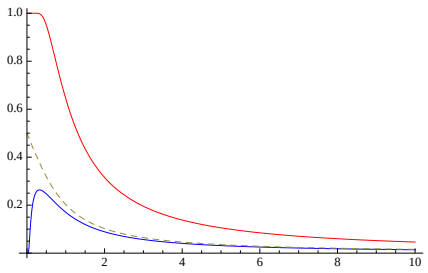

Figure 5.3: $\mathbb{P}[\zeta > 1]$, over-threshold (red), critical (dashed), under-threshold (blue). The x-axis contains the variance σ_β^2 of the infection rate β.

Deterministic δ - part 1. We analyze the probability of a non-zero limit behaviour of the solution in the case the curing rate δ is deterministic. We analyze the cases $\mathbb{E}[\beta] < \delta$ (sub-critical case), $\mathbb{E}[\beta] = \delta$ (critical case) and $\mathbb{E}[\beta] > \delta$ (super-critical case). Recall that in the deterministic case, there exists a global positive solution in the super-critical case, while in the first two situations, the solution converges to 0.

Proposition 5.4. *For a random infection rate $\beta = e^{a+bZ}$ and a curing rate δ deterministic, the probability of an endemic state is*

$$\mathbb{P}[\zeta > 1] = 1 - \frac{1}{2} erfc\left(\frac{a-c}{\sqrt{2}b}\right) \tag{5.16}$$

where $c = \ln(\delta)$.

In Figure 5.3 we see that the higher the variance the lower the probability of being over-threshold, even if we already start on this side. On the other hand, the presence of a (small) randomness allows the under-threshold case to get to a positive limit, with a positive probability.

Deterministic δ - part 2. Next, we consider the expected value of the limit solution in case it results to be positive. In the deterministic case, this happens only in the super-critical case, and the limit (in this case) is $x_\infty = 1 - \frac{\delta}{\beta}$.

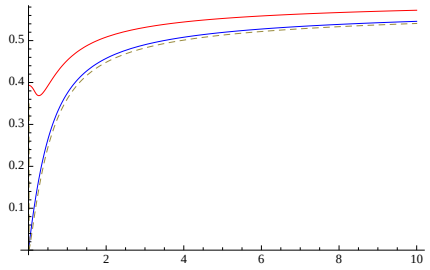

Figure 5.4: x_∞, over-threshold (red), critical (dashed), under-threshold (blue). The x-axis contains the variance σ_β^2 of the infection rate β.

In presence of noise, we have seen that there is a positive probability of survival of the infection in the limit; thus, we shall analyze the results in all the three cases.

Proposition 5.5. *The expected value of the limit infection conditioned on the persistence of the infection is*

$$x_\infty := \mathbb{E}[1 - \frac{1}{\zeta} \mid \zeta > 1] = \frac{e^{\frac{b^2}{2}-a+c} erfc\left(\frac{b^2-a+c}{\sqrt{2}b}\right)}{erfc\left(\frac{a-c}{\sqrt{2}b}\right) - 2} + 1 \tag{5.17}$$

where $c = \ln(\delta)$.

In Figure 5.3 we see that as σ_β goes to 0, the three curves converge to the deterministic values (according to the parameters' values). As σ_β goes to $+\infty$, all the three curves converge to the value $\frac{2}{3}$.

After this preliminaries results, we consider the system (5.14), investigating, via numerical experiments, the influence of the variance of independent and identically distributed infection rates, on the steady-state average fraction of infected nodes, which indicates the severity of the overall infection.

Specifically, let us consider β_{ij} that, we remember, is the rate at which the node j infect the node i. We assume that each infection rate β_{ij} has a log-normal distribution $\ln\mathcal{N}(a, b^2)$ with $\mathbb{E}[\beta_{ij}] = \mu_{\beta_{ij}} = \mu$, and $\mathrm{Var}(\beta_{ij}) = \sigma^2_{\beta_{ij}} = \sigma^2$, for all $i, j = 1, \ldots, N$; δ is assumed constant among the population.

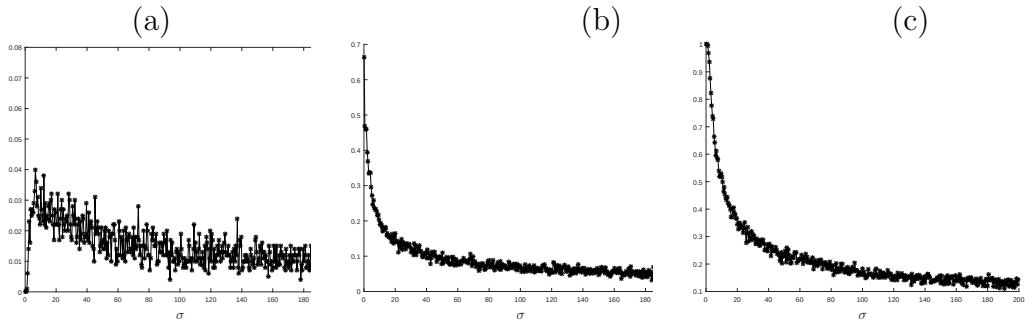

Figure 5.5: Proportion of processes on which persists a positive fraction of infected nodes, as function of σ, for a network with arbitrary topology and $N = 13$, with $\tau_c^{(1)} = 0.2045$ (a) $\mu/\delta < \tau^{(1)}$, with $\mu = 1$, $\delta = 8$ (b) $\mu/\delta = \tau_c^{(1)}$, with $\mu = 1$, $\delta = 4.89$ (c) $\mu/\delta < \tau_c^{(1)}$, with $\mu = 1$, $\delta = 4$.

In order to compare the results in Figure 5.3 we compute the proportion of processes on which persists a positive fraction of infected nodes, as function of σ, for a network with arbitrary topology and $N = 13$ (see Fig. 5.3).

We generate 1000 sample values of the random variables with log-normal distribution solving, at each step, the system (5.14): in (a) we consider the sub-critical case, $\mu/\delta < \tau_c^{(1)}$, in (b) the critical case, $\mu/\delta = \tau_c^{(1)}$, and in (c) the super-critical case, $\mu/\delta > \tau_c^{(1)}$. In the homogenous setting, with deterministic β and δ, for the critical and sub-critical case, the NIMFA model predicts the extinction in the long-term, instead in the super-critical case there is a stationary positive solution, that is globally asymptotically stable (excluding the zero vector from the set of initial conditions)[17].

In Figure 5.3 (a)(b)(c) we can clearly recognize the same behavior of the one-dimensional logistic model (see Figure 5.3) in each of three cases, the sub-critical, critical and super-critical case, respectively. Thus, the same observations regarding the influence of the infection rates' variance, on the strength of the infection, still hold.

5.4 A stochastic differential equation SIS model

Most realistic heterogeneous parameter distributions are not fixed in time, but could be considered as additional dynamical variables [100]. Here we report the results in [15], where, in order to model the fluctuations in time of the parameters, we consider white noise [6, Chapter 3], a natural starting point for the case when the functional form and properties of the stochastic process are not known [100, 57, 41].

In particular, we consider that a node i can be infected by all its infected neighbors with rate β_i, that is described by a stochastic process of the form

$$\beta_i \longrightarrow \beta + \sigma_i(x)\, \dot{w}_i(t),$$

where $\dot{w}_i(t)$ is the white-noise mapping and the functions $\sigma_i : \mathbb{R} \to [0, +\infty)$, that provides the noise level for each node, are locally Lipschitz continuous, that satisfy

$$\sup_{x\in(0,1)} \frac{\sigma_i(x)}{x} \leq M, \quad \text{for all} \quad i = 1, \ldots, N. \tag{5.18}$$

This choice implies that the intensity of the infection rate varies around a mean value, and the disturbance is small if the value of the probability of infection is small.

We shall assume that $W(t) = (w_1(t), \ldots, w_N(t))$ is an N-dimensional Brownian motion, defined on a stochastic basis $(\Omega, \mathcal{F}, \{\mathcal{F}_t\}, \mathbb{P})$ with the usual conditions (i.e. it is complete and right continuous), and with covariance matrix tI_N, where I_N is the $N \times N$ identity matrix.
For the sake of simplicity, we shall assume that the recovery rate δ is a deterministic constant. The general case does not change substantially the results that we present here.
Starting from (5.14) we can describe the system by the following Itô stocha-

stic differential equation

$$\begin{aligned} \mathrm{d}x_i(t) &= [\beta s_i(t)(1-x_i(t)) - \delta x_i(t)]\ \mathrm{d}t + \sigma_i(x_i(t))s_i(t)(1-x_i(t))\,\mathrm{d}w_i(t), \\ s_i(t) &= \sum_{j=1}^{N} a_{ij}x_j(t), \qquad i \in \{1,\dots,N\} \end{aligned} \tag{5.19}$$

with a given vector of initial conditions $(x_1(0),\dots,x_N(0))$.

We introduce also the vector-valued stochastic differential equation

$$\begin{aligned} \mathrm{d}X(t) &= f(X(t))\,\mathrm{d}t + g(X(t))\,\mathrm{d}W_t \\ X(0) &= (x_1(0),\dots,x_N(0)), \end{aligned} \tag{5.20}$$

where $X(t) = (x_1(t),\dots,x_N(t))$ while $f(X(t))$ and $g(X(t))$ are functions defined in $\mathbb{R}^N$ and $L(\mathbb{R}^N,\mathbb{R}^N)$, respectively. The j-th component of f is $\beta(1-x_j(t))s_j(t)-\delta x_j(t)$, whereas g is a diagonal matrix with entries $\sigma_j(x_j(t))(1-x_j(t))s_j(t)$. We shall denote $\Delta = (0,1)^N$.

5.4.1 Dynamics of the stochastic model

Theorem 5.4. *For any initial condition $X(0) = (x_1(0),\dots,x_N(0))$ such that $X(0) \in \Delta$, there exists a unique global solution to system (5.19) on $t \geq 0$ and the solution remains in Δ almost surely for all times.*

Proof. Since the coefficients of the equation are locally Lipschitz continuous, for any given initial value $X(0) \in (0,1)^N$ there is a unique local solution on $t \in [0,\tau_e)$, where τ_e is the explosion time (see for instance [6]).
To show this solution is global, we need to show that $\tau_e = \infty$ a.s. This is achieved if we prove a somehow stronger property of the solution, namely that it never leaves the domain Δ. Let $n_0 > 0$ be sufficiently large for $x_i(0) \in \left(\frac{1}{n_0}, 1-\frac{1}{n_0}\right)$ for all $i = 1,\dots N$. For each integer $n \geq n_0$, define the stopping time

$$\tau_n = \inf\left\{t \in [0,\tau_e) : \min_{1\leq i\leq N} x_i(t) \leq 1/n \text{ or } \max_{1\leq i\leq N} x_i(t) \geq 1-1/n\right\},$$

where, as customary, $\inf \emptyset = +\infty$ (with $\emptyset$ denoting the empty set).
Clearly τ_n is increasing as $n \to \infty$ and letting $\tau_\infty = \lim_{n\to\infty} \tau_n$, we have $\tau_\infty \leq \tau_e$ a.s. Hence we basically need to show that $\tau_\infty = \infty$ a.s; if this were not so, there would exists a pair of constants $T > 0$ and $\epsilon \in (0, 1)$ such that

$$\mathbb{P}\{\tau_\infty \leq T\} > \epsilon.$$

Accordingly, there is an integer $n_1 \geq n_0$ such that

$$\mathbb{P}\{\tau_n \leq T\} \geq \epsilon \qquad \forall n \geq n_1. \tag{5.21}$$

Now we define a function $V : (0, 1)^N \to \mathbb{R}^+$ as

$$V(X(t)) = -\sum_{i=1}^{N} \log\left[x_i(t)(1 - x_i(t))\right].$$

By Itô's formula we have

$$\begin{aligned} \mathrm{d}V(X(t)) = &\sum_{i=1}^{N} \left(\frac{1}{1-x_i} - \frac{1}{x_i}\right) \left[(\beta s_i(1-x_i) - \delta x_i)\ \mathrm{d}t + \sigma_i(x_i)s_i(1-x_i)\,\mathrm{d}w_i(t)\right] \\ &+ \frac{1}{2}\sum_{i=1}^{N} \left(\frac{1}{(1-x_i)^2} + \frac{1}{x_i^2}\right) \sigma^2(x_i)s_i^2(1-x_i)^2\,\mathrm{d}t, \end{aligned} \tag{5.22}$$

where we hide the explicit dependence on time of the processes x_i and s_i. Let L be the infinitesimal generator associated to the stochastic equation (5.20) defined, for $V \in C^\infty(\Delta)$, by

$$LV(X) = \sum_{i=1}^{N} f_i(X)\partial_{x_i}V(X) + \frac{1}{2}\sum_{i=1}^{N} g_{ii}^2(X)\partial^2_{x_ix_i}V(X), \qquad X = (x_1, \ldots, x_N); \tag{5.23}$$

then from (5.22)

$$\mathrm{d}V(X(t)) = LV(X(t))\mathrm{d}t + \mathrm{d}M(t),$$

where $M(t)$ is the (local) martingale defined by

$$M(t) = \sum_{i=1}^{N} \int_0^t \left(\frac{1}{1-x_i(t)} - \frac{1}{x_i(t)}\right) \sigma_i(x_i(t))s_i(t)(1-x_i(t))\,\mathrm{d}w_i(t).$$

Lemma 5.3. *There is a finite constant K such that $LV(X) \leq K$ for every $X \in \Delta$.*

We postpone the proof of the lemma and continue to pursue the global existence of the solution. By the lemma we have

$$\int_0^{\tau_n \wedge T} \mathrm{d}V(X(t)) \leq \int_0^{\tau_n \wedge T} K \,\mathrm{d}t + M(t), \tag{5.24}$$

and taking the expectation

$$\mathbb{E}[V\left(X(\tau_n \wedge T)\right)] \leq \mathbb{E}[V(X(0))] + K\,\mathbb{E}(\tau_n \wedge T) \leq \mathbb{E}[V(X(0))] + KT. \tag{5.25}$$

Set $\Omega_n = \{\tau_n \leq T\}$ for $n \geq n_1$. By (5.21) we have $P(\Omega_n) \geq \epsilon$. Since for every $\omega \in \Omega_n$, there is at least one of the $x_i(\tau_n, \omega)$ equaling either $1/n$ or $1 - 1/n$, then it holds

$$V\left(X(\tau_n, \omega)\right) \geq -\left(\log\left(\frac{1}{n}\right) + \log\left(1 - \frac{1}{n}\right)\right). \tag{5.26}$$

Then from (5.25) and (5.26) it follows that

$$V(X(0)) + KT \geq \mathbb{E}\left[\chi_{\Omega_n} V\left(X(\tau_n, \omega)\right)\right] \geq \epsilon\left(\log(n) + 1\right)$$

where χ_{Ω_n} is the indicator function of Ω_n. Letting $n \to \infty$ we have the following contradiction

$$\infty > V(X(0)) + KT = \infty,$$

hence we must have $\tau_\infty = \infty$ a.s. and the proof is complete. □

Proof of Lemma 5.3. Recall that

$$\begin{aligned} LV(X) = \sum_{i=1}^{N} \Bigg[& \left(\frac{1}{1-x_i} - \frac{1}{x_i}\right)\left(\beta s_i (1-x_i) - \delta x_i\right) \\ & + \frac{1}{2}\left(\frac{1}{(1-x_i)^2} + \frac{1}{x_i^2}\right)\sigma_i^2(x_i) s_i^2 (1-x_i)^2 \Bigg]; \end{aligned}$$

the last term is bounded by

$$\begin{aligned} \frac{1}{2}\left(\frac{1}{(1-x_i)^2} + \frac{1}{x_i^2}\right)\sigma^2(x_i) s_i^2 (1-x_i)^2 \leq & \frac{1}{2}\left(\frac{x_i^2 + (1-x_i)^2}{(1-x_i)^2\, x_i^2}\right) M^2\, x_i^2\, s_i^2 (1-x_i)^2 \\ \leq & M^2 (N-1)^2. \end{aligned}$$

The first term is given by

$$\left(\frac{1}{1-x_i}-\frac{1}{x_i}\right)(\beta s_i(1-x_i)-\delta x_i)=\frac{2x_i-1}{x_i(1-x_i)}\left(\beta s_i(1-x_i)-\delta x_i\right);$$

since the function

$$y(x)=\frac{2x-1}{x(1-x)}\left(\beta s(1-x)-\delta x\right), \qquad x\in(0,1)$$

has a maximum in $x_m=\frac{\sqrt{\beta s}}{\sqrt{\beta s}+\sqrt{\delta}}$ that is

$$y(x_m)=\beta s+\delta-2\sqrt{\delta\beta s},$$

in our framework, since $s_i=\sum a_{ij}x_j\leq N-1$, we finally get

$$LV(X)\leq N\left[\beta(N-1)+\delta+M^2(N-1)^2\right] \tag{5.27}$$

so the claim follows with a constant K given by the right-hand side of (5.27). □

5.4.2 Stability properties of the zero solution

Now we provide an analysis of the stability of the zero solution, i.e. the disease-free equilibrium, in order to identify the threshold condition for controlling the infection or eventually eradicating it.

Let $X_0=0$ be the vector of all zero components and let us consider the equation (5.20). Since $f(X_0)=0$ and $g(X_0)=0$ for all $t\geq 0$, it follows that the unique solution of (5.20) satisfying the initial condition $X(0)=X_0$ is the identically zero solution $X(t)=X_0$.

For the definitions and conditions on the stability of the zero solution see Chapter 2.

Remark 5.4. The contact matrix A, that is the adjacency matrix of an undirected graph, is symmetric and satisfies

$$\begin{aligned}\langle AX,X\rangle &\leq \lambda_1(A)|X|^2,\\ \langle AX,AX\rangle &\leq \lambda_1(A)^2|X|^2\end{aligned} \tag{5.28}$$

for every $X\in\mathbb{R}^N$.

Theorem 5.5. *Recall that M is the constant from (5.18). If*

$$\delta > \beta\lambda_1(A) + \frac{1}{32}M^2\lambda_1(A)^2 \tag{5.29}$$

then the null solution for (5.20), $X(t) = X_0$, is stochastically asymptotically stable in the large in $(0,1)^N$. This means that X_0 is stochastically stable and

$$\mathbb{P}\left[\lim_{t\to\infty} X(t) = 0\right] = 1,$$

for all $X(0) \in (0,1)^N$.

Proof. Let us define the Lyapunov function $V : (0,1)^N \to \mathbb{R}_+ = [0,\infty)$

$$V(X) = |X|^2;$$

recalling the definition of the infinitesimal generator L in (5.23) and setting (compare (5.19))

$$s_i = \sum_{j=1}^{N} a_{ij}x_j$$

we have

$$LV(X) = 2\beta\sum_{i=1}^{N} x_i s_i - 2\delta|X|^2 - 2\beta\sum_{i=1}^{N} x_i^2 s_i + \sum_{i=1}^{N}\sigma(x_i)^2(1-x_i)^2 s_i^2.$$

Since it holds that

$$x(1-x) \le \frac{1}{4},$$

we have from (5.28) and condition (5.18) that

$$LV(X) \le \left(2\beta\lambda_1(A) - 2\delta + \frac{1}{16}M^2\lambda_1(A)^2\right)|X|^2. \tag{5.30}$$

In order to conclude, we shall impose that $C = 2\beta\lambda_1(A) - 2\delta + \frac{1}{16}M^2\lambda_1(A)^2$ is strictly negative, i.e.,

$$\delta > \beta\lambda_1(A) + \frac{1}{32}M^2\lambda_1(A)^2$$

as required. Then under this assumption we have that

$$LV(X) \le CV(X).$$

and by Theorem 2.2, X_0 is stochastically asymptotically stable in the large in $(0,1)^N$. □

5.4.3 Stochastic permanence

We obtain, from Theorem 5.4, that the solution exists for all times and that it remains in Δ definitely. However, this property is too weak for the applications, so we search for further details about the asymptotic behaviour of the solution. First, we recall the following definition from [56].

Definition 5.1. Equation (5.19) (equivalently, (5.20)) is said to be stochastically permanent if for any $\varepsilon > 0$ there exists a constant $\chi = \chi(\varepsilon)$ such that, for any initial condition $X(0) = (x_1(0), \ldots, x_N(0)) \in \Delta$, the solution satisfies

$$\liminf_{t\to\infty} \mathbb{P}(|X(t)| \geq \chi) \geq 1 - \varepsilon. \tag{5.31}$$

At first, we prove a result that seems interesting on its own.

Theorem 5.6. *Assume that*

$$\delta < \lambda_1(A)\,\beta - \frac{1}{32} M^2 \lambda_1(A)^2. \tag{5.32}$$

Then, for any initial condition $X(0) \in \Delta$, the solution $X(t)$ satisfies

$$\sup_{t>0} \mathbb{E}\left[\frac{1}{|X(t)|^\alpha}\right] \leq C \tag{5.33}$$

where $\alpha > 0$ is small enough to have

$$\delta < \lambda_1(A)\,\beta - \frac{\alpha+1}{32} M^2 \lambda_1(A)^2$$

and C is a finite constant depending on α, the initial condition $X(0)$, the adjacency matrix A and the rates β and δ.

Proof. Let u be the Perron eigenvector of the $N \times N$ adjacency matrix A, i.e., it is the eigenvector corresponding to the spectral radius $\lambda_1(A)$, and the unique one such that $u > 0$ and $|u|_1 = 1$ [47]. Consider the function

$$\psi(X) = \frac{1}{\sum_{i=1}^{N} u_i x_i};$$

by Itô's formula the process $Y(t) = \psi(X(t))$ satisfies

$$\mathrm{d}Y(t) = L\psi(X(t))\,\mathrm{d}t + \mathrm{d}M(t),$$

where $M(t)$ is a (local) martingale and L is the infinitesimal generator of the diffusion $X(t)$, defined in (5.23). We may compute

$$\begin{aligned} L\psi(X) &= \sum_{i=1}^{N} u_i f_i(X)\partial_{x_i}\psi(X) + \frac{1}{2}\sum_{i=1}^{N} u_i^2 g_{ii}^2(X)\partial_{x_i x_i}^2\psi(X) \\ &= -\sum_{i=1}^{N} f_i(X)\psi^2(X) + \sum_{i=1}^{N} g_{ii}^2(X)\psi^3(X), \\ &\qquad X = (x_1,\dots,x_N), \quad \psi \in C^\infty(\Delta). \end{aligned}$$

Next, we introduce the process

$$Z(t) = e^{\kappa t}(1+\psi(X(t)))^\alpha, \tag{5.34}$$

where κ is a positive constant to be chosen later. Again by appealing to Itô's formula we have

$$\begin{aligned} \mathrm{d}Z(t) =& \kappa Z(t)\,\mathrm{d}t \\ &+\alpha e^{\kappa t}(1+\psi(X(t)))^{\alpha-1}\left[-\psi^2(X(t))\sum_{i=1}^{N} u_i f_i(X(t)) + \psi^3(X(t))\sum_{i=1}^{N} u_i^2 g_{ii}^2(X(t))\right]\mathrm{d}t \\ &+\frac{1}{2}\alpha(\alpha-1)e^{\kappa t}(1+\psi(X(t)))^{\alpha-2}\psi^4(X(t))\sum_{i=1}^{N} u_i^2 g_{ii}^2(X(t))\,\mathrm{d}t + \mathrm{d}\tilde{M}(t). \end{aligned} \tag{5.35}$$

Let us consider

$$-\sum_{i=1}^{N} u_i f_i(X(t)) = -\sum_{i=1}^{N}\beta u_i s_i(t) + \sum_{i=1}^{N}\beta u_i s_i(t)x_i(t) + \sum_{i=1}^{N}\delta u_i x_i(t). \tag{5.36}$$

Since $u \geq 0$, $|u|_1 = 1$, from (5.28) we have

$$\begin{aligned} \beta\sum_{i=1}^{N} u_i s_i(t)x_i(t) &= \beta\sum_{i,j=1}^{N} a_{ij}x_j(t)u_i x_i(t) \leq \beta\sum_{i,j=1}^{N} a_{ij}x_j(t)x_i(t) \\ &= \beta\langle AX(t), X(t)\rangle \leq \beta\lambda_1(A)\,|X(t)|_2^2 \leq \beta\lambda_1(A)\,\psi(X(t))^{-2}, \end{aligned}$$

moreover

$$
\begin{aligned}
-\sum_{i=1}^{N}\beta\sum_{j=1}^{N}u_i a_{ij}x_j(t)+\sum_{i=1}^{N}\delta u_i x_i(t) &= -\beta\langle u, AX(t)\rangle+\delta\langle u, X(t)\rangle \\
&= -\beta\langle A^T u, X(t)\rangle+\delta\langle u, X(t)\rangle \\
&= (-\beta\,\lambda_1(A)+\delta)\,\psi^{-1}(X(t)).
\end{aligned}
$$

Using these estimates in (5.36) we get

$$
-\sum_{i=1}^{N} f_i(X(t)) \le \beta\lambda_1(A)\,\psi^{-2}(X(t))+(-\beta\,\lambda_1(A)+\delta)\,\psi^{-1}(X(t)). \tag{5.37}
$$

Next, we consider

$$
\sum_{i=1}^{N} u_i^2 g_{ii}^2 = \sum_{i=1}^{N} u_i^2\left[\sigma_i(x_i(t))s_i(t)(1-x_i(t))\right]^2;
$$

by Theorem 5.4 we already know that $x_i(t)\in(0,1)$, then we have $x(1-x)\le 1/4$, hence the previous sum is bounded by

$$
\begin{aligned}
\frac{M^2}{16}\sum_{i=1}^{N}u_i^2\left[\sum_{j=1}^{N}a_{ij}x_j(t)\right]^2 &\le \frac{M^2}{16}\left[\sum_{i=1}^{N}\left(u_i\sum_{j=1}^{N}a_{ij}x_j(t)\right)\right]^2 \\
&= \frac{M^2}{16}\langle u, AX(t)\rangle^2 \\
&= \frac{M^2}{16}\lambda_1^2(A)\psi(X(t))^{-2},
\end{aligned}
$$

where M is the constant in (5.18). We have thus from (5.35), integrating in $(0,t)$ and taking expectation

$$
\begin{aligned}
\mathbb{E}[Z(t)]-\mathbb{E}[Z(0)] \le \alpha\,\mathbb{E}\int_0^t e^{\kappa s}(1+\psi(X(s))^{\alpha-2} \\
\cdot\left\{\left(\beta\lambda_1(A)+\frac{\kappa}{\alpha}\right)+\left(2\frac{\kappa}{\alpha}+\delta+\frac{M^2}{16}\lambda_1(A)^2\right)\psi(X(s))\right. \\
\left.+\left(\frac{\kappa}{\alpha}-\beta\,\lambda_1(A)+\delta+\frac{(\alpha+1)}{32}M^2\lambda_1(A)^2\right)\psi^2(X(s))\right\}\,\mathrm{d}s.
\end{aligned} \tag{5.38}
$$

Choose κ small enough to have

$$\delta < \lambda_1(A)\,\beta - \frac{\alpha+1}{32}M^2\lambda_1(A)^2 - \frac{\kappa}{\alpha};$$

notice that $\psi(X(s)) \geq \frac{1}{N}$, and the function

$$(1+x)^{\alpha-2}(c_0 + c_1 x - c_2 x^2)$$

satisfies, on that interval,

$$(1+x)^{\alpha-2}(c_0 + c_1 x - c_2 x^2) \leq H < +\infty$$

for every choice of $c_0, c_1 \in \mathbb{R}$ and $c_2 > 0$ and for some positive and finite constant H. Thus we obtain the inequality

$$\mathbb{E}[Z(t)] \leq \mathbb{E}[Z(0)] + \frac{\alpha H}{\kappa}e^{\kappa t}$$

and recalling definition (5.34) it follows

$$\mathbb{E}[(1+\psi(X(t)))^\alpha] \leq e^{-\kappa t}\mathbb{E}[Z(0)] + \frac{\alpha H}{\kappa}. \tag{5.39}$$

Next, observe the estimate $\psi^{-1}(X) = \langle u, X\rangle \leq |u||X| \leq |X|$, hence $\psi(X)^\alpha \geq |X|^{-\alpha}$. Thus, by using (5.39) and taking the supremum in $t > 0$,

$$\begin{aligned}\sup_{t>0}\mathbb{E}\left[\frac{1}{|X(t)|^\alpha}\right] &\leq \sup_{t>0}\mathbb{E}\left[\psi^\alpha(X(t))\right] \\ &\leq \sup_{t>0}\mathbb{E}\left[(1+\psi(X(t)))^\alpha\right] \\ &\leq \left(\mathbb{E}[(1+\psi(X(0)))^\alpha] + \frac{\alpha H}{\kappa}\right)\end{aligned}$$

as required. □

The main result in this section is the following.

Theorem 5.7. *Assume that condition* (5.32) *holds. Then the solution of the system* (5.20) *is stochastically permanent.*

Proof. The proof follows from a simple application of Markov's inequality. Let us estimate

$$\mathbb{P}(|X(t)| < \chi)$$

for some χ to be chosen. Then

$$\mathbb{P}(|X(t)| < \chi) = \mathbb{P}\left(\frac{1}{|X(t)|} > \frac{1}{\chi}\right) \leq \frac{\mathbb{E}\left[1/|X(t)|^{\alpha}\right]}{1/\chi^{\alpha}} \leq C\chi^{\alpha},$$

where C is the constant from (5.33). The above inequality holds by taking the supremum:

$$\sup_{t>0} \mathbb{P}(|X(t)| < \chi) \leq C\chi^{\alpha},$$

and therefore

$$\inf_{t>0} \mathbb{P}(|X(t)| \geq \chi) \geq 1 - C\chi^{\alpha}.$$

Since for every $\varepsilon > 0$ we can find $\chi = (\varepsilon/C)^{1/\alpha}$, inequality (5.31) is satisfied, as required. □

Remark 5.5. We can formulate condition (5.32) in terms of the ratio β/δ, then we have that the solution of (5.20) is stochastically permanent if

$$\frac{\beta}{\delta} > \tau_p^s := \frac{1}{\lambda_1(A)} + \frac{M^2\lambda_1(A)}{32\delta} = \tau_c^{(1)} + \frac{M^2\lambda_1(A)}{32\delta}.$$

On the other side, the null solution is asymptotically stable in the large provided that (5.29) holds, thus

$$\frac{\beta}{\delta} < \tau_c^s := \frac{1}{\lambda_1(A)} - \frac{M^2\lambda_1(A)}{32\delta} = \tau_c^{(1)} - \frac{M^2\lambda_1(A)}{32\delta}. \tag{5.40}$$

We see that there is a gap between the regions where the effective infection rate τ leads to extinction or persistence, respectively, whose extension depends on the intensity of the noise, through the parameter M. In the intermediate region, we perform numerical simulations to test the long term behaviour of the system.

We underline however that both Theorem 5.5 and 5.7 give us only sufficient conditions.

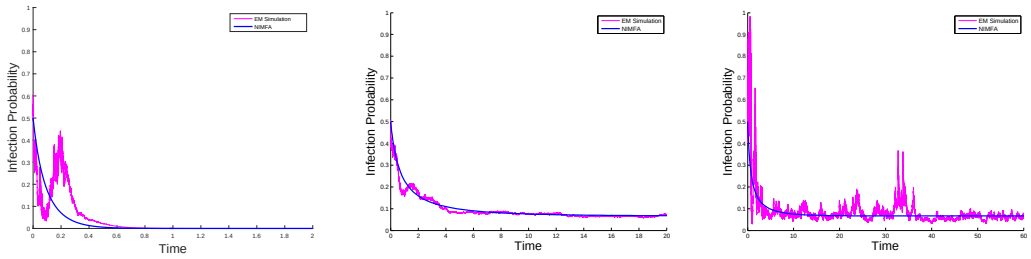

(a) (b) (c)

Figure 5.6: Dynamics of the infection probability of the node 4 in a graph with ring topology, and $N = 50$, where $\tau_c^{(1)} = 0.5$: EM approximation of the solution of (5.20) versus solution of (3.5). At time 0 the fraction of infected nodes is 0.5. a) $\beta = 4.1$, $\delta = 16.3$, $M = 8$, $\beta/\delta < \tau_c^s = 0.7454$. b) $\beta = 1.5$, $\delta = 2.8$, $\beta/\delta > \tau_p^s = 0.5143$, M=0.8. c)$\beta = 1.5$, $\delta = 2.8$, $\beta/\delta > \tau_p^s = 0.8571$, M=4.

Numerical Experiments.

We numerically simulate the solution of system (5.20) by the Euler-Maruyama (EM) method [45], and we compare it with the solution of the NIMFA system (3.5).

In Figure 5.6 (a), (b) and (c) we consider a graph with ring topology and $N = 50$. In (a) we consider values of β and δ such that $\tau < \tau_c^s$ and $M = 8$, and we plot the dynamical behaviour of one given node, by computing the solution of (5.20) along one sample path. The numerical computation confirms the stability result in Theorem 5.5. In (b) and (c), instead, we consider values of β and δ such that $\tau > \tau_p^s$ for $M = 0.8$ and $M = 4$ respectively. We can recognise the behaviour aforesaid in Theorem 5.7. Moreover we can see that, if the assumption (5.32) of Theorem 5.7 holds, the solution of (5.20) fluctuates around the endemic equilibrium of the system (3.5) and, clearly, with the decrease of the intensity of the noise, the fluctuations are smaller. The same type of numerical experiments have been done in Figure 5.7 (a), (b) and (c), for a complete graph and $N = 40$.

In Figure 5.8 (a), (b) and (c) and in Figure 5.9 (a), (b) we investigate the behaviour of the solution of (5.20), in the case where both conditions of stability (5.29) and permanence (5.32) are not satisfied.

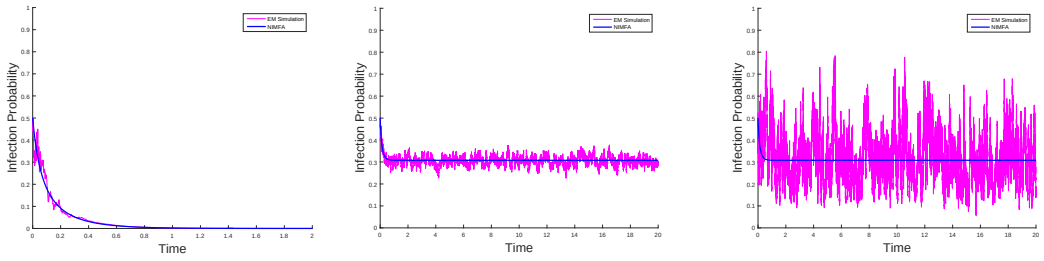

(a) (b) (c)

Figure 5.7: Dynamics of the infection probability of the node 4 in a complete graph with $N = 40$, where $\tau_c^{(1)} = 0.0256$: EM approximation of the solution of (5.20) versus solution of (3.5). At time 0 the fraction of infected nodes is 0.5. a) $\beta = 0.5$, $\delta = 23.9$, $\beta/\delta \leq \tau_c^s = 0.0210$, $M = 0.3$. b) $\beta = 0.5$, $\delta = 13.5$, $\beta/\delta > \tau_p^s = 0.0258$, $M = 0.04$. c) $\beta = 0.5$, $\delta = 13.5$, $\beta/\delta > \tau_p^s = 0.0338$, M=0.3.

Precisely, in Figure 5.8 we consider the graph with ring topology and $N = 50$; in particular, in (a) we consider the case where $0 < \beta/\delta < \tau_c^{(1)}$ and we can see that the solution of (5.20) tends to zero, as that of (3.5). In Figure 5.8 (b), instead, we analyze the case $\tau_c^{(1)} < \beta/\delta < \tau_p^s$, we can observe a different behaviour of the solution of (5.20) that does not fluctuate around the solution of (3.5), moreover in (c) the EM solution is averaged over 100 sample paths always in the case $\tau_c^{(1)} < \beta/\delta < \tau_p^s$; we can see that, in this case, NIMFA provides an upper bound of our infection probabilities dynamics. The same behavior, in the region $\tau_c^{(1)} < \beta/\delta < \tau_p^s$, of one sample path, and of the averaged solution, is depicted also by Figure 5.9 (a) and (b) respectively, where we consider a graph with an arbitrary topology and $N = 13$.

Thus, we see that, in the intermediate region, our system tends to have the same long-term behaviour of the deterministic model, with some differences in the level of infection, due to the randomness of the environment.

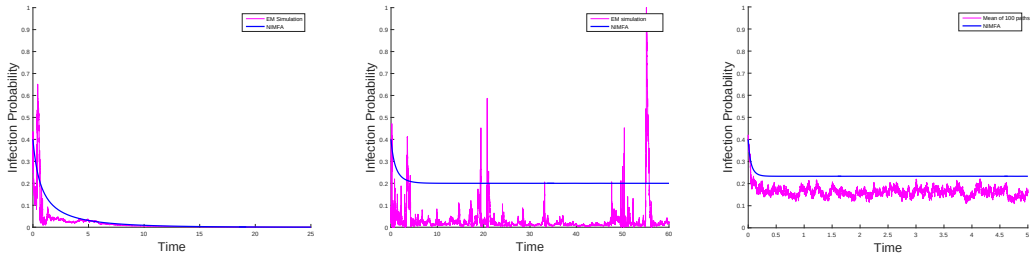

(a) (b) (c)

Figure 5.8: Dynamics of the infection probability of the node 4 for a graph with ring topology, and $N = 50$, where $\tau_c^{(1)} = 0.5$: EM approximation of the solution of (5.20) versus solution of (3.5). At time 0 the fraction of infected nodes is 0.4. a) $\beta = 1.5$, $\delta = 3.2$, $M = 10$, $0 < \beta/\delta < \tau_c^{(1)}$. b) $\beta = 1.5$, $\delta = 2.4$, $M = 40$, $\tau_c^{(1)} < \beta/\delta < \tau_p^s$. c) EM approximation of the solution of (5.20) averaged over 100 sample paths versus. $\beta = 30$, $\delta = 46$, $M = 30$, $\tau_c^{(1)} < \beta/\delta < \tau_p^s$.

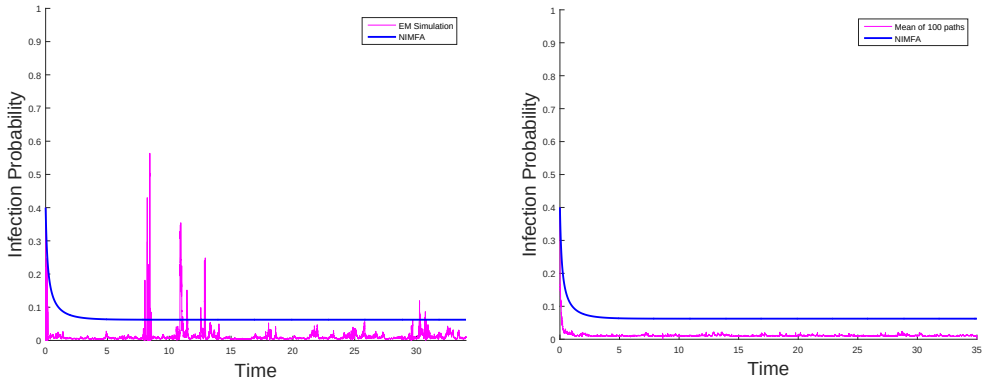

(a) (b)

Figure 5.9: Dynamics of the infection probability of the node 4 in a graph with arbitrary topology and $N = 13$, where $\tau_c^{(1)} = 0.2045$. At time 0 the fraction of infected nodes is 0.4. $\beta = 2.2$, $\delta = 10$, $M = 40$, $\tau_c^{(1)} < \beta/\delta < \tau_p^s$. (a) EM approximation of (5.20) versus solution of (3.5). (b) EM approximation of the solution of (5.20) averaged over 100 sample paths versus solution of (3.5).$\beta = 2.2$, $\delta = 10$, $M = 40$.

Appendix A

Bisection Algorithm

We report on the algorithm `OptimalImmunization2D` that solves the $2D$ immunization problem 5.5 analyzed in Section 5.2.1.
In Tab. A.1 we report on the pseudocode of the algorithm. It employs three additional functions `LeftCorner` (Tab. A.2) `RightCorner` and `BisectionThreshold` (Tab. A.3).

`LeftCorner` identifies via bisection feasible point $(\delta_0^{\min}, \delta_1^{\max})$; the bisection search operated by `LeftCorner` – see proof of Thm. 5.3 – is performed along values $\delta_1 = f(\delta_0)$. The companion function `RightCorner` identifies the point $(\delta_0^{\max}, \delta_1^{\min})$, the pseudocode is omitted.

Procedure `isNegativeDefinite` is the standard test for a real symmetric matrix A to be negative definite; it requires to verify $\det(A_k) = (-1)^k$ where A_k is the k-th principal minor of A, i.e., the matrix obtained considering the first k rows and columns only.

Finally, the `OptimalImmunization2D` algorithm performs a bisection search based on a subgradient descent over the utility function $U(\delta_0) = c_0\delta_0 + c_1\phi(\delta_0)$.

Remark A.1. In Tab. A.1 we have reported an implementation assuming the calculation of the subgradient ∂U at each mid point x. However, it is sufficient to evaluate the increment at a point $x + \epsilon_1$ within the feasibility region for some $\epsilon_1 > 0$: if $U(x) < U(x+\epsilon_1)$, then, due to convexity, the whole

Table A.1: `OptimalThreshold2D`: solves the $2D$ optimal immunization problem via the bisection search.

$(\delta_0^*, \delta_1^*) =$ `OptimalThreshold2D`(Q, c_0, c_1)
Receives: Q, c_0, c_1
Returns: δ_0^*, δ_1^*
Initialize: $(\delta_l, \delta_1^{\max}) =$ `LeftCorner`(Q, c_0, c_1)
$(\delta_1^{\min}, \delta_r) =$ `RightCorner`(Q, c_1, c_0)
$k \leftarrow 1$, $U_{k-1} \leftarrow 0$, $U_k \leftarrow \infty$
1: `WHILE` $\lvert U_k - U_{k-1} \rvert > \epsilon$
2: $\delta_0^* = (\delta_l + \delta_r)/2$
3: $\delta_1^* \leftarrow$ `BisectionThreshold`(Q, δ_0^*)
4: $U_{k+1} = c_0\,\delta_0^* + c_1\,\delta_1^*$
5: `IF` $\partial U_k < 0$ % (see Rem. A.1)
6: `THEN` $\delta_r = \delta_0^*$
7: `ELSE` $\delta_l = \delta_0^*$
8: `END`
9: $k \leftarrow k + 1$
9: `END`

interval $[x+\epsilon_1, +\infty)$ can be discarded. Conversely, if $U(x) > U(x+\epsilon_1)$, then, due to convexity, the whole interval $[0, x)$ can be discarded during the search. This operation can be performed at a cost $O(1)$ when $U(x)$ and $U(x + \epsilon_1)$ are known, i.e., at the cost of two calls of `BisectionThreshold`.

Theorem A.1 (Correctness)**.** *`OptimalThreshold2D` is an ϵ approximation of an optimal solution Δ_2^*.*

Proof. The algorithm operates a bisection search for a global minimum of $U(\Delta_2) = c_1\delta_0 + c_1\phi(\delta_0)$, where $U(\Delta_2)$ is a convex function. Let $V = U_{l_{\max}}$: from the properties of the bisection search on (quasi-)convex functions [18][Ch. 4, pp. 145], the accuracy at step $r = \lfloor V/\epsilon \rfloor$ of the algorithm is $U_r - U(\Delta_2^*) < 2^{-r}V = \epsilon$. □

Table A.2: `LeftCorner`: identifies the left corner of $\Gamma' \subseteq \Gamma$ (Thm. 5.3); the pseudocode of the dual function $(\delta_0^{\max}, \delta_1^{\min}) =$ `RightCorner`(Q, c_0, c_1) is omitted for the sake of space.

$(\delta_0^{\min}, \delta_1^{\max}) =$ `LeftCorner`(Q, c_0, c_1)
Receives: Q, c_0, c_1
Returns: $\delta_0^{\min}$
Initialize: $U_{\max} \leftarrow (c_0 + c_1) l_{\max}$
1: `REPEAT`
2: $\delta_0^{\min} = (\delta_l + \delta_r)/2$
3: $\delta_1^{\max} \leftarrow \frac{U_{\max} - c_0 \delta_0^{\min}}{c_1}$
4: $D = \operatorname{diag}(\delta_0^{\min} \mathbf{1}_m, \delta_1^{\max} \mathbf{1}_{m'})$
5: $X \leftarrow$ `isNegativeDefinite`$(Q - D)$
6: `IF`$X =$ `true`
7: `THEN` $\delta_r = \delta_0^*$ % discard larger values
8: `ELSE` $\delta_l = \delta_0^*$ % discard smaller values
9: `END`
10: $T = \det(Q - D)$
12: `UNTIL` $X ==$`TRUE` `AND` $\lvert T \rvert < \epsilon$ % Termination condition

Furthermore, we can characterize the computational complexity of the algorithm.

Theorem A.2 (Complexity)**.** *The time complexity of* `OptimalThreshold2D` *is* $O(\epsilon^{-2} n^{1+\ell} \log^2 n)$ *where* $\ell = 2.373$.

Proof. The number of iterations of the bisection search `WHILE` loop (lines 1 to 9 in Tab. A.1) is $O(\epsilon^{-1} \log n)$. This follows again from elementary properties of bisection search [18][Ch. 4, pp. 145]. In fact, the bisection search operates for $0 \leq U(\delta_0) \leq U_{l_{\max}}$ and $U_{l_{\max}} = l_{\max}(c_0 + c_1)$. Finally, indeed, $l_{\max} \leq (n-1) \max_{i,j} q_{ij}$.

Using the same argument on the measure of the search intervals of `BisectionThreshold`, `LeftCorner` and `RightCorner` we conclude that they require $O(\epsilon^{-1} \log n)$ ite-

Table A.3: `BisectionThreshold`: given feasible δ_0, finds δ_1 such that (δ_0, δ_1) lies on the frontier of the feasibility region.

$\delta_1 =$ `BisectionThreshold`(Q, δ_0)
Receives: Q, δ_0
Returns: δ_1
Initialize: $T \leftarrow \inf$, $\delta_l = 0$, $\delta_r \leftarrow \max_i \sum_j a_{ij}$
1: `REPEAT`
2: $\delta_1 = (\delta_l + \delta_r)/2$
3: $D \leftarrow \mathrm{diag}(\delta_0 \mathbf{1}_m, \delta_1 \mathbf{1}_{m'})$
4: $X \leftarrow$ `isNegativeDefinite`$(Q - D)$
5: `IF` $X =$ `true`
6: `THEN` $\delta_r = \delta_1$ % discard larger values
7: `ELSE` $\delta_l = \delta_1$ % discard smaller values
8: `END`
9: $T = \det(Q - D)$
10: `UNTIL` $X ==$`TRUE` `AND` $\lvert T\rvert < \epsilon$ % Termination condition

rations of the `REPEAT` loop as well.

Finally, test `isNegativeDefinite` appearing in `Threshold2D`, `LeftCorner` and `RightCorner` requires the computation of $n-1$ determinants of the principal minors of $A - D$ at cost $O(n^{1+\ell})$. Here ℓ is the exponent for fast matrix multiplication [1]. In the case of the Coppersmith-Winograd algorithm for fast matrix multiplication it holds $\ell = 2.373$.

□

We note that `REPEAT` loop stops when $\epsilon > \prod |\lambda_i| = |\det(Q - D)| > |\lambda_1|^n$, i.e., when $|\lambda_1| < (\epsilon)^{1/n}$. Furthermore, the termination condition in `BisectionThreshold`, `LeftCorner` and `RightCorner` requires Δ_2 to lie within the feasible region *and* the determinant to be smaller than ϵ.

Finally, in Tab. A.4 we compare the performance of a `SDPT3` solver applied to Prob. 5.5 and the solution provided by our algorithm `OptimalThreshold2D`.

Table A.4: Accuracy of `OptimalThreshold2D`.

	`OptimalThreshold2D`			`SDPT3`		
k	$U^*(10^4)$	δ_0^*	$k \cdot \delta_1^*$	$U^*(10^4)$	δ_0^*	$k \cdot \delta_1^*$
10	0.8635	31.8661	13.3640	0.8636	31.8605	13.4162
20	0.9975	34.5574	26.7174	0.9978	34.5438	26.8328
30	1.1315	37.2509	40.0516	1.1319	37.2270	40.2493
40	1.2655	39.9458	53.3731	1.2661	39.9103	53.6658
50	1.3994	42.6389	66.6937	1.4003	42.5936	67.0822
60	1.5333	45.3384	79.9757	1.5344	45.2769	80.4984
70	1.6672	48.0397	93.2366	1.6686	47.9602	93.9148
80	1.8010	50.7338	106.5281	1.8027	50.6436	107.3306
90	1.9347	53.4384	119.7527	1.9369	53.3267	120.7479
100	2.0684	56.1414	132.9698	2.0711	56.0101	134.1635

The comparison is performed on a graph with $m = 50$ central nodes and for $c_i^0 = c_i^1 = 1$, $i = 1 \dots m$, for increasing values of the terminal community dimension k. We observe that the solution provided by `OptimalThreshold2D` is more accurate. The reason is that the algorithm performs the search on the frontier of the feasibility region – where the optimal solution is found based on Cor. 5.1 – whereas interior point methods such as the one used by the `SDPT3` solver tested here tend to provide more conservative solutions.* Namely, solutions tend to lie in the interior of the feasibility region, bounding $\lambda_1(Q-D)$ more far from zero than those generated by `OptimalThreshold2D`.

*More precisely, a solution is generated by `SDPT3` using a primal-dual interior-point algorithm which leverages on infeasible path-following paradigm [88].

Bibliography

[1] A. Aho, J. Hopcroft, and J. Ullman. *The Design and Analysis of Computer Algorithms*. Addison-Wesley, 1974.

[2] E. Allen. *Modeling with Itô stochastic differential equations*, volume 22. Springer Science & Business Media, 2007.

[3] L. Allen. An introduction to stochastic epidemic models. In F. Brauer, P. van den Driessche, and J. Wu, editors, *Mathematical Epidemiology*, volume 1945 of *Lecture Notes in Mathematics*, pages 81–130. Springer Berlin Heidelberg, 2008.

[4] L. Allen, B. Bolker, Y. Lou, and A. Nevai. Asymptotic profiles of the steady states for an sis epidemic patch model. *SIAM Journal on Applied Mathematics*, 67(5):1283–1309, 2007.

[5] R. M. Anderson, R. M. May, and B. Anderson. *Infectious diseases of humans: dynamics and control*, volume 28. Wiley Online Library, 1992.

[6] L. Arnold. Stochastic differential equations: theory and applications. 1974. *A Wiley-Interascience Publications*.

[7] N. T. Bailey et al. *The mathematical theory of infectious diseases and its applications*. Charles Griffin & Company Ltd, 5a Crendon Street, High Wycombe, Bucks HP13 6LE., 1975.

[8] D. Balcan, V. Colizza, B. Gonçalves, H. Hu, J. J. Ramasco, and A. Vespignani. Multiscale mobility networks and the spatial spreading of infectious diseases. *Proceedings of the National Academy of Sciences*, 106(51):21484–21489, 2009.

[9] F. Ball, T. Britton, T. House, V. Isham, D. Mollison, L. Pellis, and G. S. Tomba. Seven challenges for metapopulation models of epidemics, including households models. *Epidemics*, 10:63–67, 2015.

[10] F. Ball, D. Mollison, and G. Scalia-Tomba. Epidemics with two levels of mixing. *The Annals of Applied Probability*, pages 46–89, 1997.

[11] F. Ball and P. Neal. A general model for stochastic sir epidemics with two levels of mixing. *Mathematical biosciences*, 180(1):73–102, 2002.

[12] F. Ball and P. Neal. Network epidemic models with two levels of mixing. *Mathematical biosciences*, 212(1):69–87, 2008.

[13] F. Ball, D. Sirl, and P. Trapman. Analysis of a stochastic sir epidemic on a random network incorporating household structure. *Mathematical Biosciences*, 224(2):53–73, 2010.

[14] S. Boccaletti, V. Latora, Y. Moreno, M. Chavez, and D.-U. Hwang. Complex networks: Structure and dynamics. *Physics reports*, 424(4):175–308, 2006.

[15] S. Bonaccorsi and S. Ottaviano. Epidemics on networks with heterogeneous population and stochastic infection rates. *arXiv preprint, arXiv:1602.01501*, 2016.

[16] S. Bonaccorsi, S. Ottaviano, F. De Pellegrini, A. Socievole, and P. Van Mieghem. Epidemic outbreaks in two-scale community networks. *Phys. Rev. E*, 90:012810, Jul 2014.

[17] S. Bonaccorsi, S. Ottaviano, D. Mugnolo, and F. De Pellegrini. Epidemic outbreaks in networks with equitable or almost-equitable partitions. *SIAM Journal of Applied Mathematics*, 75(6):2421 – 2443, 2015.

[18] S. Boyd and L. Vandenberghe. *Convex optimization*. Cambridge University Press, 2004.

[19] S. P. Boyd. Semidefinite programming. *SIAM review*, 38:49–95, 1994.

[20] P. Brémaud. *Markov chains: Gibbs fields, Monte Carlo simulation, and queues*, volume 31. Springer Science & Business Media, 2013.

[21] T. Britton. Stochastic epidemic models: a survey. *Mathematical biosciences*, 225(1):24–35, 2010.

[22] D. M. Cardoso, C. Delorme, and P. Rama. Laplacian eigenvectors and eigenvalues and almost equitable partitions. *European journal of combinatorics*, 28(3):665–673, 2007.

[23] E. Cator, R. Van de Bovenkamp, and P. Van Mieghem. Susceptible-infected-susceptible epidemics on networks with general infection and cure times. *Physical Review E*, 87(6):062816, 2013.

[24] E. Cator and P. Van Mieghem. Second-order mean-field susceptible-infected-susceptible epidemic threshold. *Physical review E*, 85(5):056111, 2012.

[25] E. Cator and P. Van Mieghem. Nodal infection in Markovian SIS and SIR epidemics on networks are non-negatively correlated. *Physical Review E*, 89(5):052802, 2014.

[26] D. Chakrabarti, Y. Wang, C. Wang, J. Leskovec, and C. Faloutsos. Epidemic thresholds in real networks. *ACM Transactions on Information and System Security (TISSEC)*, 10(4):1, 2008.

[27] V. Colizza and A. Vespignani. Epidemic modeling in metapopulation systems with heterogeneous coupling pattern: Theory and simulations. *Journal of theoretical biology*, 251(3):450–467, 2008.

[28] D. J. Daley, J. Gani, and J. M. Gani. *Epidemic modelling: an introduction*, volume 15. Cambridge University Press, 2001.

[29] L. Danon, A. P. Ford, T. House, C. P. Jewell, M. J. Keeling, G. O. Roberts, J. V. Ross, and M. C. Vernon. Networks and the epidemiology of infectious disease. *Interdisciplinary perspectives on infectious diseases*, 2011, 2011.

[30] C. Dargatz. A diffusion approximation for an epidemic model. Discussion Paper 517, Ludwig-Maximilians-Universitat Munchen - Collaborative Research Centre 386, 2006.

[31] J. N. Darroch and E. Seneta. On quasi-stationary distributions in absorbing continuous-time finite markov chains. *Journal of Applied Probability*, 4(1):192–196, 1967.

[32] O. Diekmann, J. Heesterbeek, and J. A. Metz. On the definition and the computation of the basic reproduction ratio r 0 in models for infectious diseases in heterogeneous populations. *Journal of mathematical biology*, 28(4):365–382, 1990.

[33] M. Draief and L. Massouli. *Epidemics and rumours in complex networks*. Cambridge University Press, 2010.

[34] W. Feller. *An introduction to probability theory and its applications*, volume 2. John Wiley & Sons, 2008.

[35] B. Frank, S. David, T. Pieter, et al. Threshold behaviour and final outcome of an epidemic on a random network with household structure. *Advances in Applied Probability*, 41(3):765–796, 2009.

[36] A. Ganesh, L. Massoulié, and D. Towsley. The effect of network topology on the spread of epidemics. In *INFOCOM 2005. 24th Annual Joint Conference of the IEEE Computer and Communications Societies. Proceedings IEEE*, volume 2, pages 1455–1466. IEEE, 2005.

[37] T. C. Gard. *Introduction to stochastic differential equations*. M. Dekker, 1988.

[38] G. P. Garnett and R. M. Anderson. Sexually transmitted diseases and sexual behavior: insights from mathematical models. *Journal of Infectious Diseases*, 174(Supplement 2):S150–S161, 1996.

[39] C. Godsil. Feasibility conditions for the existence of walk-regular graphs. *Linear Algebra and its Applications*, 30:15–61, 1980.

[40] S. Gómez, A. Arenas, J. Borge-Holthoefer, S. Meloni, and Y. Moreno. Discrete-time markov chain approach to contact-based disease spreading in complex networks. *EPL (Europhysics Letters)*, 89(3):38009, 2010.

[41] A. Gray, D. Greenhalgh, L. Hu, X. Mao, and J. Pan. A stochastic differential equation SIS epidemic model. *SIAM J. Appl. Math.*, 71(3):876–902, 2011.

[42] A. Hakan and B. Tom. Stochastic epidemic models and their statistical analysis. *Lecture Notes in Statistics*, 151, 2000.

[43] I. Hanski and O. Ovaskainen. Metapopulation theory for fragmented landscapes. *Theoretical population biology*, 64(1):119–127, 2003.

[44] I. A. Hanski and O. E. Gaggiotti. *Ecology, genetics and evolution of metapopulations*. Academic Press, 2004.

[45] D. J. Higham. An algorithmic introduction to numerical simulation of stochastic differential equations. *SIAM review*, 43(3):525–546, 2001.

[46] A. L. Hill, D. G. Rand, M. A. Nowak, and N. A. Christakis. Emotions as infectious diseases in a large social network: the sisa model. *Proceedings of the Royal Society of London B: Biological Sciences*, 277(1701):3827–3835, 2010.

[47] R. A. Horn and C. R. Johnson, editors. *Matrix Analysis*. Cambridge University Press, New York, NY, USA, 2012.

[48] T. House. Non-markovian stochastic epidemics in extremely heterogeneous populations. *arXiv preprint arXiv:1403.2878*, 2014.

[49] T. House, G. Davies, L. Danon, and M. J. Keeling. A motif-based approach to network epidemics. *Bulletin of Mathematical Biology*, 71(7):1693–1706, 2009.

[50] M. Keeling. The implications of network structure for epidemic dynamics. *Theoretical population biology*, 67(1):1–8, 2005.

[51] J. G. Kemeny and J. L. Snell. Finite markov chains. undergraduate texts in mathematics, 1976.

[52] R. Khasminskii. *Stochastic stability of differential equations*, volume 66. Springer Science & Business Media, 2011.

[53] T. G. Kurtz. Limit theorems for sequences of jump markov processes approximating ordinary differential processes. *Journal of Applied Probability*, 8(2):344–356, 1971.

[54] A. Lajmanovich and J. A. Yorke. A deterministic model for Gonorrhea in a non-homogeneous population. *Mathematical Biosciences*, 28(34):221 – 236, 1976.

[55] C. Li, R. van de Bovenkamp, and P. Van Mieghem. Susceptible-infected-susceptible model: A comparison of n-intertwined and heterogeneous mean-field approximations. *Physical Review E*, 86(2):026116, 2012.

[56] X. Li and X. Mao. Population dynamical behavior of non-autonomous Lotka-Volterra competitive system with random perturbation. *Discrete Contin. Dyn. Syst.*, 24(2):523–545, 2009.

[57] X. Mao, G. Marion, and E. Renshaw. Environmental Brownian noise suppresses explosions in population dynamics. *Stochastic Process. Appl.*, 97(1):95–110, 2002.

[58] N. Masuda. Effects of diffusion rates on epidemic spreads in metapopulation networks. *New Journal of Physics*, 12(9):093009, 2010.

[59] R. K. McCormack and L. J. S. Allen. Stochastic sis and sir multihost epidemic models. In R. P. Agarwal and K. Perera, editors, *Proceedings of the Conference on Differential and Difference Equations and Applications*, pages 775–786. Hindawi, New York, Cairo, 2006.

[60] S. Merler, M. Ajelli, A. Pugliese, and N. M. Ferguson. Determinants of the spatiotemporal dynamics of the 2009 h1n1 pandemic in europe: implications for real-time modelling. 2011.

[61] C. D. Meyer. *Matrix analysis and applied linear algebra*. Siam, 2000.

[62] C. D. Meyer, editor. *Matrix Analysis and Applied Linear Algebra*. Society for Industrial and Applied Mathematics, Philadelphia, PA, USA, 2000.

[63] H. Minc. Non-negative matrices. *New York*, 1988.

[64] D. Mugnolo. *Semigroup methods for evolution equations on networks*. Springer, 2014.

[65] I. Nåsell. The quasi-stationary distribution of the closed endemic sis model. *Advances in Applied Probability*, pages 895–932, 1996.

[66] I. Nåsell. Stochastic models of some endemic infections. *Mathematical biosciences*, 179(1):1–19, 2002.

[67] M. E. Newman. The structure and function of complex networks. *SIAM review*, 45(2):167–256, 2003.

[68] S. Ottaviano, F. De Pellegrini, and S. Bonaccorsi. Heterogeneous sis model for directed community networks and optimal immunization. *arXiv preprint arXiv:1602.04679*.

[69] R. Pastor-Satorras, C. Castellano, P. Van Mieghem, and A. Vespignani. Epidemic processes in complex networks. *arXiv preprint arXiv:1408.2701*, 2014.

[70] R. Pastor-Satorras and A. Vespignani. Epidemic spreading in scale-free networks. *Physical review letters*, 86(14):3200, 2001.

[71] L. Pellis, F. Ball, and P. Trapman. Reproduction numbers for epidemic models with households and other social structures. i. definition and calculation of r 0. *Mathematical biosciences*, 235(1):85–97, 2012.

[72] L. Perko. *Differential equations and dynamical systems*, volume 7. Springer Science & Business Media, 2013.

[73] C. Poletto, S. Meloni, V. Colizza, Y. Moreno, and A. Vespignani. Host mobility drives pathogen competition in spatially structured populations. *PLOS Comp Bio*, 9(8):1003169, 2013.

[74] P. Pollett. Quasi-stationary distributions: a bibliography. *Disponiblea http://www. maths. uq. edu. au/ pkp/papers/qsds/qsds. pdf*, 2008.

[75] P. Pollett and A. Roberts. A description of the long-term behaviour of absorbing continuous-time markov chains using a centre manifold. *Advances in applied probability*, pages 111–128, 1990.

[76] B. A. Prakash, L. Adamic, T. Iwashyna, H. Tong, and C. Faloutsos. Fractional immunization in networks. *Austin, Texas, USA*, 2013.

[77] V. M. Preciado, M. Zargham, C. Enyioha, A. Jadbabaie, and G. Pappas. Optimal vaccine allocation to control epidemic outbreaks in arbitrary networks. *CoRR*, abs/1303.3984, 2013.

[78] B. Qu and H. Wang. Sis epidemic spreading with heterogeneous infection rates. *arXiv preprint arXiv:1506.07293*, 2015.

[79] D. Rand. Correlation equations and pair approximations for spatial ecologies. *Advanced ecological theory: principles and applications*, 100, 1999.

[80] J. V. Ross, T. House, and M. J. Keeling. Calculation of disease dynamics in a population of households. *PLoS One*, 5(3):e9666, 2010.

[81] F. D. Sahneh, C. Scoglio, and P. Van Mieghem. Generalized epidemic mean-field model for spreading processes over multilayer complex networks. *Networking, IEEE/ACM Transactions on*, 21(5):1609–1620, 2013.

[82] R. J. Sánchez-García, E. Cozzo, and Y. Moreno. Dimensionality reduction and spectral properties of multilayer networks. *Physical Review E*, 89(5):052815, 2014.

[83] A. J. Schwenk. Computing the characteristic polynomial of a graph. In *Graphs and Combinatorics*, pages 153–172. Springer, 1974.

[84] J. R. Silvester. Determinants of block matrices. *The Mathematical Gazette*, 84(501):pp. 460–467, 2000.

[85] P. L. Simon, M. Taylor, and I. Z. Kiss. Exact epidemic models on graphs using graph-automorphism driven lumping. *Journal of mathematical biology*, 62(4):479–508, 2011.

[86] B. Spagnolo, D. Valenti, and A. Fiasconaro. Noise in ecosystems: a short review. *Math. Biosci. Eng.*, 1(1):185–211, 2004.

[87] D. Stanescu and B. M. Chen-Charpentier. Random coefficient differential equation models for bacterial growth. *Math. Comput. Modelling*, 50(5-6):885–895, 2009.

[88] R. H. Tütüncü, K. C. Toh, and M. J. Todd. Solving semidefinite-quadratic-linear programs using SDPT3. *Mathematical Programming*, 95(2):189–217, 2003.

[89] P. Van Mieghem. *Graph spectra for complex networks*. Cambridge University Press, 2010.

[90] P. Van Mieghem. Decay towards the overall-healthy state in sis epidemics on networks. *arXiv preprint arXiv:1310.3980*, 2013.

[91] P. Van Mieghem. Exact markovian sir and sis epidemics on networks and an upper bound for the epidemic threshold. *arXiv preprint arXiv:1402.1731*, 2014.

[92] P. Van Mieghem. Exact markovian sir and sis epidemics on networks and an upper bound for the epidemic threshold. *arXiv preprint arXiv:1402.1731*, 2014.

[93] P. Van Mieghem and E. Cator. Epidemics in networks with nodal self-infection and the epidemic threshold. *Physical Review E*, 86(1):016116, 2012.

[94] P. Van Mieghem and J. Omic. In-homogeneous virus spread in networks. *arxiv: 1306.2588*, 2013.

[95] P. Van Mieghem, J. Omic, and R. Kooij. Virus spread in networks. *Networking, IEEE/ACM Tran. on*, 17(1):1–14, Feb 2009.

[96] P. Van Mieghem and R. Van de Bovenkamp. Non-markovian infection spread dramatically alters the susceptible-infected-susceptible epidemic threshold in networks. *Physical review letters*, 110(10):108701, 2013.

[97] P. Van Mieghem and R. Van de Bovenkamp. Accuracy criterion for the mean-field approximation in susceptible-infected-susceptible epidemics on networks. *Physical Review E*, 91(3):032812, 2015.

[98] W. Wang, Z. Wu, C. Wang, and R. Hu. Modelling the spreading rate of controlled communicable epidemics through an entropy-based thermodynamic model. *Science China Physics, Mechanics and Astronomy*, 56(11):2143–2150, 2013.

[99] Y. Wang, D. Chakrabarti, C. Wang, and C. Faloutsos. Epidemic spreading in real networks: An eigenvalue viewpoint. In *Reliable Distributed Systems, 2003. Proceedings. 22nd International Symposium on*, pages 25–34. IEEE, 2003.

[100] A. Widder and C. Kuehn. Heterogeneous population dynamics and scaling laws near epidemic outbreaks. *arXiv preprint arXiv:1411.7323*, 2014.